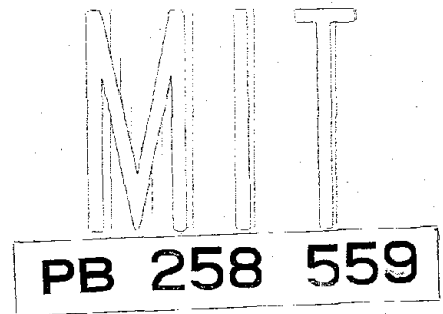


294002

Publication No. R76-40

Order No. 557



Evaluation of Seismic Safety of Buildings

Report No. 8

INELASTIC RESPONSE SPECTRUM DESIGN PROCEDURES FOR STEEL FRAMES

by

Richard W. Haviland

John M. Biggs

Stavros A. Anagnostopoulos

September 1976

DEPARTMENT

OF

CIVIL

ENGINEERING



SCHOOL OF ENGINEERING

MASSACHUSETTS INSTITUTE OF TECHNOLOGY

Cambridge, Massachusetts 02139

Sponsored by the National Science Foundation
Division of Advanced Environmental Research
and Technology
Grant ATA 74-06935

REPRODUCED BY
**NATIONAL TECHNICAL
INFORMATION SERVICE**
U. S. DEPARTMENT OF COMMERCE
SPRINGFIELD, VA. 22161

Additional Copies May be Obtained from
National Technical Information Service
U.S. Department of Commerce
5285 Port Royal Road
Springfield, Virginia 22151

BIBLIOGRAPHIC DATA SHEET		1. Report No. MIT-CE-R76-40	2.	3. Recipient's Accession No.
4. Title and Subtitle INELASTIC RESPONSE SPECTRUM DESIGN PROCEDURES FOR STEEL FRAMES, Evaluation of Seismic Safety of Buildings			5. Report Date September 1976	6.
7. Author(s) Haviland, Richard W., Biggs, John M., and Anagnostopoulos,			8. Performing Organization Rept. No. R76-40; Order 557	
9. Performing Organization Name and Address Massachusetts Institute of Technology Dept. of Civil Engineering Cambridge, Mass. 02139			10. Project/Task/Work Unit No. Stavros A.	
12. Sponsoring Organization Name and Address National Science Foundation 1800 "G" Street, N.W. Washington, D.C. 20550			11. Contract/Grant No. ATA 74-06935	
			13. Type of Report & Period Covered Research - 9/75 - present	
15. Supplementary Notes Eighth Report in a Series			14.	
16. Abstracts Reported is an evaluation of aseismic design procedures based upon inelastic response spectra. Steel frames of different heights are designed for a desired level of yielding using elastic modal analysis. Responses in terms of maximum ductility ratios are computed for simulated ground motions derived from the design spectrum. Both shear beam models and point hinge models are utilized and compared. Results are given in terms of maximum local and story ductility ratios as compared with the design values. The effect of gravity loads on the computed response and the effect of including such loads in the design procedure and investigated. In general, local ductility ratios exceed the desired design level. The use of seismic load factors to improve performance is investigated. It is concluded that the inelastic response spectrum approach is promising, but that further study and development are necessary before it could be adopted with confidence.				
17. Key Words and Document Analysis. 17a. Descriptors Inelastic Dynamic Analysis / Design Nonlinear Dynamic Analysis / Design Inelastic Response Spectrum Modal Analysis				
17b. Identifiers/Open-Ended Terms Yielding Modal Analysis Response Spectrum Dynamic Analysis Design				
17c. COSATI Field/Group 13 02 Civil Engineering ; 13 13 Structural Engineering				
18. Availability Statement Release Unlimited			19. Security Class (This Report) UNCLASSIFIED	
			21. No. of Pages	



Massachusetts Institute of Technology
Department of Civil Engineering
Constructed Facilities Division
Cambridge, Massachusetts 02139

Evaluation of Seismic Safety of Buildings

Report No. 8

INELASTIC RESPONSE SPECTRUM DESIGN
PROCEDURES FOR STEEL FRAMES

by

Richard W. Haviland
John M. Biggs
Stavros A. Anagnostopoulos

September, 1976

Sponsored by National Science Foundation
Division of Advanced Environmental Research
and Technology
Grant ATA 74-06935

Publication No. R76-40

Order No. 557

ABSTRACT

Reported herein is an evaluation of aseismic design procedures based upon inelastic response spectra. Steel frames of different heights are designed for a desired level of yielding using elastic modal analysis. Responses in terms of maximum ductility ratios are computed for simulated ground motions derived from the design spectrum. Both shear beam models and point hinge models are utilized and compared. Results are given in terms of maximum local and story ductility ratios as compared with the design values.

The effect of gravity loads on the computed response and the effect of including such loads in the design procedure are investigated.

In general, local ductility ratios exceed the desired design level. The use of seismic load factors to improve performance is investigated.

It is concluded that the inelastic response spectrum approach is promising, but that further study and development are necessary before it could be adopted with confidence.

PREFACE

This is the eighth report prepared under National Science Foundation Grant ATA 74-06935. This report is derived from a thesis written by Richard William Haviland in partial fulfillment of the requirements for the degree of Master of Science in Civil Engineering. The research was supervised by Stavros A. Anagnostopoulos, Research Associate, and John M. Biggs, Professor, both of the Department of Civil Engineering at the Massachusetts Institute of Technology. The purpose of the supporting project is to evaluate the effectiveness of the total seismic design process, which consists of steps beginning with seismic risk analysis through dynamic analysis and the design of structural components. The project seeks to answer the question: "Given a set of procedures for these steps, what is the actual degree of protection against earthquake damage provided?" Alternative methods of analysis and design are being considered. Specifically, these alternatives are built around three methods of dynamic analysis: (1) time-history analysis, (2) response spectrum modal analysis, and (3) random vibration analysis.

The formal reports produced thus far are:

1. Arnold, Peter, Vanmarcke, Erik H., and Gazetas, George, "Frequency Content of Ground Motions during the 1971 San Fernando Earthquake," M.I.T. Department of Civil Engineering Research Report R76-3, Order No. 526, January 1976.
2. Gasparini, Dario, and Vanmarcke, Erik H., "Simulated Earthquake Motion Compatible with Prescribed Response Spectra," M.I.T. Department of Civil Engineering Research Report R76-4, Order No. 527, January 1976.
3. Vanmarcke, Erik H., Biggs, J.M., Frank, Robert, Gazetas, George, Arnold, Peter, Gasparini, Dario A., and Luyties, William, "Comparison of Seismic Analysis Procedures for Elastic Multi-degree Systems," M.I.T. Department of Civil Engineering Research Report R76-5, Order No. 528, January 1976.
4. Frank, Robert, Anagnostopoulos, Stavros, Biggs, J.M., and Vanmarcke, Erik H., "Variability of Inelastic Structural Response Due to Real and Artificial Ground Motions," M.I.T. Department of Civil Engineering Research Report R76-6, Order No. 529, January 1976.
5. Haviland, Richard, "A Study of the Uncertainties in the Fundamental Translational Periods and Damping Values for Real Buildings," Supervised by Professors J.M. Biggs and Erik H. Vanmarcke, M.I.T. Department of Civil Engineering Research Report R76-12, Order No. 531, February 1976.

6. Luyties, William H. III, Anagnostopoulos, Stavros, and Biggs, John M., "Studies on the Inelastic Dynamic Analysis and Design of Multi-Story Frames," M.I.T. Department of Civil Engineering Research Report R76-29, Order No. 548, July 1976.
7. Gazetas, George, "Random Vibration Analysis of Inelastic Multi-Degree-of-Freedom Systems Subjected to Earthquake Ground Motions," Supervised by Professor Erik H. Vanmarcke, M.I.T. Department of Civil Engineering Research Report R76-39, Order No. 556, August 1976.
8. Haviland, Richard W., Biggs, John M., and Anagnostopoulos, Stavros A., "Inelastic Response Spectrum Design Procedures for Steel Frames," M.I.T. Department of Civil Engineering Research Report R76-40, Order No. 557, September 1976.

These reports are based upon a series of Internal Study Reports which were prepared during the course of the work. Those prepared to date are:

1. Arnold, Peter, "The Influence of Site Azimuth and Local Soil Conditions on Earthquake Ground Motion Spectra," January 1975.
2. Arnold, Peter, "Structural Response to Earthquake Ground Motions by Random Vibrations," January 1975.
3. Gasparini, Dario, "SIMQKE", A Program for Artificial Motion Generation," January 1975.
4. Frank, Robert and Gasparini, Dario, "Evaluation of Seismic Safety of Buildings: Progress Report on Statistical Studies of Responses of MDOF Systems to Real and Artificial Ground Motions," January 1975.
5. Gazetas, George, "Study of the Effect of Local Soil Conditions on the San Fernando Earthquake Response Spectra, Using Regression Analysis," January 1975.
6. Frank, Robert, "A Statistical Study on the Nonlinear Response of MDOF Systems to Real and Artificial Earthquake Ground Motions," August 1975.
7. Frank, Robert, "A Study of the 'Effective Period' Change for SDOF Systems Responding Inelastically to a Sinusoidal Base Motion," August 1975.
8. Frank, Robert, "A Statistical Study of the Response Spectra of the 39 Real Earthquake Records," August 1975.
9. Gazetas, George, and Vanmarcke, Erik H., "Evaluation of Random Vibration Analysis of Elastic MDOF Systems," August 1975.
10. Gasparini, Dario, "Some Parametric Studies Using the Earthquake Simulation Program SIMQKE," August 1975.
11. Frank, Robert, "A Study of the Effect of the Distribution of Stiffness on the Response, Elastic and Inelastic, of MDOF Systems to Real and Artificial Earthquake Motions," September 1975.
12. Frank, Robert, "A Study on the Effect of the Motion Intensity on the Nonlinear Response of MDOF Systems," September 1975.

13. Gazetas, George, "Approximate, Random-Vibration Based Analysis of Elastoplastic, Shear-Type, Multi-DOF Structures," January 1976.
14. Haviland, Richard, "Discussion of the Incorporation of Uncertainty in Member Resistance into a Seismic Safety Analysis of Buildings," July 1976.

The project is supervised by Professors John M. Biggs and Erik H. Vanmarcke of the Civil Engineering Department. They have been assisted by Dr. Stavros Anagnostopoulos, a Research Associate in the Department. The research assistants on the project have been Peter Arnold, George Gazetas, Dario Gasparini, Robert Frank, William Luyties, and Richard Haviland.



TABLE OF CONTENTS

	<u>Page</u>
Title Page	i
Abstract	ii
Preface	1
Table of Contents	4
List of Figures	6
List of Tables	10
CHAPTER 1 - Introduction	13
1.1 General	13
1.2 Objectives and Scope	15
CHAPTER 2 - Frame Selection and Design	17
2.1 Description of Frames	17
2.2 Gravity Load Effects	22
2.3 Earthquake Load Effects	24
2.3.1 Inelastic Spectra	24
2.3.2 Modal Analysis	30
2.4 Determination of Member Strength	33
CHAPTER 3 - Inelastic Dynamic Analysis	37
3.1 Mathematical Models for Determination of Inelastic Dynamic Response	37
3.1.1 Point Hinge Model	37
3.1.2 Shear Beam Model	41
3.2 Measures of Inelastic Response	42
3.2.1 Member Level Parameters	42
3.2.2 Story Level Parameters	46
3.3 Simulated Motions	49
3.4 Comparisons of Parameters and Response of Point Hinge and Shear Beam Models	55

TABLE OF CONTENTS
(continued)

	<u>Page</u>
CHAPTER 4 - Behavior of Frames Designed for Inelastic Response	59
4.1 Results for Designs at a Ductility Level of 4, Including Gravity Effects	59
4.2 Results for Designs at a Ductility Level of 2, Including Gravity Effects	76
4.3 Results for Analyses Ignoring Gravity Effects	90
4.4 Results for Designs Ignoring Gravity Effects	104
4.5 Results for Designs Using Factored Spectral Forces	114
CHAPTER 5 - Commentary	123
5.1 Conclusions	123
5.2 Recommendations	128
References	130
Appendix A - Properties of Equivalent Shear Beam Models	133
Appendix B - Strength Properties for Inelastic Designs	135

LIST OF FIGURES

<u>Figure No.</u>	<u>Title</u>	<u>Page</u>
2.1.1	Properties of Four Story Frame	18
2.1.2	Properties of Ten Story Frame	19
2.1.3	Properties of Eighteen Story Frame	20
2.3.1	Elastic and Inelastic Design Spectra - After Newmark and Hall, Redrawn from Reference 11	25
2.3.2	Elastic and Inelastic Design Spectra, $\mu = 2$	26
2.3.3	Elastic and Inelastic Design Spectra, $\mu = 4$	27
2.3.4	Elastic and Elastoplastic Resistance- Deformation Functions	29
2.4.1	Member End Forces Resulting From Gravity and Earthquake Loads	34
2.4.2	Moment Diagram for Girder Hinged at Both Ends	34
3.1.1	Moment-Rotation Relationship at the End of a Member	39
3.1.2	Column Interaction Diagram	39
3.2.1	Definition of Rotational Ductility	43
3.2.2	Definition of Moment Ductility	43
3.2.3	Definition of Story Ductility	48
3.3.1	Response Spectrum for Simulated Motion 1	50
3.3.2	Response Spectrum for Simulated Motion 2	51
3.3.3	Response Spectrum for Simulated Motion 3	52
3.3.4	Intensity Function	54
3.4.1	Comparison of Maximum Lateral and Interstory Displacements of Point Hinge and Shear Beam Models	57

7
LIST OF FIGURES
(continued)

<u>Figure No.</u>	<u>Title</u>	<u>Page</u>
4.1.1	Maximum Ductility Factors for Gravity and Earthquake Design - $\mu = 4$; 4-Story Frame; Motions 1, 2, 3	63
4.1.2	Maximum Story Level Parameters for Gravity and Earthquake Design - $\mu = 4$; 4-Story Frame; Motions 1, 2, 3	64
4.1.3	Maximum Girder Ductility Factors for Gravity and Earthquake Design - $\mu = 4$; 10-Story Frame; Motions 1, 2, 3	65
4.1.4	Maximum Column Ductility Factors for Gravity and Earthquake Design - $\mu = 4$; 10-Story Frame; Motions 1, 2, 3	66
4.1.5	Maximum Story Level Parameters for Gravity and Earthquake Design - $\mu = 4$; 10-Story Frame; Motions 1, 2, 3	67
4.1.6	Maximum Girder Ductility Factors for Gravity and Earthquake Design - $\mu = 4$; 18-Story Frame; Motion 2	68
4.1.7	Maximum Column Ductility Factors for Gravity and Earthquake Design - $\mu = 4$; 18-Story Frame; Motion 2	69
4.1.8	Maximum Forces for Gravity and Earthquake Design - $\mu = 4$; 18-Story Frame; Motion 2	70
4.1.9	Maximum Displacements for Gravity and Earthquake Design - $\mu = 4$; 18-Story Frame; Motion 2	71
4.2.1	Maximum Response Parameters for Gravity and Earthquake Design - $\mu = 2$; 4-Story Frame; Motion 2	77
4.2.2	Maximum Ductility Factors for Gravity and Earthquake Design - $\mu = 2$; 10-Story Frame; Motion 2	78
4.2.3	Maximum Story Level Parameters for Gravity and Earthquake Design - $\mu = 2$; 10-Story Frame; Motion 2	79

8
LIST OF FIGURES
(continued)

<u>Figure No.</u>	<u>Title</u>	<u>Page</u>
4.2.4	Maximum Girder Ductility Factors for Gravity and Earthquake Design - $\mu=2$; 18-Story Frame; Motion 2	80
4.2.5	Maximum Column Ductility Factors for Gravity and Earthquake Design - $\mu=2$; 18-Story Frame; Motion 2	81
4.2.6	Maximum Forces for Gravity and Earthquake Design - $\mu=2$; 18-Story Frame; Motion 2	82
4.2.7	Maximum Displacements for Gravity and Earthquake Design - $\mu=2$; 18-Story Frame; Motion 2	83
4.3.1	Maximum Response Parameters for Analysis Without Gravity - $\mu=4$; 4-Story Frame; Motion 1	92
4.3.2	Maximum Response Parameters for Analysis Without Gravity - $\mu=4$; 4-Story Frame; Motion 2	93
4.3.3	Maximum Response Parameters for Analysis Without Gravity - $\mu=4$; 4-Story Frame; Motion 3	94
4.3.4	Maximum Ductility Factors for Analysis Without Gravity - $\mu=4$; 10-Story Frame; Motion 1	95
4.3.5	Maximum Story Level Parameters for Analysis Without Gravity - $\mu=4$; 10-Story Frame; Motion 1	96
4.3.6	Maximum Ductility Factors for Analysis Without Gravity - $\mu=4$; 10-Story Frame; Motion 2	97
4.3.7	Maximum Story Level Parameters for Analysis Without Gravity - $\mu=4$; 10-Story Frame; Motion 2	98
4.3.8	Maximum Ductility Factors for Analysis Without Gravity - $\mu=4$; 10-Story Frame; Motion 3	99

LIST OF FIGURES
(continued)

<u>Figure No.</u>	<u>Title</u>	<u>Page</u>
4.3.9	Maximum Story Level Parameters for Analysis Without Gravity - $\mu = 4$; 10-Story Frame; Motion 3	100
4.4.1	Maximum Ductility Factors for Earthquake Design - $\mu = 4$; 4-Story Frame; Motions 1, 2, 3	106
4.4.2	Maximum Story Level Parameters for Earthquake Design - $\mu = 4$; 4-Story Frame; Motions 1, 2, 3	107
4.4.3	Maximum Girder Ductility Factors for Earthquake Design - $\mu = 4$; 10-Story Frame; Motions 1, 2, 3	108
4.4.4	Maximum Column Ductility Factors for Earthquake Design - $\mu = 4$; 10-Story Frame; Motions 1, 2, 3	109
4.4.5	Maximum Story Level Parameters for Earthquake Design - $\mu = 4$; 10-Story Frame; Motions 1, 2, 3	110
4.5.1	Maximum Ductility Factors for Gravity and Factored Spectral Design - $\mu = 4$; 4-Story Frame; Motion 2	116
4.5.2	Maximum Story Level Parameters for Gravity and Factored Spectral Design - $\mu = 4$; 4-Story Frame; Motion 2	117
4.5.3	Maximum Girder Ductility Factors for Gravity and Factored Spectral Design - $\mu = 4$; 10-Story Frame; Motion 2	118
4.5.4	Maximum Column Ductility Factors for Gravity and Factored Spectral Design - $\mu = 4$; 10-Story Frame; Motion 2	119
4.5.5	Maximum Story Level Parameters for Gravity and Factored Spectral Design - $\mu = 4$; 10-Story Frame; Motion 2	120

LIST OF TABLES

<u>Table No.</u>	<u>Title</u>	<u>Page</u>
4.1.1	Average Ductility Factors for Gravity and Earthquake Design - $\mu = 4$; 4-Story Frame; Motions 1, 2, 3	72
4.1.2	Story Ductility Factors for Gravity and Earthquake Design - $\mu = 4$; 4-Story Frame; Motions 1, 2, 3	72
4.1.3	Average Ductility Factors for Gravity and Earthquake Design - $\mu = 4$; 10-Story Frame; Motions 1, 2, 3	73
4.1.4	Story Ductility Factors for Gravity and Earthquake Design - $\mu = 4$; 10-Story Frame; Motions 1, 2, 3	74
4.1.5	Average Ductility Factors for Gravity and Earthquake Design - $\mu = 4$; 18-Story Frame; Motion 2	75
4.1.6	Story Ductility Factors for Gravity and Earthquake Design - $\mu = 4$; 18-Story Frame; Motion 2	75
4.2.1	Average Ductility Factors for Gravity and Earthquake Design - $\mu = 2$; 4-Story Frame; Motion 2	84
4.2.2	Story Ductility Factors for Gravity and Earthquake Design - $\mu = 2$; 4-Story Frame; Motion 2	84
4.2.3	Average Ductility Factors for Gravity and Earthquake Design - $\mu = 2$; 4-Story Frame; Motion 2	85
4.2.4	Story Ductility Factors for Gravity and Earthquake Design - $\mu = 2$; 10-Story Frame; Motion 2	85
4.2.5	Average Ductility Factors for Gravity and Earthquake Design - $\mu = 2$; 18-Story Frame; Motions 2	86
4.2.6	Story Ductility Factors for Gravity and Earthquake Design - $\mu = 2$; 18-Story Frame; Motion 2	86

11
LIST OF TABLES
(continued)

<u>Table No.</u>	<u>Title</u>	<u>Page</u>
4.2.7	Normalized Maximum Ductility Factors for 4-Story Frame	87
4.2.8	Normalized Maximum Ductility Factors for 10-Story Frame	88
4.2.9	Normalized Maximum Ductility Factors for 18-Story Frame	89
4.3.1	Average Ductility Factors for Analysis Without Gravity - $\mu = 4$; 4-Story Frame; Motions 1, 2, 3	101
4.3.2	Story Ductility Factors for Analysis Without Gravity - $\mu = 4$; 4-Story Frame; Motions 1, 2, 3	101
4.3.3	Average Ductility Factors for Analysis Without Gravity - $\mu = 4$; 10-Story Frame; Motions 1, 2, 3	102
4.3.4	Story Ductility Factors for Analysis Without Gravity - $\mu = 4$; 10-Story Frame; Motions 1, 2, 3	103
4.4.1	Average Ductility Factors for Earthquake Design - $\mu = 4$; 4-Story Frame; Motions 1, 2, 3	111
4.4.2	Story Ductility Factors for Earthquake Design - $\mu = 4$; 4-Story Frame; Motions 1, 2, 3	111
4.4.3	Average Ductility Factors for Earthquake Design - $\mu = 4$; 10-Story Frame; Motions 1, 2, 3	112
4.4.4	Story Ductility Factors for Earthquake Design - $\mu = 4$; 10-Story Frame; Motions 1, 2, 3	113
4.5.1	Average Ductility Factors for Gravity and Factored Spectral Design - $\mu = 4$; 4-Story Frame; Motion 2	121
4.5.2	Story Ductility Factors for Gravity and Factored Spectral Design - $\mu = 4$; 4-Story Frame; Motion 2	121

LIST OF TABLES
(continued)

<u>Table No.</u>	<u>Title</u>	<u>Page</u>
4.5.3	Average Ductility Factors for Gravity and Factored Spectral Design - $\mu = 4$; 10-Story Frame; Motion 2	122
4.5.4	Story Ductility Factors for Gravity and Factored Spectral Design - $\mu = 4$; 10-Story Frame, Motion 2	122
A.1	Equivalent Shear Beam Properties for 4-Story Frame	134
A.2	Equivalent Shear Beam Properties for 10-Story Frame	134
B.1	Properties of 4-Story Frame for Section 4.1	136
B.2	Properties of 10-Story Frame for Section 4.1	136
B.3	Properties of 18-Story Frame for Section 4.1	137
B.4	Properties of 4-Story Frame for Section 4.2	137
B.5	Properties of 10-Story Frame for Section 4.2	138
B.6	Properties of 18-Story Frame for Section 4.2	138
B.7	Properties of 4-Story Frame for Section 4.4	139
B.8	Properties of 10-Story Frame for Section 4.4	139
B.9	Properties of 4-Story Frame for Section 4.5	139
B.10	Properties of 10-Story Frame for Section 4.5	140



CHAPTER 1 - INTRODUCTION1.1 General

Several sources exist for the dissipation of the energy transmitted to the base of a building structure which is subjected to earthquake ground motion. These include: the kinetic energy associated with the acceleration of the building mass, the strain energy due to elastic deformations of the structural components, internal work done by damping forces, the redundancy provided by non-structural elements, and nonlinear behavior. The degree of flexibility related to increasing the amount of external work dissipated in each of the alternative sources is described in what follows.

The mass is generally not considered as a design parameter. Live and dead loads are a function of the material, intended purpose, and architecture of the building which restricts the total weight to a relatively narrow range. Proportioning the strength of a structure to remain elastic in active seismic regions results in an uneconomical design, a fact which has been recognized by building codes. Damping mechanisms are not well understood, allowing limited control or certainty related to the amount of damping available. Current trends in engineering practice favor high-rise construction with few interior partitions and glass or other light exterior cladding. Faced with these difficulties, increased interest has developed within the past 15 years for the potential hysteretic dissipation of energy through ductile action of structural elements.

Investigations concerning inelastic response are characterized by the following:

- 1) Type of model used to idealize the dynamic behavior -either a shear beam model with nonlinear springs specified for an individual story, point hinge model to determine concentration of nonlinear deformations at the ends of a member, or fiber model to study the spread of plasticity.
- 2) The form of input base motion including pulse-type, recorded accelerograms, and simulated motions.
- 3) The complexity of the structural system in terms of number of degrees-of-freedom.
- 4) The force-deformation relationship governing the hysteretic action such as elastoplastic, bilinear, trilinear, Ramberg - Osgood, and stiffness degrading.
- 5) Whether the intention is to study the parameters influencing response, analysis techniques, or approaches to design.

In order to incorporate the knowledge acquired on the response of nonlinear systems into practical applications for building codes, safe and economical methods to design multistory buildings must be proposed and tested for their validity. Although several efforts have been directed toward determining the ductility requirements of typical buildings proportioned by existing philosophies (4, 12, 14, 15, 17, 20, 23), only recently has the control of nonlinear deformations to a specified level of ductility been attempted (7, 8, 10, 18, 19). This latter

capability is necessary to insure that ductility criteria established for the detailing of elements and joints are sufficient to prevent excessive damage or ultimate collapse.

1.2 Objectives and Scope

The primary objectives of the research reported herein were to develop and evaluate methods for predicting the nonlinear response of multi-degree-of-freedom systems subjected to earthquake ground motion. The basic design philosophy is an extension of simplified rules suggested by Newmark and Hall (11) which relate the response spectra of single-degree-of-freedom elastic and inelastic systems. The structural type is restricted to moment-resisting plane steel frames.

The process of selecting frame properties and proportioning member resistances is described in Chapter 2. A 4-, 10- and 18-story frame are under consideration having stiffness, mass and geometry typical of similar frames reported in the literature. Influences of the presence of gravity loads are examined and static analyses performed to obtain end forces due to a uniform distribution of dead and live load. Earthquake load effects are computed using an elastic modal analysis with an inelastic design response spectrum as input. Strength properties of members are expressed as a function of the applied design loads.

Chapter 3 presents the inelastic dynamic analysis procedures. Assumptions regarding the mathematical models and computer programs used to determine response are outlined. Output parameters are defined to characterize the nonlinear deformations at the member and story level. The earthquake excitation consists of 3 simulated motions, generated to

match the elastic design spectrum. Comparisons are made of the story level response of a 4- and 10-story frame with the point hinge and shear beam models.

Results of the behavior of the inelastic designs are detailed in Chapter 4. Performance of the proposed procedure is assessed in terms of nonlinear deformations occurring at the ends of individual columns and girders, and the forces and displacements associated with each story. Effects of the design ductility level, including gravity load in the design and analysis, and factoring spectral forces are considered.

Chapter 5 contains a summary of conclusions and recommendations concerning the information gained and potential areas for expanded research, respectively, in developing methods for the inelastic design of multi-degree-of-freedom systems.

CHAPTER 2 - FRAME SELECTION AND DESIGN2.1 Description of Frames

Properties of the 4-, 10-, and 18-story frames employed in the investigation of design procedures are depicted in Figures 2.1.1, 2.1.2, and 2.1.3, respectively. The 4- and 10-story frames have been used by Luyties, Anagnostopoulos and Biggs in a portion of a previous report (10).

The configurations of the 3 frames are similar, each consisting of a regular rectangular plane grid in elevation which is symmetric about its vertical centerline and has 3 equal spans at 16 ft. 8 in. Story heights are 12 ft. above the 15 ft. lower story. The selection of the total number of stories for the 3 frames is intended to represent the range of typical low- to high-rise steel buildings.

In all frames, the distribution of stiffness decreases at intervals of one or several stories with an increase in height, generating an approximately linear variation. Reduction in member size reflects conventional economic considerations for optimum utilization of material. Relative moments of inertia of columns and girders and areas of columns govern the extent of taper and have been determined based on comparisons of similar frame designs published in the literature. Areas are not specified for girders due to the relative insignificance of their axial deformations.

The reference stiffness, I , coincident with the uppermost exterior column, is adjusted to give preselected values of the fundamental periods of vibration. Period values of 0.47 sec., 1.37 sec., and 2.92 sec. were designated for the 4-, 10-, and 18-story frames, respectively,

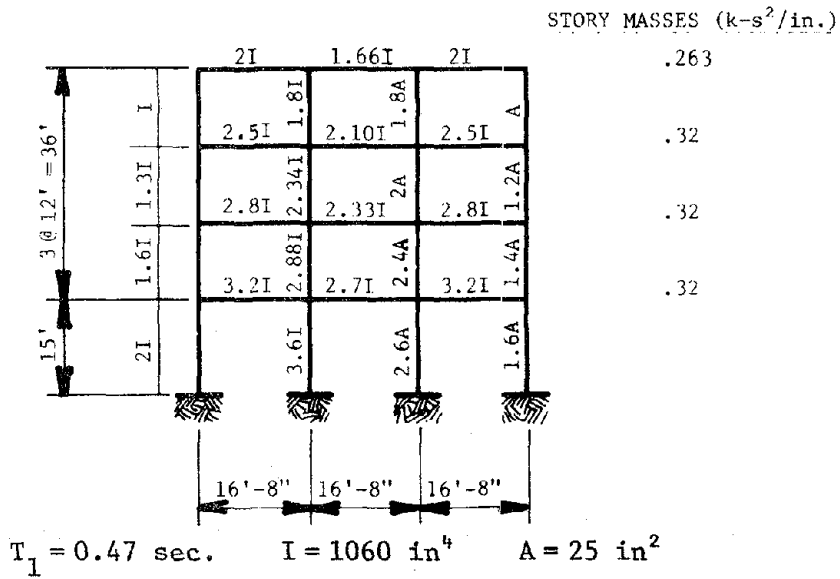


FIGURE 2.1.1 - PROPERTIES OF FOUR STORY FRAME

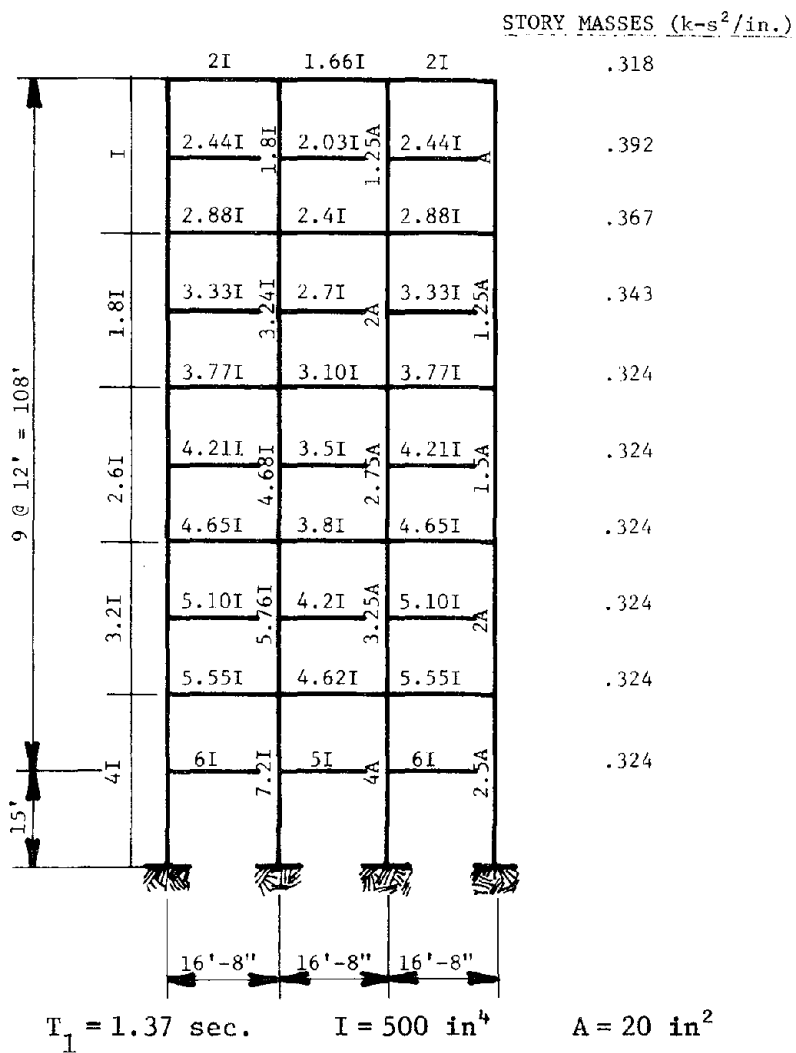
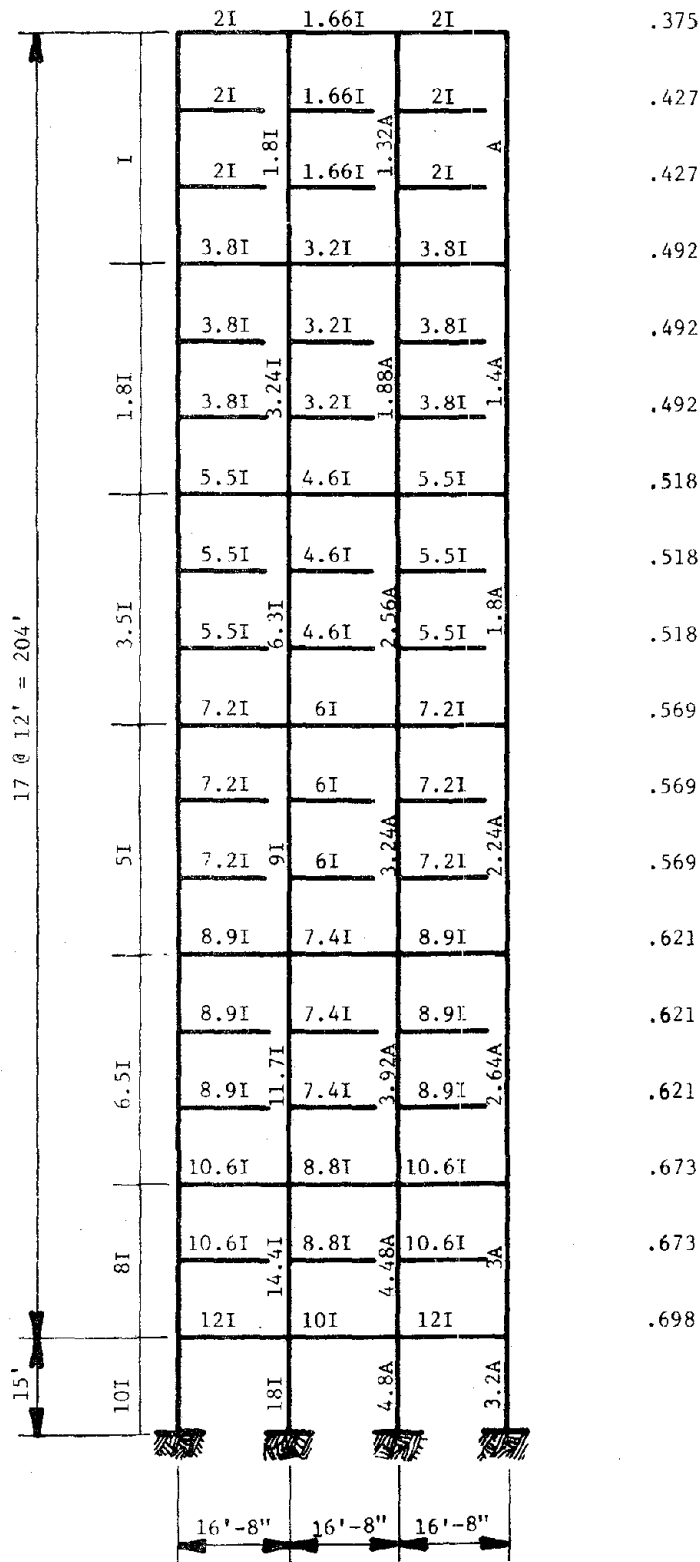


FIGURE 2.1.2 - PROPERTIES OF TEN STORY FRAME

STORY MASSES (k-s²/in.)



$T_1 = 2.92 \text{ sec.}$ $I = 300 \text{ in}^4$ $A = 25 \text{ in}^2$

FIGURE 2.1.3 - PROPERTIES OF EIGHTEEN STORY FRAME

to be within the range of experimental period determinations for moment-resisting steel frame buildings of the same height (6).

Story masses correspond to full dead plus live load, without load factors, distributed uniformly over the 3 spans.

It is possible to determine gravity and earthquake elastic load effects given the mass, stiffness and geometry of the frames described herein, as discussed in Sections 2.2 and 2.3. Subsequently, the individual member strength can be expressed as a function of the design load effects, independent of actual structural shapes (e.g., WF sections), as shown in Section 2.4.

2.2 Gravity Load Effects

The sophistication of the mathematical models employed in investigations of the nonlinear dynamic behavior of buildings has generally influenced the extent of incorporation regarding the effects of vertical dead and live load. Numerous studies, based on lumped parameter systems of the shear beam type, have necessarily neglected gravity loads due to the degree of idealization in which only story level response is evaluated (1, 2, 3, 7, 12, 13, 20, 24). In order to justify the lack of vertical load considerations, the available resistance for lateral earthquake loads must be assumed to be independent of the gravity load demands. Initial advancements to more complex member level models only provided for lateral loading conditions; Clough and Benuska (23) included the effective horizontal forces resulting from the displacement of static vertical loads, whereas Goel and Berg (17) omitted gravity effects entirely. The motivation to more adequately represent actual building performance has led to recently expanded capabilities to simulate the presence of static vertical loads (4, 5, 8, 10, 16, 18, 19, 26).

Significant aspects of static gravity loads, which influence the response of inelastic systems, are listed below.

- 1) Axial forces reduce the plastic moment capacity of column elements in connection with a yield interaction surface.
- 2) Initial end moments alter the mechanisms to first yield by increasing or decreasing the plastic moment capacity of a

cross-section available to resist earthquake moments depending on the sense of the applied loads (e.g., if the gravity and earthquake moments are of the same sign the capacity is reduced to first yield and the reverse condition occurs if the moments are of opposite signs). The importance of this phenomenon relates primarily to the girders where the larger static end moments are located.

- 3) The mass of the structure, which is a function of the dead and live load, enters directly into the inertial terms of the equations of motion.
- 4) The $P-\Delta$ effect introduces additional lateral forces necessary to sustain equilibrium. This occurs as sideways displacement transforms the relationship of the frame geometry to the direction of action of gravity loads.

The latter effect is not taken into account, herein, either through an increase in design shear or in the dynamic analysis.

The first two factors act to alter strength capacities of cross-sections, thereby influencing the pattern of yielding mechanisms, and are related to the magnitude and position of gravity loading. Member end forces are calculated from a uniform distribution of load over the 3 equal spans typical to all test frames. The total load corresponds to the story masses (as presented in Section 2.1) which remain constant throughout all design and analysis procedures.

The computer program, STRUDL (31), was used to compute static member forces by a standard stiffness analysis.

2.3 Earthquake Load Effects

2.3.1 Inelastic Design Spectra

Earthquake loading represents an extremely uncertain event, both in terms of time and location of occurrence and ensuing characteristics such as intensity, duration, frequency content, and number of strong motion pulses. An elastic design response spectrum reported by Newmark and Hall (11) was adopted to fully describe the potential seismic hazard for the sites of all frames under study.

The elastic spectrum has been constructed, utilizing a tripartite logarithmic format, in Figures 2.3.2 and 2.3.3 for 5% critical damping. Corresponding maximum ground motion (not shown) parameters have been scaled to an acceleration of 0.33 g, velocity of 15.84 in/sec, and displacement of 11.88 in. Application of the recommended amplification factors for 5% damping yields the bounds defining the elastic response spectrum: 0.86 g, 30.1 in/sec, and 16.63 in.

Approximate rules have been proposed by Newmark and Hall (11) and are used here to produce inelastic acceleration and displacement spectra from the design elastic spectrum. Investigations of the maximum deformations of single-degree-of-freedom elastic and elastoplastic systems subject to various types of input motion form the basis for these simplified procedures (1, 2, 3, 24, 25). Figure 2.3.1 illustrates the relationship between the three spectra as a function of frequency. Line DVAA₀ indicates the elastic response spectrum. The amplified acceleration, velocity, and displacement regions are symbolized by

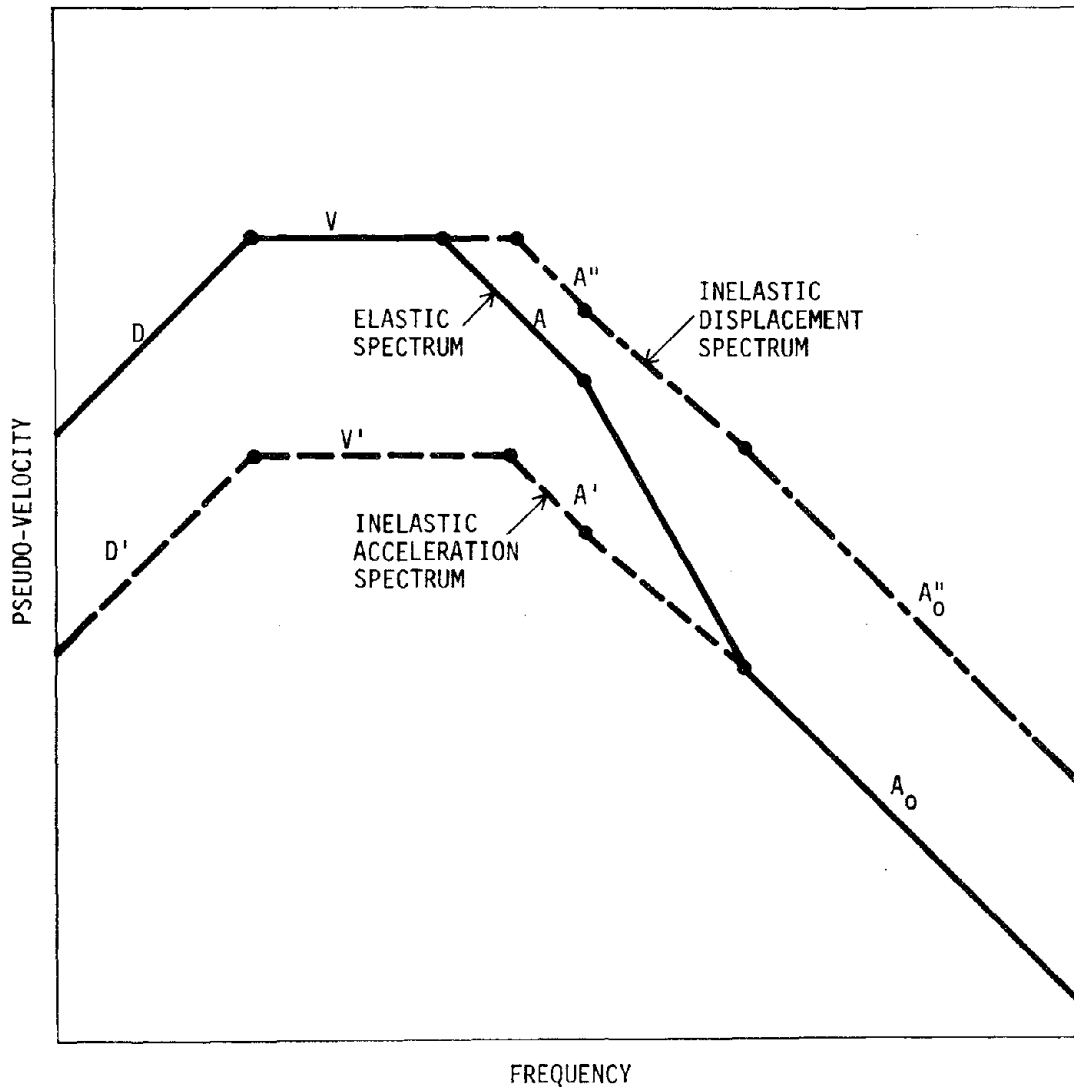


FIGURE 2.3.1 - ELASTIC AND INELASTIC DESIGN SPECTRA -
 AFTER NEWMARK AND HALL
 Redrawn from Reference 11

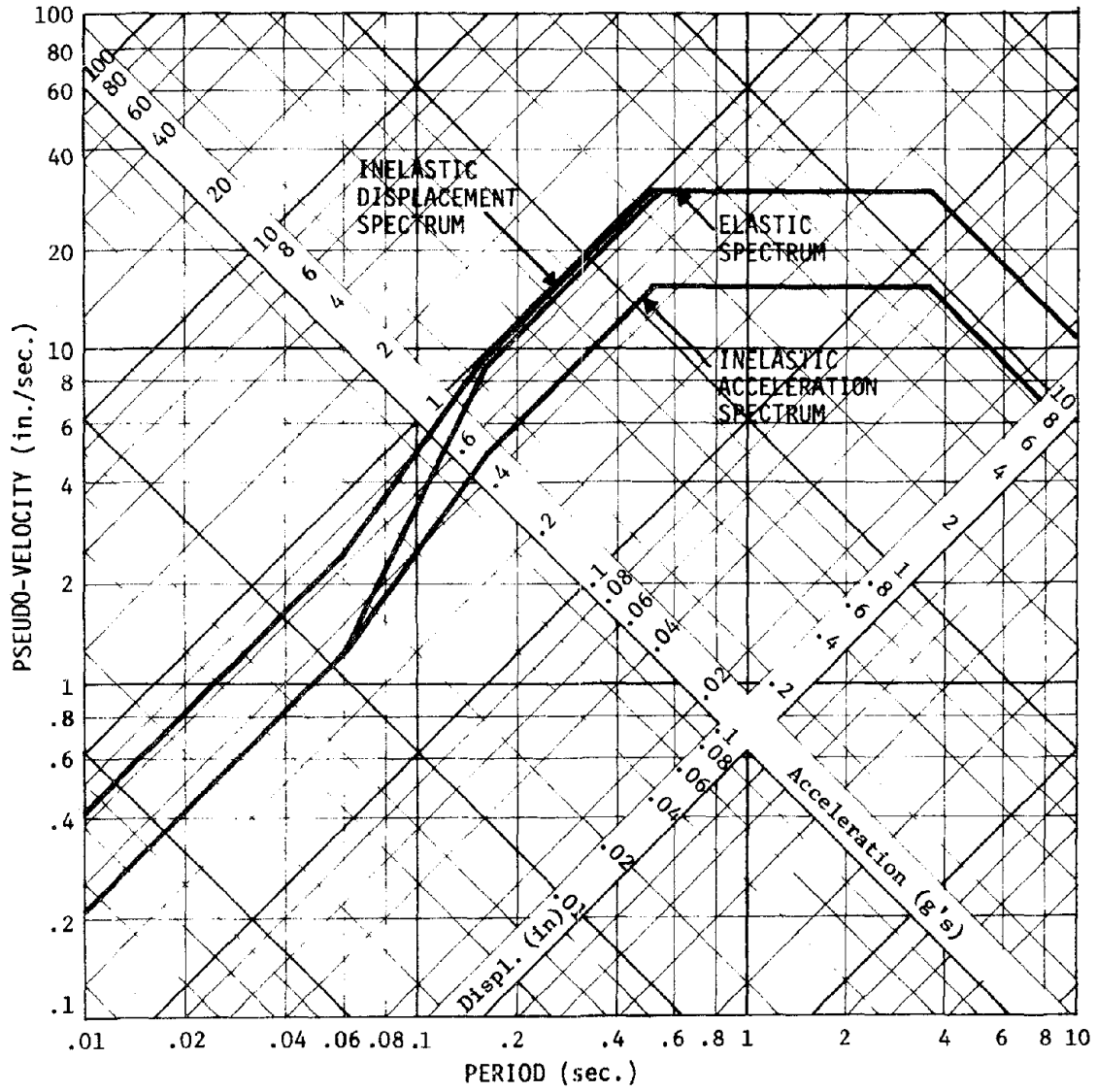


FIGURE 2.3.2 - ELASTIC AND INELASTIC DESIGN SPECTRA, $\mu = 2$

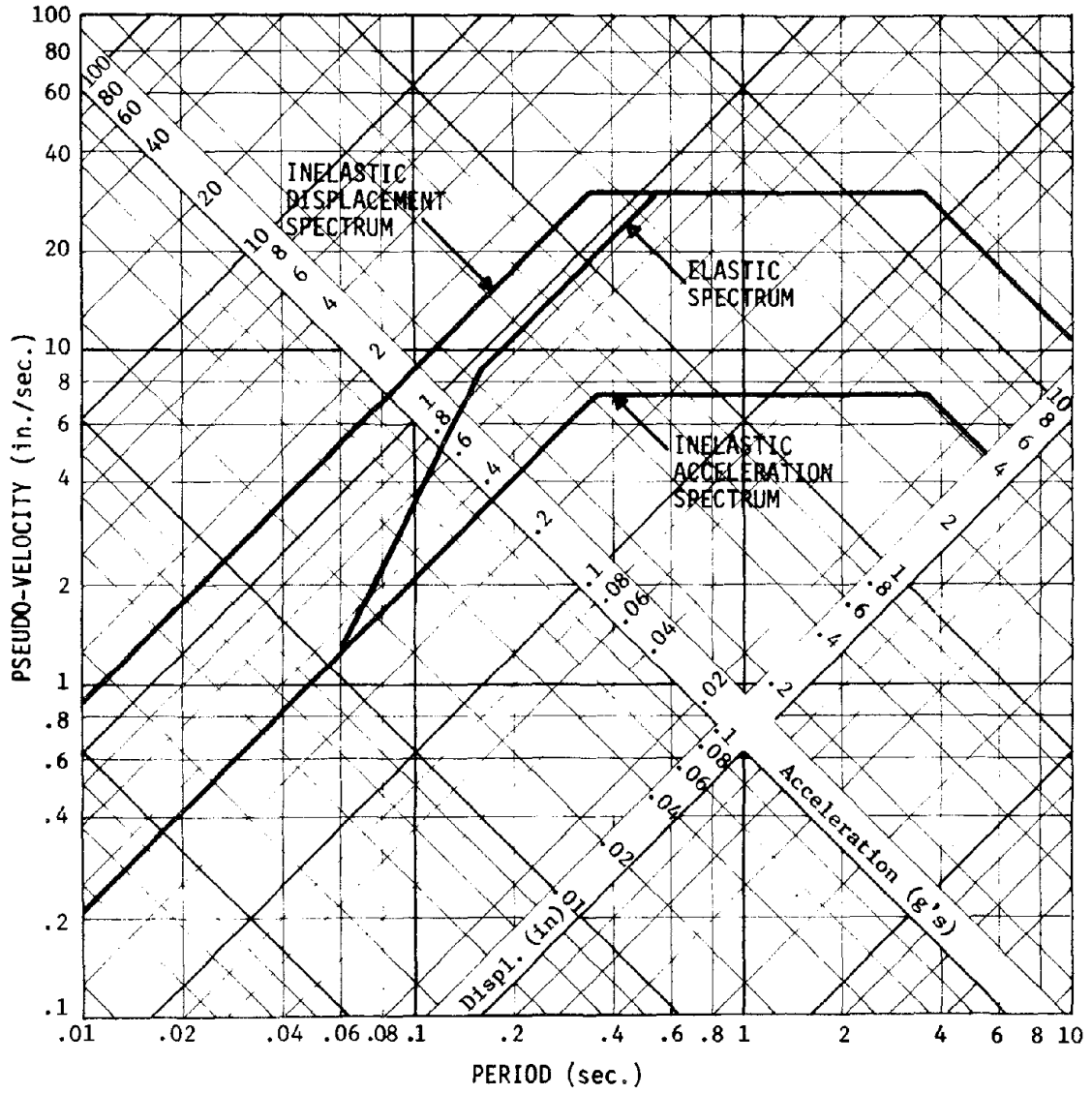


FIGURE 2.3.3 - ELASTIC AND INELASTIC DESIGN SPECTRA, $\mu = 4$

A, V, and D, respectively. Frequencies at the intersection of segments comprising the different curves which are common among spectra are identified by blackened circles.

In the high frequency range, the inelastic acceleration or yield displacement spectrum (D'V'A'A₀) coincides with the elastic spectrum (segment A₀) which is bounded by the maximum ground acceleration. Segments A' and A are parallel, inclined at 45° and differ by a factor derived by requiring that the energy absorption associated with the resistance functions of comparable elastic and elastoplastic systems (i.e., having the same mass, damping and initial stiffness) be equivalent. Referring to Figure 2.3.4:

$$\frac{1}{2}(u_y)(K u_y) + (u_2 - u_y)(K u_y) = \frac{1}{2}(u_1)(K u_1)$$

and by definition $u_2 = \mu u_y$

$$\frac{u_y}{u_1} = \frac{1}{\sqrt{2\mu - 1}}$$

where μ = ductility factor; K = initial stiffness; u_y = yield deformation of elastoplastic system; u_1 = absolute maximum deformation of elastic system; u_2 = absolute maximum deformation of elastoplastic system.

Section D'V' is parallel and diminished by the ductility factor with respect to DV. The fifth and unlabeled segment is an acceleration transition zone defined by connecting the endpoints of A' and A₀.

The maximum inelastic displacement spectrum (DVA"A₀"), consistent with the definition of ductility, follows the shape of the acceleration

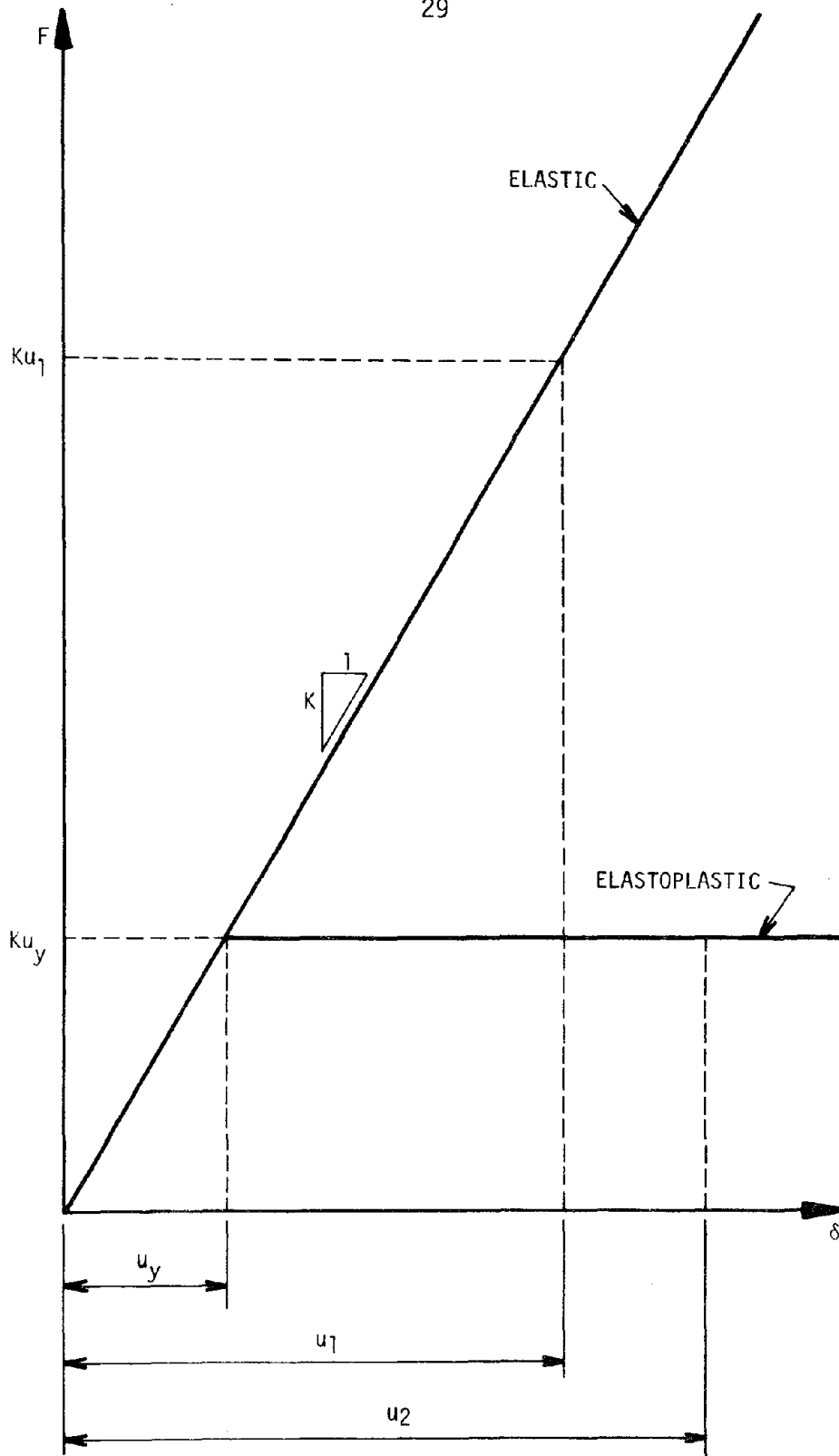


FIGURE 2.3.4 - ELASTIC AND ELASTOPLASTIC RESISTANCE-DEFORMATION FUNCTIONS

spectrum magnified by μ for all frequencies. In the low frequency region, indicative of flexible systems, the elastic and inelastic displacements are considered the same.

Inelastic design spectra, obtained by applying the Newmark and Hall rules to transform the design elastic response spectrum (previously detailed), are shown in Figures 2.3.2 and 2.3.3 for two different levels of ductility (i.e., $\mu = 2$ and $\mu = 4$).

2.3.2 Modal Analysis

Extensions of these simple concepts to the design of multi-degree-of-freedom (MDOF) structures have been examined in a limited number of studies (7, 8, 9, 19). The state-of-the-art in response spectrum methods for elastic design, being firmly established and familiar to structural engineers, suggests that a convenient and approximate approach to the treatment of complex nonlinear systems may be by performing a modal analysis with an inelastic spectrum. Although modal procedures are appropriate for their practicality, provisions for code implementation have not been advanced due to the lack of sufficient research.

Major criticisms of this methodology are inherent in the incongruent mixture of elastic and inelastic behavior. Decomposition of the solution into a set of uncoupled modal equations and application of the principle of superposition to produce the response by combining the effects of a desired number of modes is not valid for nonlinear systems. Confronted with the alternative of executing multiple time

integration analyses in a costly and time consuming iterative design scheme, modal analysis is selected for use in the prediction of non-linear behavior. Adequacy of this initial assumption can only be determined by testing frames proportioned utilizing elastic modal procedures which are outlined in what follows.

Mode shapes and frequencies are computed by solution of the following eigenvalue problem (9):

$$\left\{ [K]_L - \omega_n^2 [M]_D \right\} \{ a_n \} = 0$$

where $[K]_L$ = lateral stiffness matrix; $[M]_D$ = diagonal matrix containing masses lumped at each floor level; ω_n = natural frequency of mode n (eigenvalues); $\{ a_n \}$ = shape for mode n (eigenvectors).

Although higher modes are sometimes neglected if their contributions are insignificant, all calculations of response parameters, performed herein, include the total number of modes corresponding to the number of masses lumped at the story levels.

The modal displacement with respect to the ground is expressed as:

$$\{ u_n \} = \Gamma_n \frac{S_a}{\omega_n^2} \{ a_n \}$$

where $\{ u_n \}$ = vector displacements for mode n; Γ_n = modal participation factor for mode n = $\{ a_n \}^T [M]_D / \{ a_n \}^T [M]_D \{ a_n \}$; S_a = ordinate of the inelastic acceleration spectrum at ω_n .

The remaining vertical and rotational degrees-of-freedom (denoted by the subscript r) are obtained from the following matrix statement.

$$[K] \{\Delta\} = \begin{bmatrix} [K_{rr}] & [K_{ru}] \\ [K_{ur}] & [K_{uu}] \end{bmatrix} \begin{Bmatrix} \{r\} \\ \{u\} \end{Bmatrix} = \begin{Bmatrix} \{F_r\} \\ \{F_u\} \end{Bmatrix} = \{F\}$$

in which $[K]$ = total stiffness matrix; $\{\Delta\}$ = vector of joint deformations; $\{F\}$ = vector of joint loads. The vector $\{F_r\}$ is set equal to zero in the condensation scheme for determining the lateral stiffness matrix.

$$[K]_L = [K_{uu}] - [K_{ur}][K_{rr}]^{-1}[K_{ru}]$$

The unknown joint deformations are

$$\{r\} = -[K_{rr}]^{-1} [K_{ru}] \{u\}$$

where the vector of horizontal displacements has been computed for each mode.

For each vector of joint deformations associated with a given mode n , member forces are derived utilizing stiffness matrix conversions from the global to local reference frames. Maximum design values of response measures (e.g., member forces, lateral displacements), composed of contributions from the uncoupled modal responses, are evaluated by the square root of the sum of the squares rule (SRSS).

All elastic modal analyses were performed with the computer program, APPLE PIE (29).

2.4 Determination of Member Strength

The end forces obtained by the elastic static and dynamic analyses are shown in Figure 2.4.1. The ultimate strength of a member is expressed as a function of these design forces, independent of actual structural shapes, as described below. Strain hardening effects, buckling in compression members, shear forces, axial forces in the girders, and load factors are not considered.

This investigation seeks to develop procedures which yield satisfactorily inelastic behavior under the design conditions; hence simulated motions were generated to match the elastic spectrum (Section 3.3). Load factors which are intended to provide some level of safety against severe load combinations above the design conditions, are not applicable.

Girder capacities are determined as

$$M_y = \max \{ M_{EQ} \text{ or } wl^2/8 \}$$

where M_y = yield moment; M_{EQ} = spectral moment; w = uniform dead plus live load; l = span length. Gravity moments, M_{GR} , are not added to increase the resistance of girders due to the effect discussed in Section 2.2. After first yield, static end moments do not alter the plastic capacity, allowing the section to be proportioned only for lateral load. Evidence of the temporary nature of the influence of gravity loads on response has been reported by Anderson and Gupta (18). Time histories of plastic rotations indicate that after a brief interval in which the initial yield mechanisms form, similar hinge rotations occur concurrently at both ends of a girder typical of behavior associated with earthquake loads acting alone.

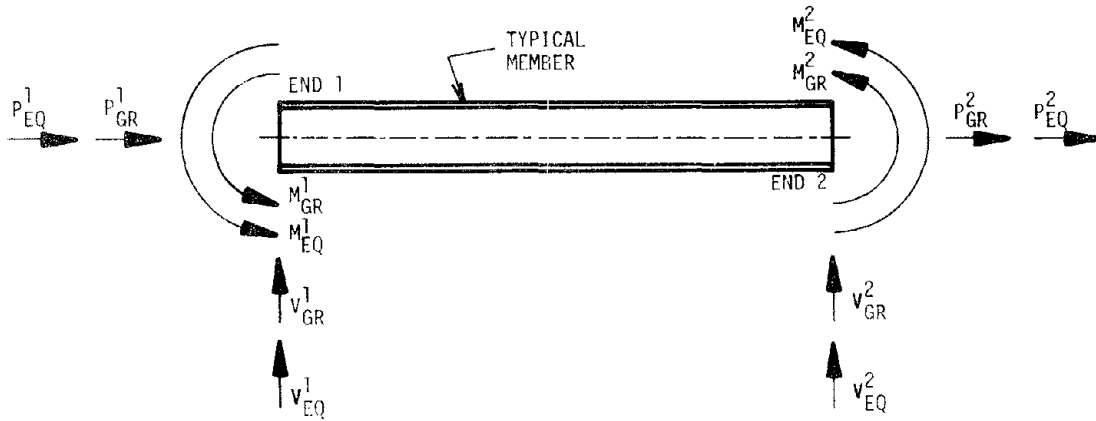


FIGURE 2.4.1 - MEMBER END FORCES RESULTING FROM GRAVITY AND EARTHQUAKE LOADS

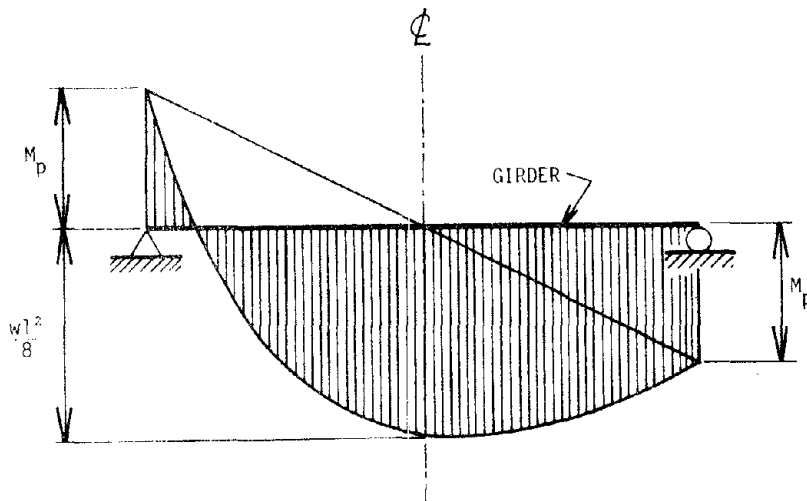


FIGURE 2.4.2 - MOMENT DIAGRAM FOR GIRDER HINGED AT BOTH ENDS

The second condition, that the capacity be at least $wl^2/8$, controls only in girders within the top floors of a frame. This is enforced to reduce the possibility of the formation of a plastic hinge at midspan of a girder which is hinged at both ends as shown in Figure 2.4.2. Although the location and value of the maximum ordinate for the parabolic moment diagram depend on the relative magnitude of the section capacity and the uniform load, the simple beam approximation is adopted for convenience.

Column resistances are based on AISC formula 2.4.3 to account for axial-flexural interaction (22).

$$\frac{P}{P_y} + \frac{M}{1.18 M_y} \leq 1.0 \quad ; \quad M \leq M_y$$

Assuming a constant ratio of plastic modulus, Z , to area, A , for all sections equal to 6,

$$M_y \geq 6P + M/1.18 \quad ; \quad M_y \geq M$$

$$P_y = M_y/6$$

where P_y = plastic axial capacity. The applied design moment, M , is taken as

$$M = \max \left\{ M_{EQ} \quad \text{or} \quad M_{GR} \right\}$$

which is consistent with the concept that static end moments only alter the capacity of a member prior to first yield. Due to the permanent reduction in plastic moment capacity caused by gravity axial forces, the design load, P , is given by

$$P = P_{EQ} + P_{GR}$$

End moments, obtained from the elastic analyses, differ in absolute value at both ends of the same member. Luyties, Anagnostopoulos and Biggs (10) have found that using an average of the end moments may produce a more favorable distribution of resistance in terms of inelastic response compared to proportioning the member based on the maximum moment at either end. Based on these results, the design moments used in the expressions above are

$$M_{EQ} = (M_{EQ}^1 + M_{EQ}^2)/2$$

$$M_{GR} = (M_{GR}^1 + M_{GR}^2)/2$$

where the superscripts refer to ends 1 and 2 as in Figure 2.4.1.

3.1 Mathematical Models for Determination of Inelastic Dynamic Response

3.1.1 Point Hinge Model

The equations of motion for a multi-degree-of-freedom system subjected to earthquake ground motion is:

$$[M]_D \{\ddot{u}\} + [C] \{\dot{u}\} + [K]_L \{u\} = -[M]_D \ddot{y}_g$$

where $[M]_D$ = diagonal mass matrix, $[C]$ = damping matrix, $[K]_L$ = lateral stiffness matrix, u = relative displacement with respect to ground, \ddot{y}_g = input ground acceleration. The solution of these equations for nonlinear response, in which the stiffness is variable and the behavior cannot be uncoupled into modal contributions, requires the use of numerical time integration techniques. The computer program, FRIEDA, developed by Aziz (26) and subsequently revised by Anagnostopoulos, Roesset, and Luyties (10, 30) was utilized to perform the inelastic dynamic analyses of multimember plane frame structures.

Assumptions and aspects regarding the method of analysis are summarized as follows:

- 1 - Shear deformation is neglected.
- 2 - Axial deformation in the girders is neglected.
- 3 - Each joint has lateral, vertical and rotational degrees-of-freedom.
- 4 - Masses are lumped at the floor levels.
- 5 - The earthquake excitation is due entirely to horizontal components of ground motion which are parallel to the frame.

- 6 - Member behavior is modelled by an elastic and elastoplastic component acting in parallel, referred to as a two-component or Clough model (14, 15, 23). Superposition of the components produces an element with a bilinear moment-rotation relationship governing the hysteretic action at each end, as shown in Figure 3.1.1. The second slope or strain-hardening branch has 5% of the initial stiffness. The more general term, point-hinge model, refers to the fundamental concept of restricting plasticity to concentrated hinges at the ends of a member when the yield moment is exceeded.
- 7 - Axial - flexural interaction is accounted for by altering the yield moment of a member in each time step as a function of the axial load. The yield interaction surface corresponds to that recommended in AISC formula 2.4-3 (22):

$$\frac{P}{P_y} + \frac{M}{1.18M_y} \leq 1.0; \quad M \leq M_p$$

$$\frac{M}{M_y} = 1.0; \quad \frac{P}{P_y} \leq 0.15$$

where P = applied axial load; M = applied moment; P_y = plastic axial capacity; M_y = yield moment.

- 8 - Overshooting errors occur when the yielded capacity of a section is exceeded in any given time step. In order to compensate for this equilibrium unbalance, correction forces are applied as joint loads in the next time step. Referring to the notation of Section 2.3.2, the form of computation

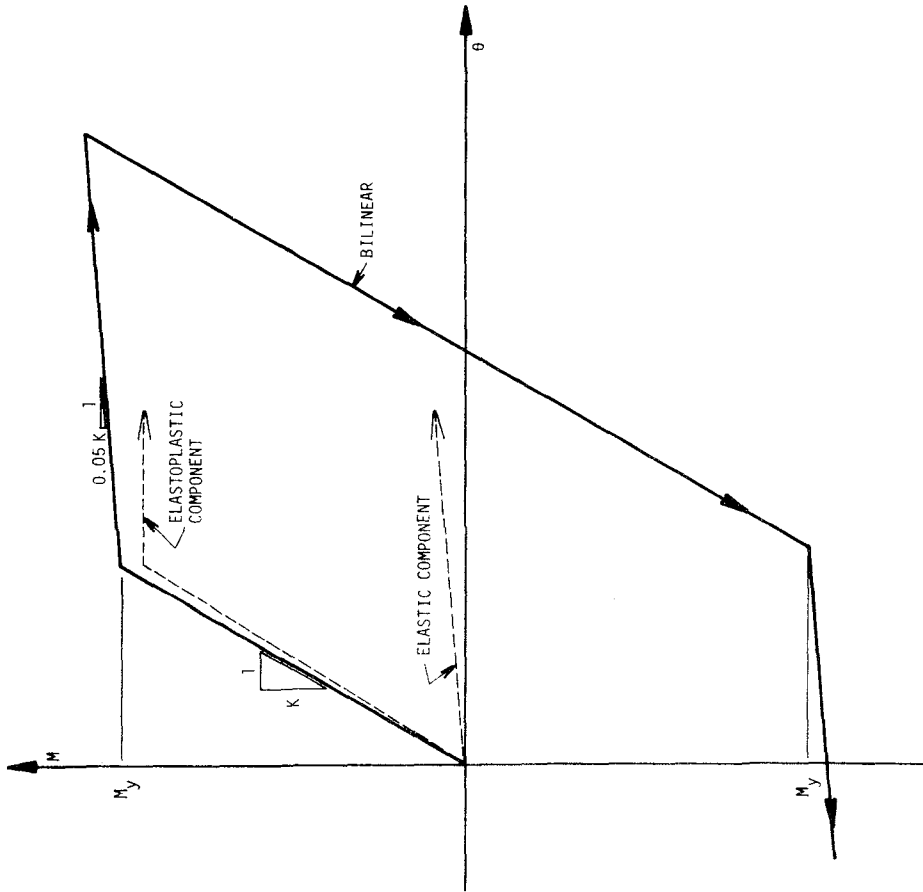


FIGURE 3.1.1 - MOMENT-ROTATION RELATIONSHIP AT THE END OF A MEMBER

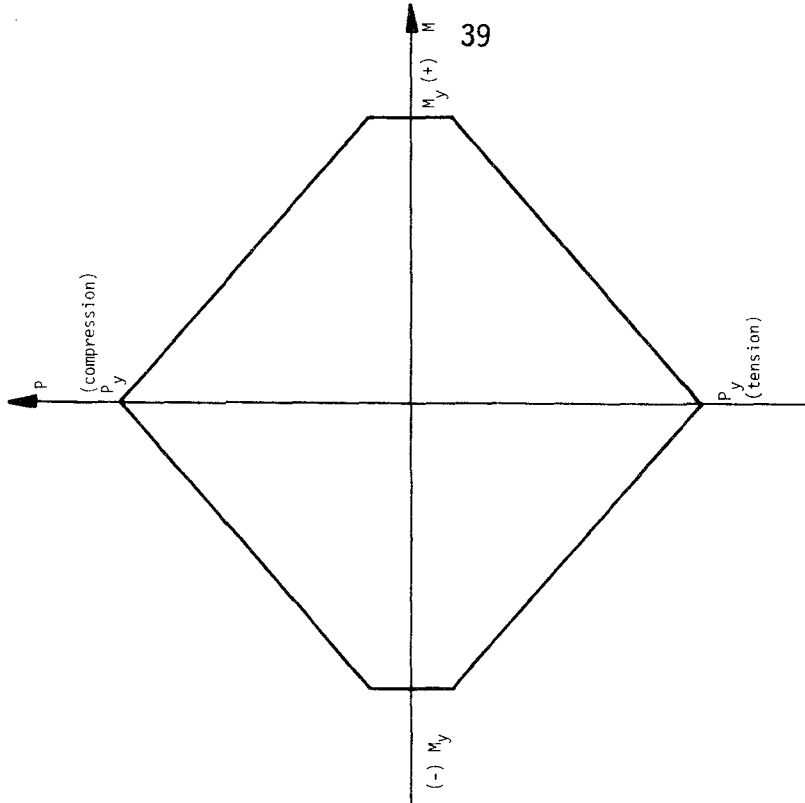


FIGURE 3.1.2 - COLUMN INTERACTION DIAGRAM

is (10):

$$[K]_L \{u\} = \{F_u\} - [K_{ur}] [K_{rr}]^{-1} \{F_r\}$$

where $\{F_r\}$ = column of applied loads consisting of terms corresponding to the sum of the moments in excess of the yielded capacity for all sections at a particular joint.

- 9 - The numerical integration assumes a constant velocity in each time step following the first step in which a Runge - Kutta method is used for initialization (26).
- 10 - The time step for all analyses is 0.01 sec, which is within a range 1/5 to 1/7 of the smallest natural period for the 3 frames.
- 11 - A constant 5% critical damping is specified in each mode. The damping matrix, $[C]$, which permits this option is (26):

$$[C] = [M]_D [\phi] [B] [\phi]^T [M]_D$$

where $[\phi]$ = matrix composed of system eigenvectors which is normalized as $[\phi]^T [M]_D [\phi] = 1$; $[B]$ = diagonal matrix containing terms of the form $2\beta_i \omega_i$; β_i = percent damping in mode $i = 5\%$.

- 12 - Static fixed end member forces are input to simulate the presence of gravity loads.
- 13 - The P - Δ effect is not considered.
- 14 - The base of the frames is fixed representing a rigid foundation.

15 - Joint size effects are neglected; all dimensions are centerline to centerline.

Details concerning the incremental tangent stiffness formulation, yield conditions for the two-component model, and numerical techniques can be found in the references cited in this section.

3.1.2 Shear Beam Model

The shear beam model has been utilized extensively in research (1, 2, 3, 7, 12, 13, 20, 24) due primarily to its inexpensive costs. Comparisons between the response of point hinge and shear beam models are presented in Section 3.4 to investigate the relationship of story level parameters.

As the term implies, this model considers that the lateral distortion of the structure is of the shear type. Floor systems, which are assumed infinitely rigid in their horizontal planes, remain parallel. Similar to the point hinge model, masses are lumped at the floor levels, only horizontal components of ground motion are input, a constant velocity routine is employed for the numerical integration and the same form for the damping matrix is adopted. The structure is idealized as a close-coupled system with lumped masses connected by nonlinear springs representing the force-deformation behavior of each individual story.

The computer program, STAVROS, implemented by Anagnostopoulos (20), was used for inelastic analyses with the shear beam model.

3.2 Measures of Inelastic Response

3.2.1 Member Level Parameters

The concept of an inelastic design depends on the capacity of element cross-sections to sustain load subsequent to yielding. Nonlinear deformations of the structural members function as the principal source for the energy dissipation of earthquake forces. Ductility factors, commonly employed to evaluate the extent of inelastic action, express the ratio of the maximum value of a deformation parameter to its yield limit value. Two definitions of ductility at the member level have attained general usage in the literature; one is based on rotations and the other on curvatures. Other forms of component ductility related to energy dissipation and cyclic deformation (5) have been proposed, but are not considered here.

The rotational ductility is (14, 15, 23):

$$\mu_R = \frac{\theta_y + \theta_i}{\theta_y} = 1 + \frac{\theta_i}{\theta_y}$$

where θ_i = maximum plastic hinge rotation at the end of a member during any inelastic excursion; $\theta_y = M_y L / 6EI$ = yield limit rotation corresponding to a girder deformed by the application of anti-symmetric yield moments, M_y , as depicted in Figure 3.2.1. The yield rotation applies only to this simple loading condition; it is actually a function of the behavior of the entire structure. The presence of gravity loads, unsymmetrical end restraints or irregular geometry decrease the accuracy of the assumed anti-symmetrical deformed shape. The rotational ductility represents the maximum plastic rotation at a section normalized by a constant factor

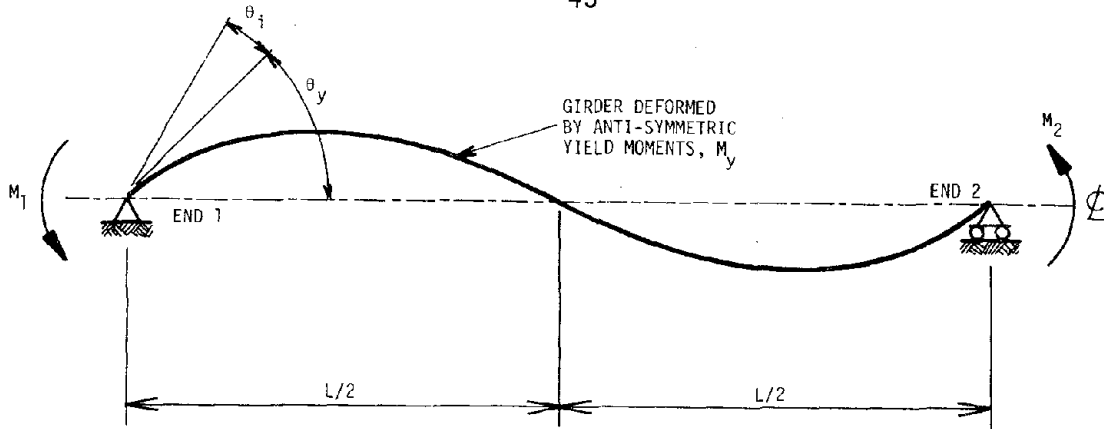


FIGURE 3.2.1 - DEFINITION OF ROTATIONAL DUCTILITY

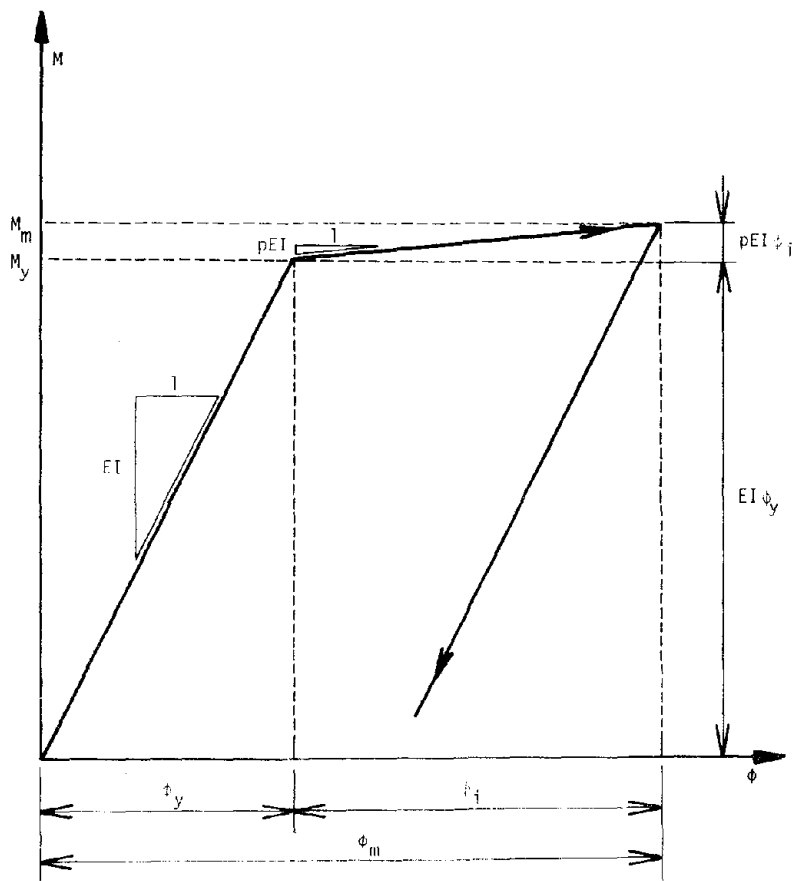


FIGURE 3.2.2 - DEFINITION OF MOMENT DUCTILITY

which depends on the yield moment. Although this definition may not precisely determine yield conditions, it permits useful comparisons of relative inelastic action. Plastic hinge rotations may be back-figured for evaluation with respect to experimental data compiled for similar sections.

The value of μ_R is taken as unity when no yielding occurs.

Although the second factor is based on curvatures at the end of a member, it is referred to as moment ductility, μ_M , due to the form of computation (4, 5, 8, 18).

$$\begin{aligned}\mu_M &= \frac{\phi_m}{\phi_y} = 1 + \frac{\phi_i}{\phi_y} \\ &= 1 + \left(\frac{M_m - M_y}{p EI} \right) \left(\frac{EI}{M_y} \right) \\ &= 1 + \frac{M_m - M_y}{p M_y}\end{aligned}$$

where ϕ_m = maximum curvature; ϕ_y = yield limit curvature; M_m = maximum moment; M_y = yield moment; E = modulus of elasticity; I = moment of inertia of cross-section; p = percent second slope. Figure 3.2.2 shows a typical moment - curvature relationship.

In a given analysis, the yield moments and percent second slope are prescribed constants for the girders. The maximum moments occurring at the left and right ends in the positive and negative directions during the time history are stored to allow computation of the 4 ductility values at the completion of the integration process. Column yield moments change as a function of the interaction diagram requiring the calculation of the moment ductility in each time step. The maximum

value at the top and bottom of a column is obtained. The factor derived from moment - curvature relationships appears more reasonable than rotational ductility since the yield limit is not denoted by an arbitrary constant.

Values less than one are possible if a section remains elastic. Under this condition, the moment ductility is defined as the ratio of the maximum moment to the yield moment of the member.

The parameters selected to characterize the nonlinear member response are the following:

- 1) Maximum exterior and interior girder ductility in a particular floor.
- 2) Maximum exterior and interior column ductility in a particular story.
- 3) Average of maximum ductility factors over height.
- 4) Average of girder ductility factors for all cross-sections in a particular floor.
- 5) Average of column ductility factors for all cross-sections in a particular story.

Both definitions of ductility, moment and rotational, are reported for comparison in each of the five categories.

Structural element capacities for ductile action are assumed unlimited for the purpose of analysis. The observed inelastic deformations represent ductility requirements which must be provided by proper detailing of the members in order to sustain the integrity of the frame.

3.2.2 Story Level Parameters

Measures of subassemblage response, chosen to describe the earthquake imposed deformations, are summarized below.

- 1) Maximum lateral displacement of a given floor with respect to the support.
- 2) Maximum story distortions or interstory displacements.
- 3) Maximum story shear.
- 4) Maximum story bending moment or overturning moment.
- 5) Maximum story ductility factor.

The first and second parameters are significant with relation to the amount of damage experienced by structural and non-structural elements, respectively. Examination of maximum story shears and bending moments allows comparisons with the elastic design values. The story ductility factor, μ_S , indicates the degree of inelastic action associated with the maximum story distortion. Concentrations of yielding in a particular story may bring about imminent collapse if the demand on ductility exceeds the capacity.

The conventional definition of ductility, common to investigations conducted with shear beam models, is the ratio of the maximum to yield interstory displacement. This interpretation applies to the level of ductility experienced by single-degree-of-freedom systems in the formulation of the simplified rules which have been prescribed for the construction of the design inelastic displacement and acceleration spectra (1, 2, 3, 11, 24, 25). The force - deformation relationships for the

nonlinear springs (e.g., elastoplastic, bilinear, trilinear) connecting the story masses in a shear beam model are specified to possess clearly defined yield points and to be composed of straight line segments.

The computation of μ_S is not convenient nor obvious for complex hysteretic systems in which the member end moment - rotation relationship is designated. The difficulties involved have impeded prevalent use of the μ_S in the evaluation of inelastic designs modelled at the member level. Bertero and Kamil have reported a displacement ductility factor for a story (8); the yield displacement was obtained by an inelastic static analysis and the maximum interstory displacement was obtained from the inelastic dynamic analysis. The resistance function produced by an inelastic static analysis is sensitive to the distribution over height of applied forces or imposed deformations, the rate of monotonically increasing load or displacement increments, and the interpretation of the resulting curvilinear form (27).

The force - deformation behavior observed during the inelastic dynamic analysis forms the basis of an approximation for μ_S developed herein. Figure 3.2.3 shows a typical computer plot of interstory shear versus interstory displacement. A bilinear relationship is constructed by the intersection of two lines; one is drawn through the origin parallel to the initial slope and the other estimates the bound of ultimate slope. The yield displacement obtained in this manner corresponds to the yield shear had the structure remained elastic and is subject to the inaccuracies of graphical interpretation.

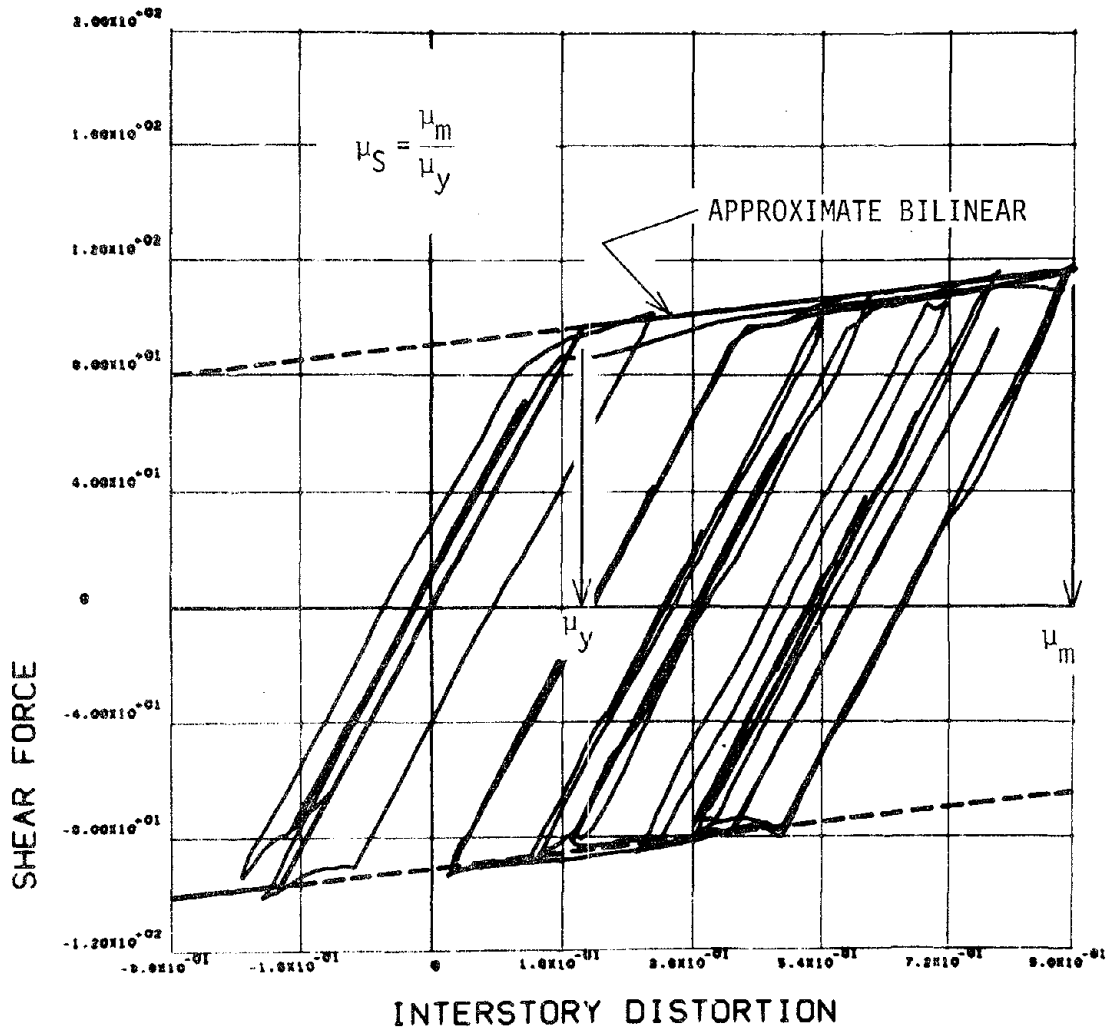


FIGURE 3.2.3 - DEFINITION OF STORY DUCTILITY

3.3 Simulated Motions

Analysis of inelastic dynamic response, involving the application of numerical techniques in the time integration solution of the equations of motion (Section 3.1), requires as input a digital acceleration record of the base motion. In order to examine the behavior of the frame designs within the range of the design earthquake excitation, three simulated motions were generated. Figures 3.3.1 to 3.3.3 compare the response spectra of the simulated motions to the Newmark and Hall design elastic response spectrum termed the target spectrum. The critical damping value of 5% is common to all spectra.

The methodology and capabilities of the computer program, SIMQKE, utilized in the simulation process, have been documented by Gasparini and Vanmarcke (21). Applying random vibration-based techniques, a stationary power spectral density function (s.d.f.) is calculated from the ordinates of the smooth target spectrum which are specified as input.

The simulated motion, $z(t)$, is computed as the sum of n sinusoids (21):

$$z(t) = I(t) \sum_n A_n \sin(\omega_n t + \phi_n)$$

The sum of the squares of the amplitudes, A_n , is proportional to the total power of $z(t)$; thus the s.d.f. provides sufficient information for deriving A_n . Interpolation of the s.d.f. occurs at frequencies, ω_n . The phase angle information, ϕ_n , is unknown; it is randomly generated with values from 0 to 2π following a uniform distribution. Different distributions of ϕ_n create different motions suggesting that an

RESPONSE SPECTRUM

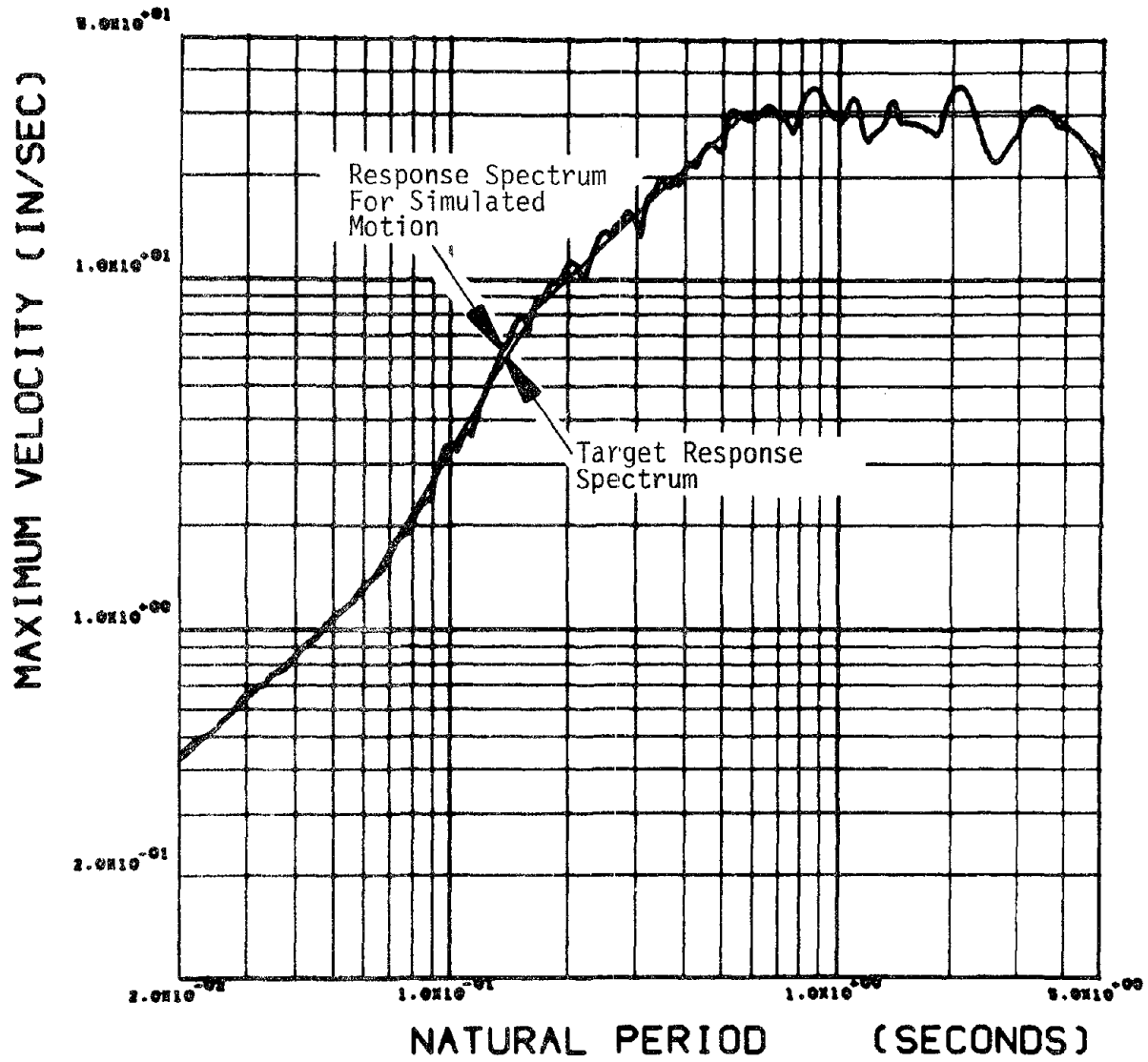


FIGURE 3.3.1 - RESPONSE SPECTRUM FOR SIMULATED MOTION 1

RESPONSE SPECTRUM

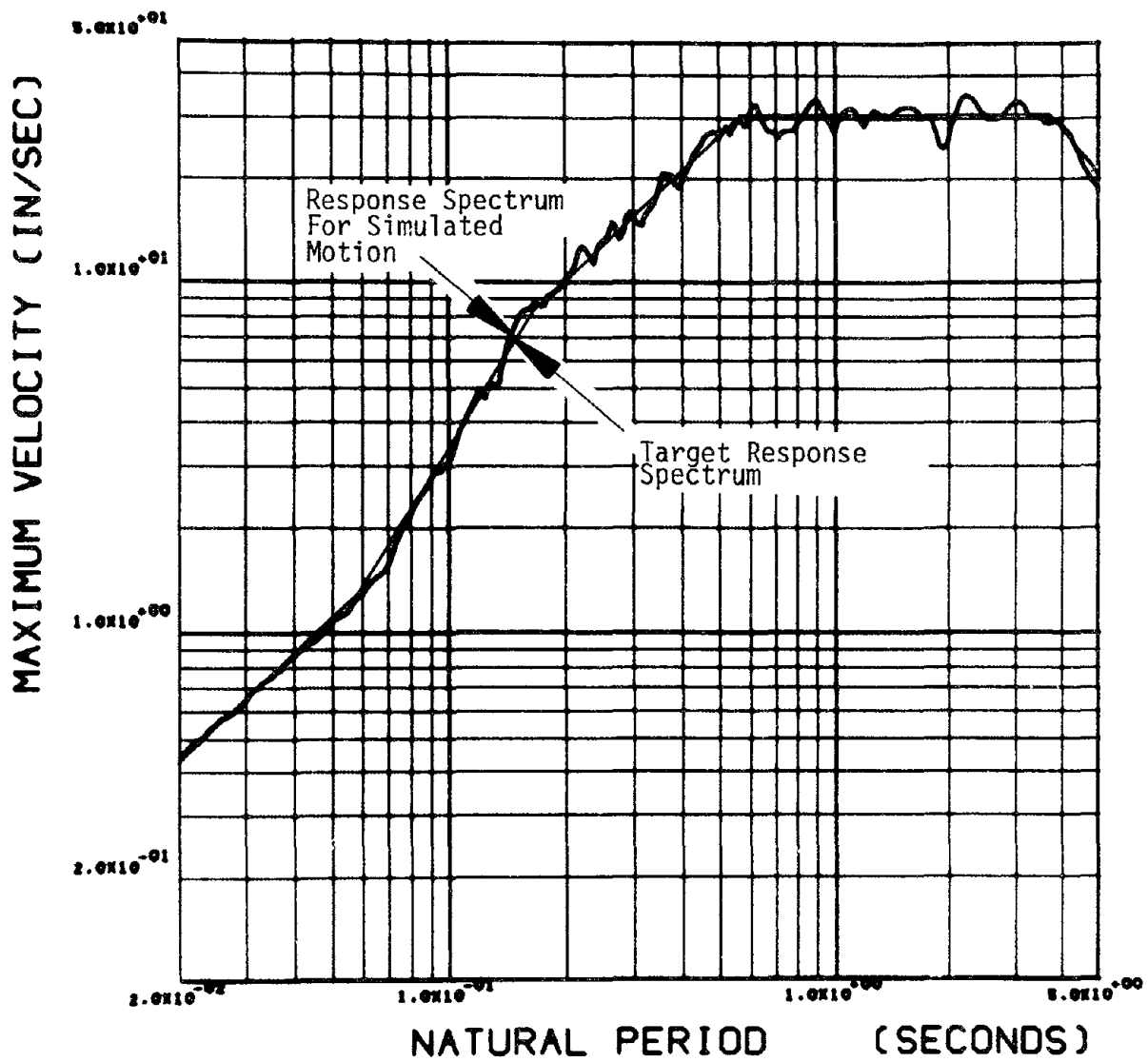


FIGURE 3.3.2 - RESPONSE SPECTRUM FOR SIMULATED MOTION 2

RESPONSE SPECTRUM

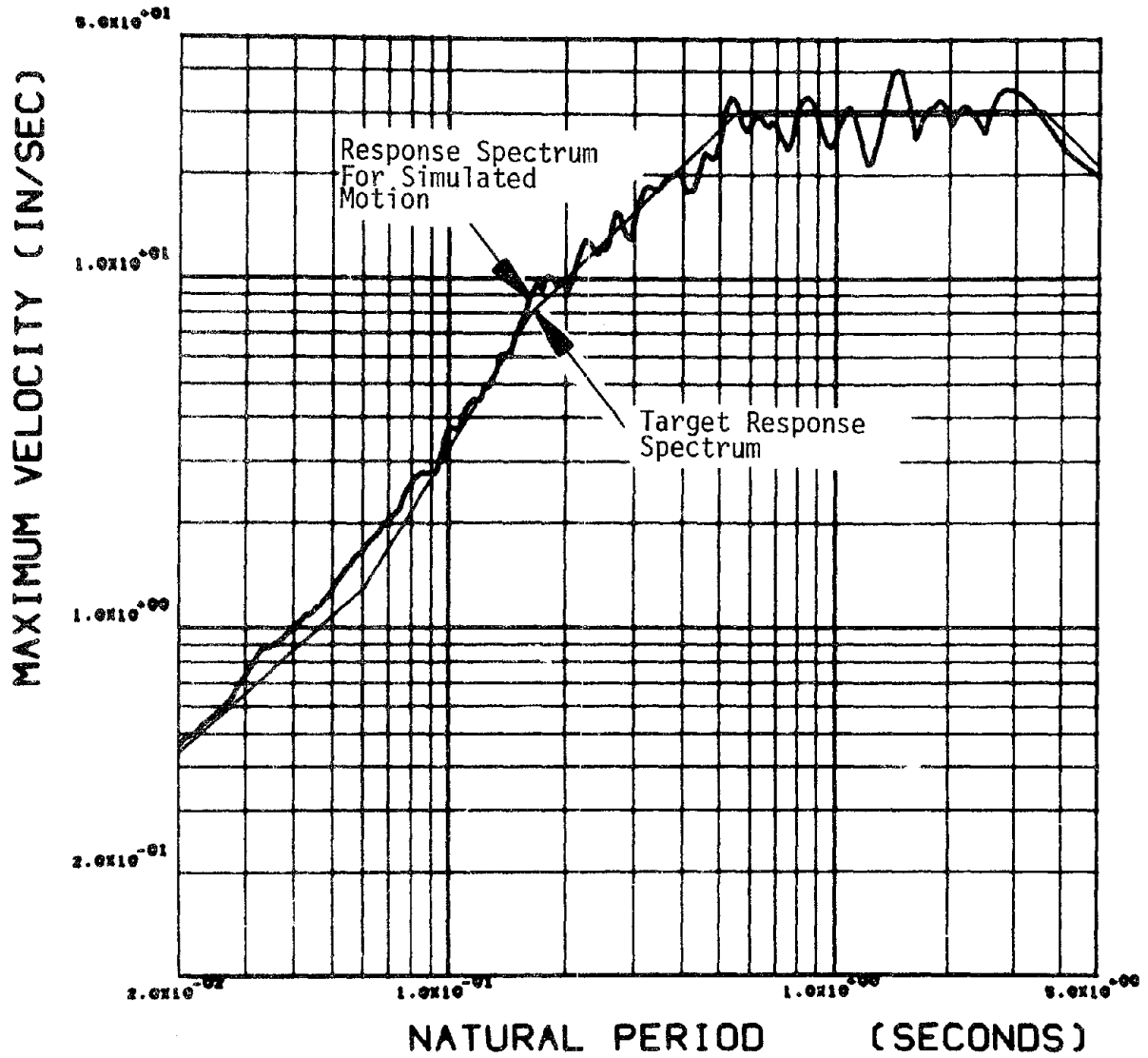


FIGURE 3.3.3 - RESPONSE SPECTRUM FOR SIMULATED MOTION 3

unlimited number of motions are possible for the same s.d.f.

The intensity function, $I(t)$, shown in Figure 3.3.4, modifies $z(t)$ to account for the transient nature of earthquakes. Parameters defining $I(t)$, used in generating the 3 motions are: rise time = 1 sec., level time = 8 sec., and duration = 10 sec.

The match between the target spectrum and the computed spectrum has been improved by 3 cycling operations (iterative scheme) in which the s.d.f. is modified by the square of the ratio of the target spectrum to the computed spectrum values. The accelerograms, produced with equal time intervals of 0.01 sec., have been corrected to achieve a peak acceleration of 0.33 g and a zero ground velocity at the end of the record.

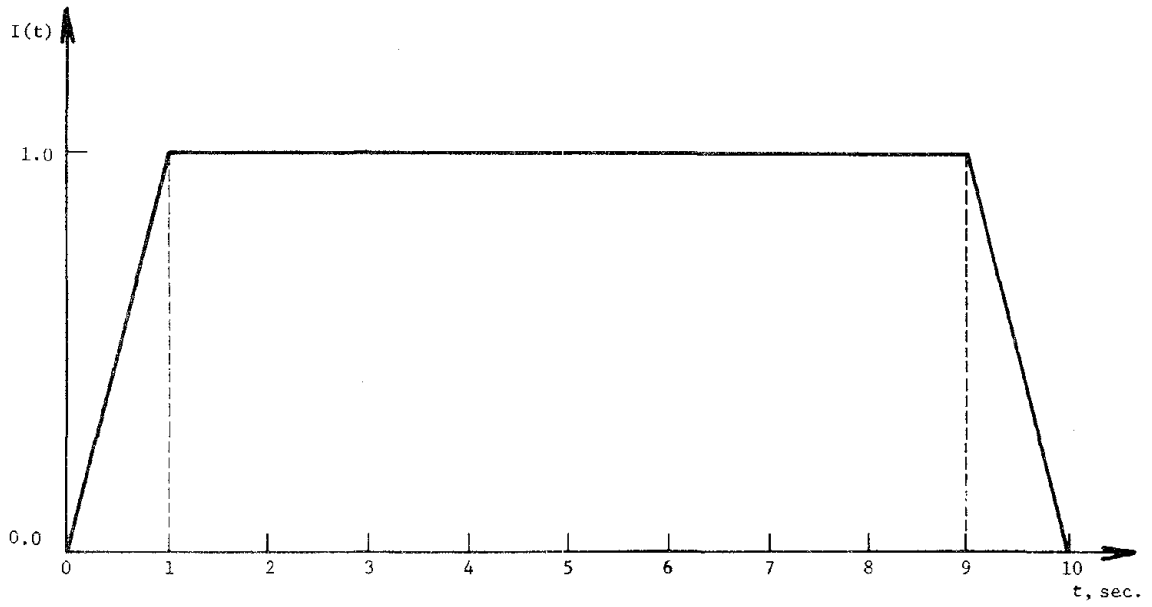


FIGURE 3.3.4 - INTENSITY FUNCTION

3.4 Comparisons of Parameters and Response of Point Hinge and Shear Beam Models

The concept of a story ductility factor for complex hysteretic systems was introduced in Section 3.2. The intention of such a factor is to provide a basis of comparison to the specified level of ductility in the inelastic spectra and to the results of shear beam studies. The assumption of bilinear behavior and the approximate graphical technique may generate inaccuracies in the computations of μ_S .

Evaluation of the validity of the definition of μ_S was performed as follows:

- 1) Bilinear resistance functions were constructed on computer plots of story shear versus interstory displacement (see Figure 3.2.3) obtained from a time integration analysis with the point hinge model.
- 2) Measured properties of the force-deformation relationships were used to delineate the nonlinear springs of a shear beam model at the same story levels; these included the initial and second stiffness and the yield limit shear. The masses and floor-to-floor dimensions remained the same for the lumped parameter system.
- 3) A time integration analysis of the "equivalent" shear beam model was performed with the same ground motion that produced the estimated spring characteristics using the member level model.
- 4) Lateral and interstory displacements were compared.

This procedure was applied to a 4- and 10-story frame for simulated motion 2. Member resistances for the 4-story frame correspond to those of Section 4.1. The 10-story frame was designed in the same manner as the frames of Section 4.1, except that the Z/A ratio was assumed equal to 7 instead of 6. Properties of the "equivalent" shear beam models are listed in Appendix A. The results are shown in Figure 3.4.1.

The interstory displacement of the 10-story frame exhibits the poorest match with differences of 12% at levels 1 and 5, and 16% at levels 7, 8 and 9. However, with these exceptions, agreement between the response of the associated systems is within 10%.

The results lend support to the following:

- 1) The story force-deformation relationship of the point hinge model may be approximated as a bilinear.
- 2) The definition of the story ductility factor may be valid for multimember systems.
- 3) Shear beam models may adequately represent the response of more complex models.

These observations apply only to the frames as designed herein. The bilinear behavior is perhaps related to the philosophy of allowing large amounts of yielding activity. Yield transitional regions are relatively insignificant with respect to the post-yield regions which possess extensive strain-hardening branches for this type of design.

Although the method for comparison of models was intended to reinforce the concept of story ductility, practical approaches for obtaining

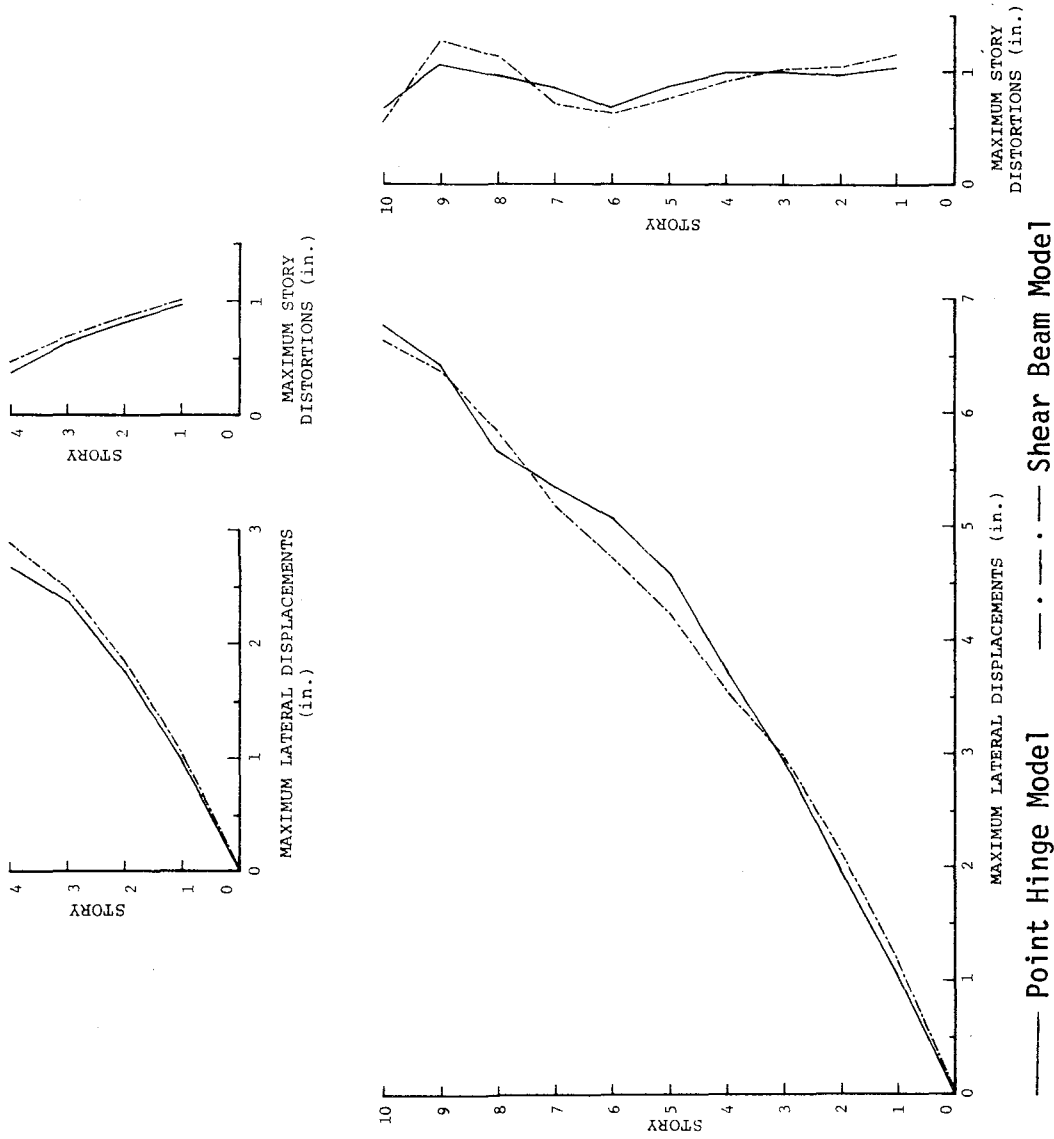


FIGURE 3.4.1 - COMPARISON OF MAXIMUM LATERAL AND INTERSTORY DISPLACEMENTS OF POINT HINGE AND SHEAR BEAM MODELS

the properties of an "equivalent" shear beam model are of interest due to potential applications for inexpensive analysis of member systems. Concurrent research is being conducted to determine story resistance parameters employing an inelastic static analysis (27).

CHAPTER 4 - BEHAVIOR OF FRAMES DESIGNED FOR INELASTIC RESPONSE

The results of the inelastic response calculations using point-hinge models are presented in this chapter. These provide a general evaluation of the inelastic response spectrum approach to design, the effects of design ductility level and gravity load, and the possibility of applying factors to the spectral forces to improve performance.

Section 4.1 contains results for designs including gravity effects and based on $\mu = 4$. In Section 4.2, the designs are based on $\mu = 2$. The effect of gravity loads on response is investigated in Section 4.3 and the effect of ignoring gravity in the design in Section 4.4. Finally, the possible use of factored seismic forces is studied in Section 4.5.

Prior to a discussion of the results, the following parameter definitions, common throughout Chapter 4 are re-stated for clarity.

- 1) Both definitions of local ductility are reported - rotational (μ_R) and moment (μ_M).
- 2) The maximum local girder ductility at a floor is defined as the largest value occurring at any of the 4 exterior girder end cross-sections or any of the 2 interior girder end cross-sections in the floor.
- 3) The maximum local column ductility in a story is defined as the largest value occurring at any of the 4 exterior or 4 interior column end cross-sections in the story.
- 4) The average over the height is simply the average of the maximum ductilities as described in #2 and #3 above.
- 5) The average column or girder ductility is defined as the average of all column cross-sections in a particular story (i.e., 8) or all girder cross-sections in a particular floor (i.e., 6).
- 6) Story ductility factors (μ_S) are based upon maximum interstory displacements (see Section 3.2.2).

- 7) The envelop of maximum inelastic response in terms of story shear, overturning moment, lateral displacement and inter-story displacement are plotted against height. Values corresponding to the elastic modal analysis with the inelastic acceleration spectrum are denoted as SRSS in the figures.

4.1 Results for Designs at a Ductility Level of 4, Including Gravity Effects

The 4-, 10- and 18-story frames were designed as detailed in Section 2.4 for a ductility (μ) of 4, including gravity loads. The 4- and 10-story designs are subjected to simulated motions 1, 2 and 3; the 18-story is analyzed only for motion 2. Appendix B summarizes the corresponding resistances for the three frames.

Maximum local ductility factors for the four-story frame are plotted in Fig. 4.1.1 for the three simulated motions. Overall story responses are plotted in Fig. 4.1.2. The same results for the 10-story frame are shown in Figs. 4.1.3 - 4.1.5, and for the 18-story frame in Figs. 4.1.6 - 4.1.9 (motion 2 only). Average girder and column ductilities are tabulated in Table 4.1.1 (4-story), Table 4.1.3 (10-story), and Table 4.1.5 (18-story). Overall story ductilities are tabulated in Tables 4.1.2, 4.1.4, and 4.1.6. Comments on these results follow.

Local column ductility varies more than girder ductility with height for the moment definition as seen in Figures 4.1.1, 4.1.3, 4.1.4, 4.1.6 and 4.1.7. At the bottom of the 10-story frame, the difference in μ_M between the first and second stories is greater than 6 in the exterior column. Sudden increases of μ_M (in exterior column of 10-story) occur at the 4th, 5th, and 6th floors for motions 2, 3 and 1, respectively, indicating an interesting difference in the response to the three motions. It is felt that these large local values are due to the application of a large bending

moment when the plastic capacity is reduced from the simultaneous action of a large axial force. The plots of rotational ductility do not show the same jagged pattern for columns. However, the definition of μ_R does not include interaction effects which may explain the anomaly.

The excessive values of μ_M at the base of the frames is attributed to the assumption of a rigid foundation and base connection; using the average of the end moments for design causes the bottom section of the lower story columns to be somewhat underdesigned.

Girder ductility decreases within the top floors, forcing more yielding into the columns. This occurs where the $wl^2/8$ condition controls, which causes the girders to be overdesigned.

In general, more yielding takes place in exterior column and girder sections than interior, as shown by the larger averages of maximum ductility over height. For columns, the difference may be due to a larger fluctuation in earthquake axial force created by the overturning moment, of which the exterior columns support the larger portion. The reason for the difference in girders is not as clear.

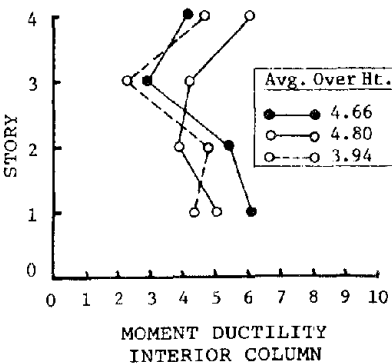
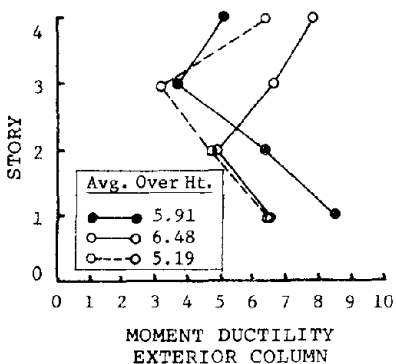
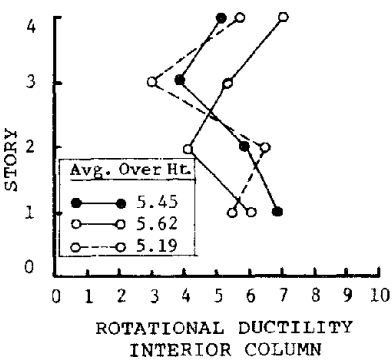
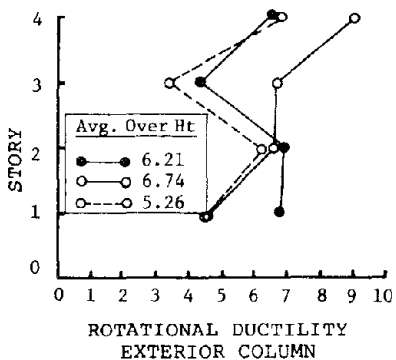
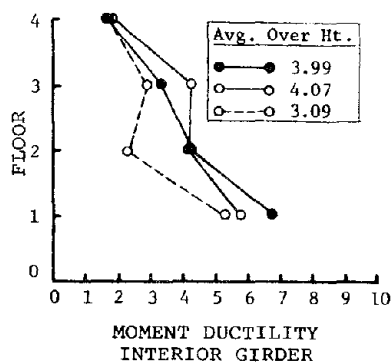
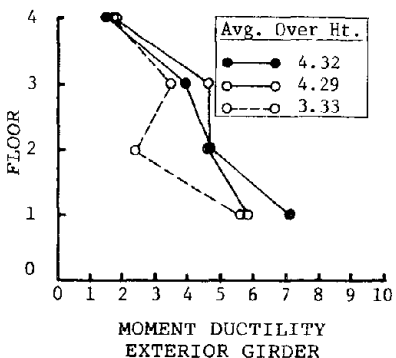
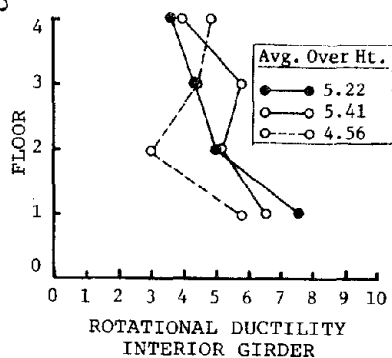
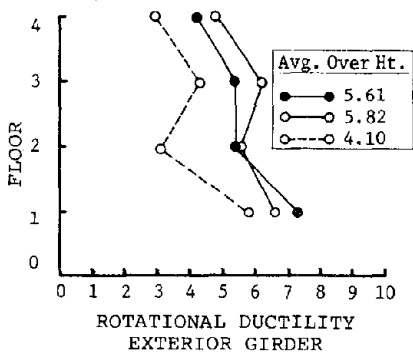
The story shears and overturning moments exceed the design values (SRSS) due to the strain-hardening effect. (See Figures 4.1.2, 4.1.5, and 4.1.8).

The average of the maximum ductility factors (Tables 4.1.1, 4.1.3, 4.1.5) is greater for columns than girders in terms of μ_M and vice versa for μ_R . Assuming that μ_M is a better index of nonlinear deformation (this is discussed in Section 4.3), it appears that the spectral design results in "weak" columns. However, the averages of μ_M at all column or girder cross-sections at a particular height are within the same range regardless of the type of element. Thus, columns are the more critical elements in terms of concentrations of maximum ductility, although the distribution of

yielding is fairly even between columns and girders when considering all cross-sections in the frame. The ductility demand is not uniform over the height with respect to maxima or averages.

Details of the ground motion produce variations in maximum member ductility at the same height (about 5 in some locations). However, the difference generally ranges from 2 to 3. The more notable result is the change in distribution of ductility throughout the frames even though the motions were generated to match the same target spectrum.

In some cases, local ductility exceeds the design value ($\mu = 4$) by more than 9 whereas the story ductility factor (μ_S) equals 3.9 (e.g., μ_M for exterior column, motion 1). Generally, μ_S is less than the design level of ductility; the maximum value is 6.1 (Tables 4.1.2, 4.1.4, 4.1.6). Limiting the nonlinear response of a given story does not indicate that inelastic action will occur to the same degree for individual members. The inelastic spectrum approach does not ensure the desired value of maximum local ductility, the average of the maximum ductility over the height, nor the average of all cross-section ductilities at a given height.



●—● motion 1 ○—○ motion 2 ○---○ motion 3

FIGURE 4.1.1 - MAXIMUM DUCTILITY FACTORS FOR GRAVITY AND EARTHQUAKE DESIGN - $\mu = 4$; 4-Story Frame; Motions 1, 2, 3

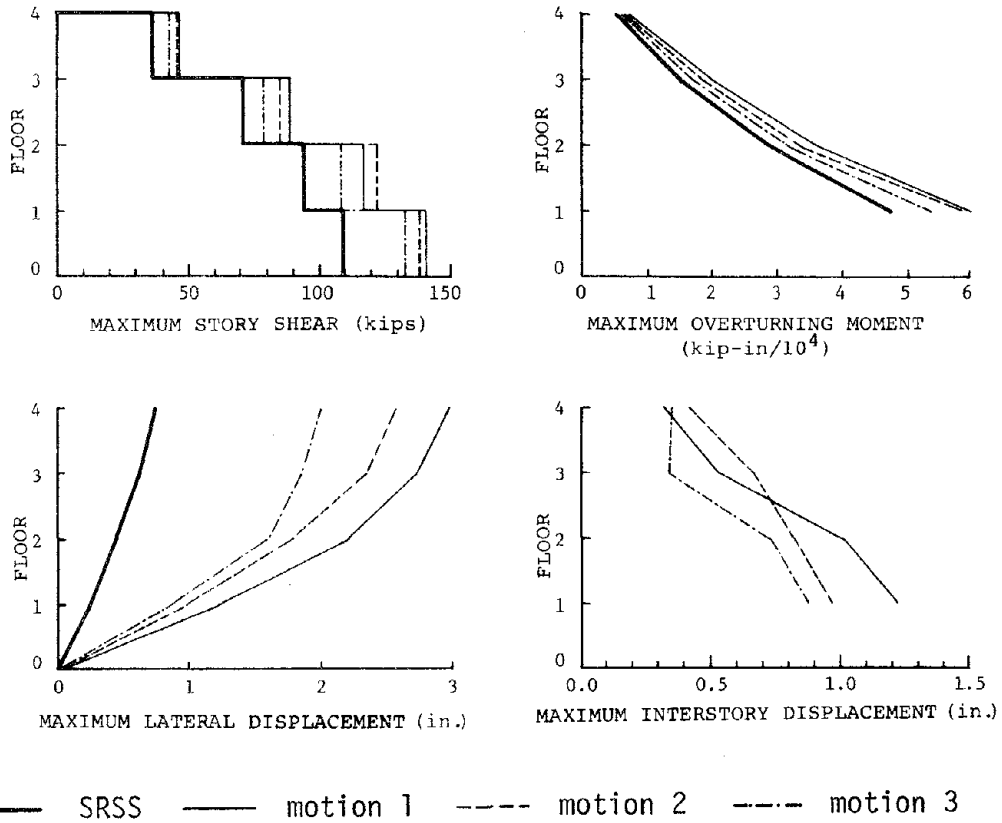
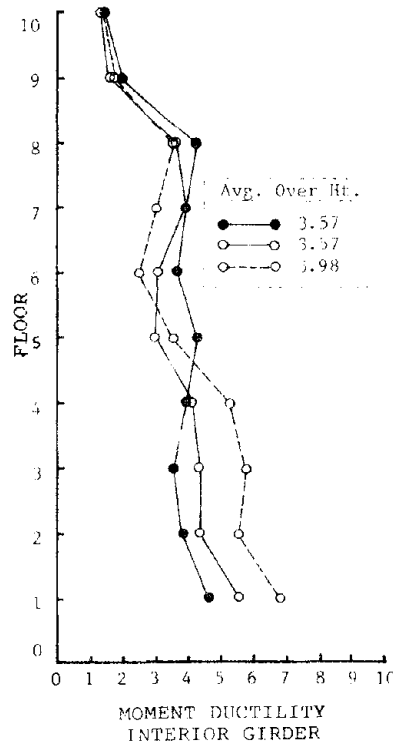
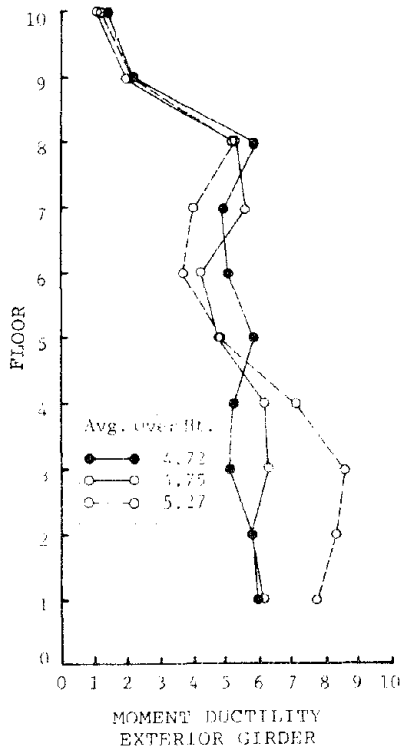
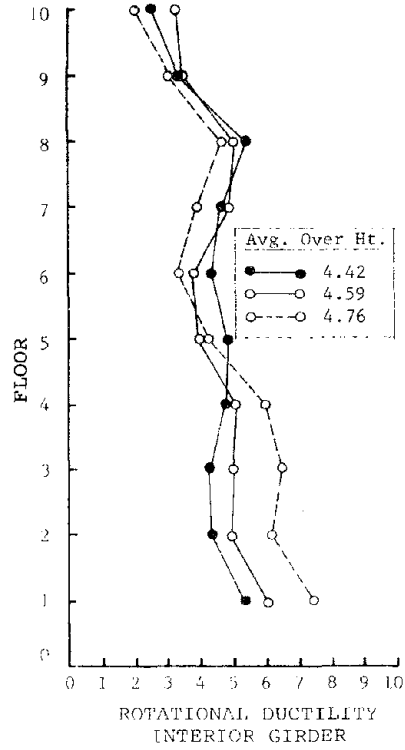
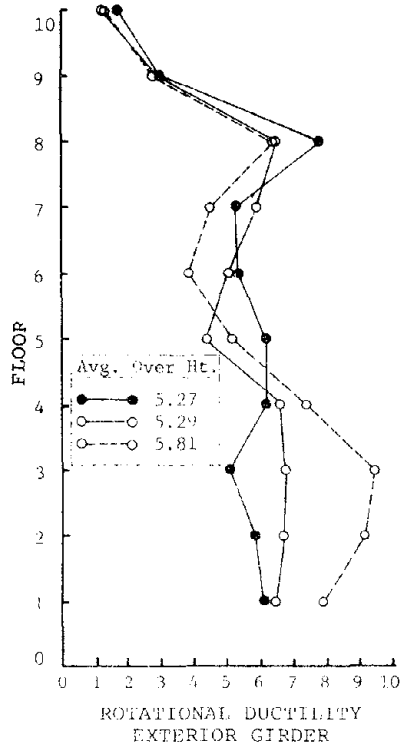
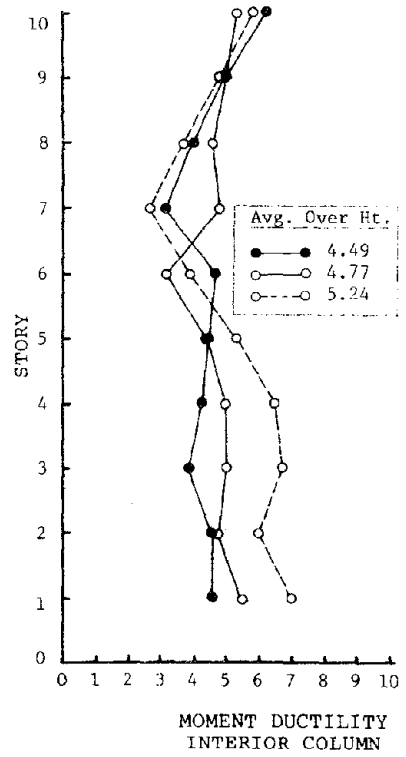
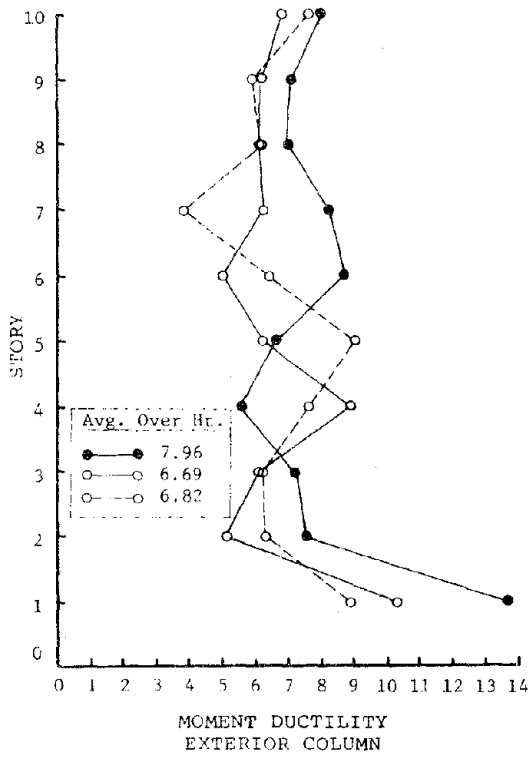
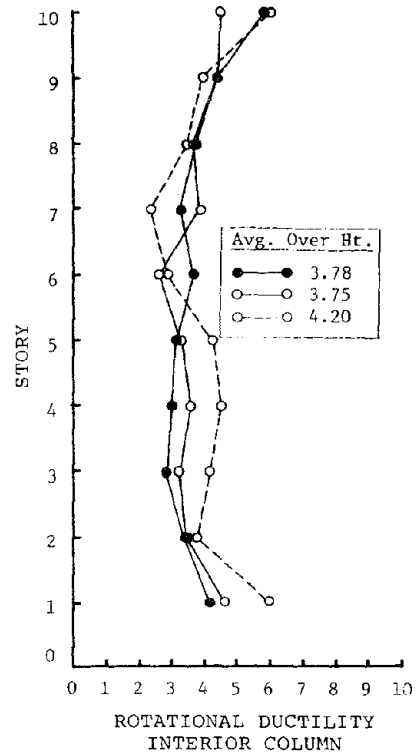
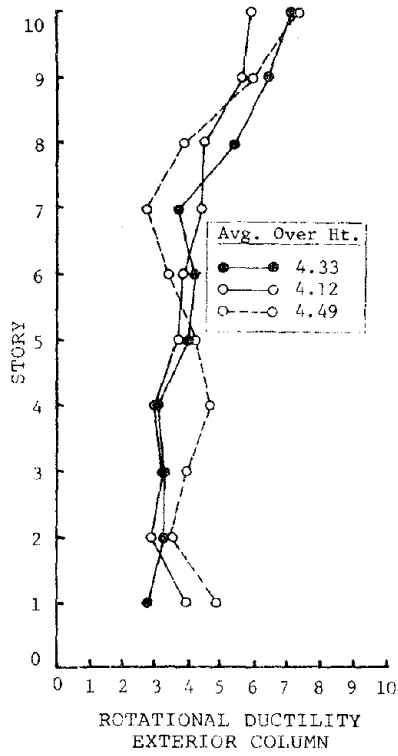


FIGURE 4.1.2 - MAXIMUM STORY LEVEL PARAMETERS FOR GRAVITY AND EARTHQUAKE DESIGN - $\mu = 4$; 4-Story Frame; Motions 1, 2, 3



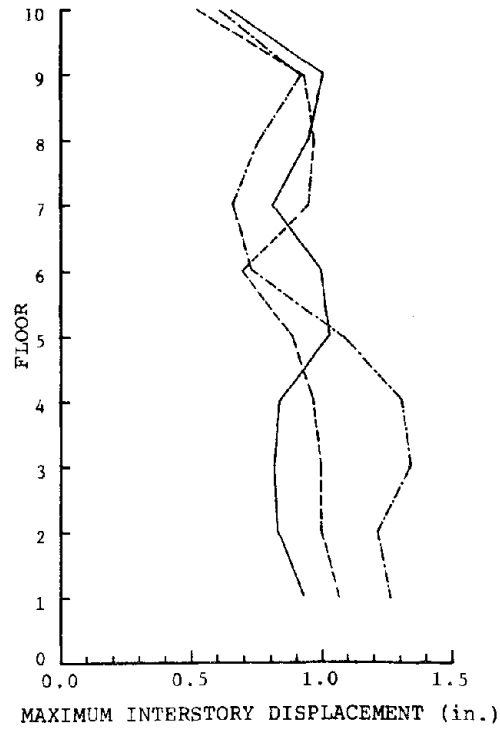
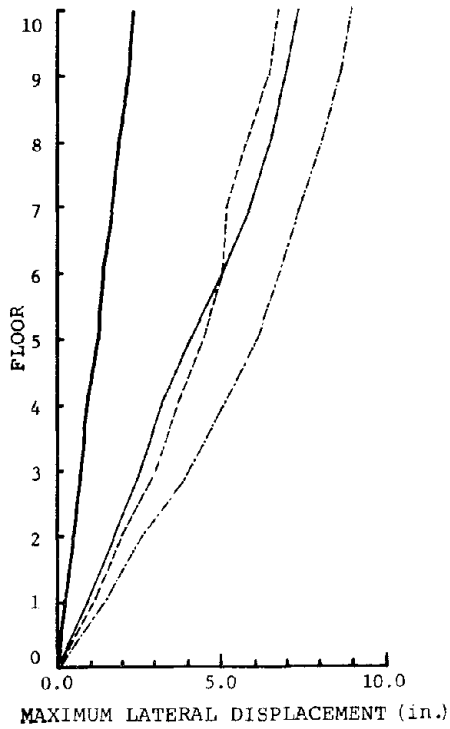
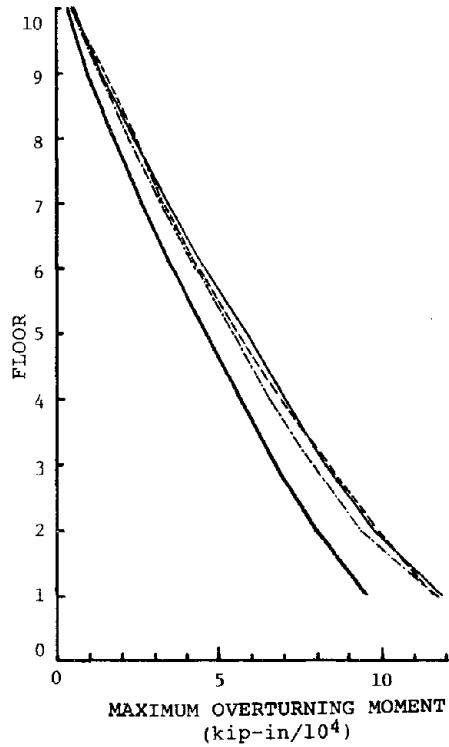
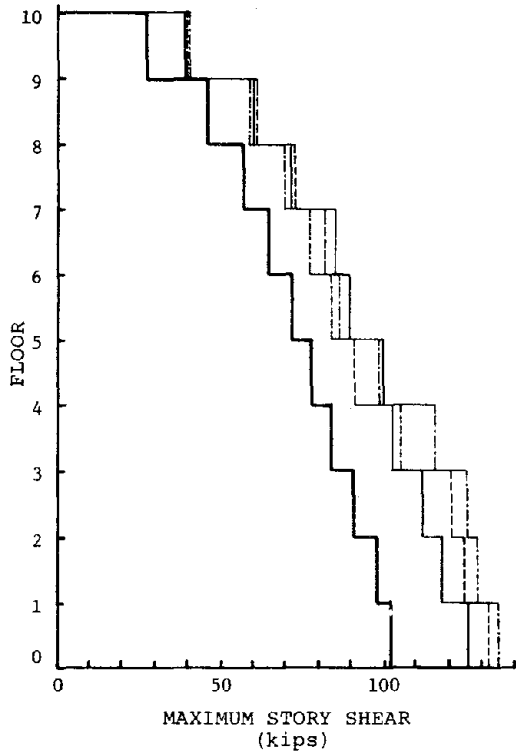
●—● Motion 1 ○—○ Motion 2 ○---○ Motion 3

FIGURE 4.1.3 - MAXIMUM GIRDER DUCTILITY FACTORS FOR GRAVITY AND EARTHQUAKE DESIGN
 $\mu = 4$; 10-Story Frame; Motions 1, 2, 3



●—● Motion 1 ○—○ Motion 2 ○—○ Motion 3

FIGURE 4.1.4 - MAXIMUM COLUMN DUCTILITY FACTORS FOR GRAVITY AND EARTHQUAKE DESIGN
 $\mu = 4$; 10-Story Frame; Motions 1, 2, 3



— SRSS - - - motion 1 . . . motion 2 - . - motion 3

FIGURE 4.1.5 - MAXIMUM STORY LEVEL PARAMETERS FOR GRAVITY AND EARTHQUAKE DESIGN
 $\mu = 4$; 10-Story Frame; Motions 1, 2, 3

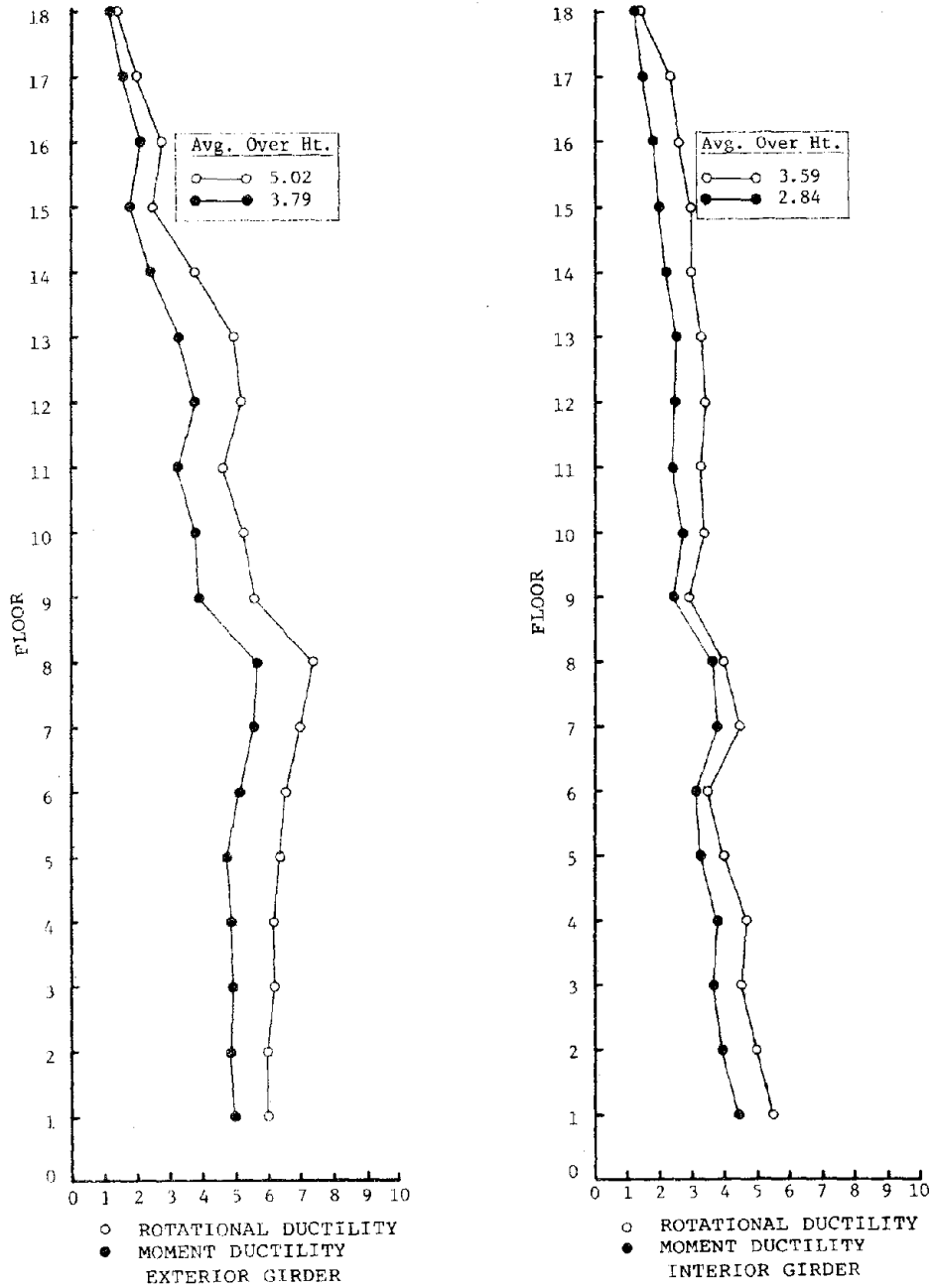


FIGURE 4.1.6 - MAXIMUM GIRDER DUCTILITY FACTORS FOR GRAVITY AND EARTHQUAKE DESIGN
 $\mu = 4$; 18-Story Frame; Motion 2

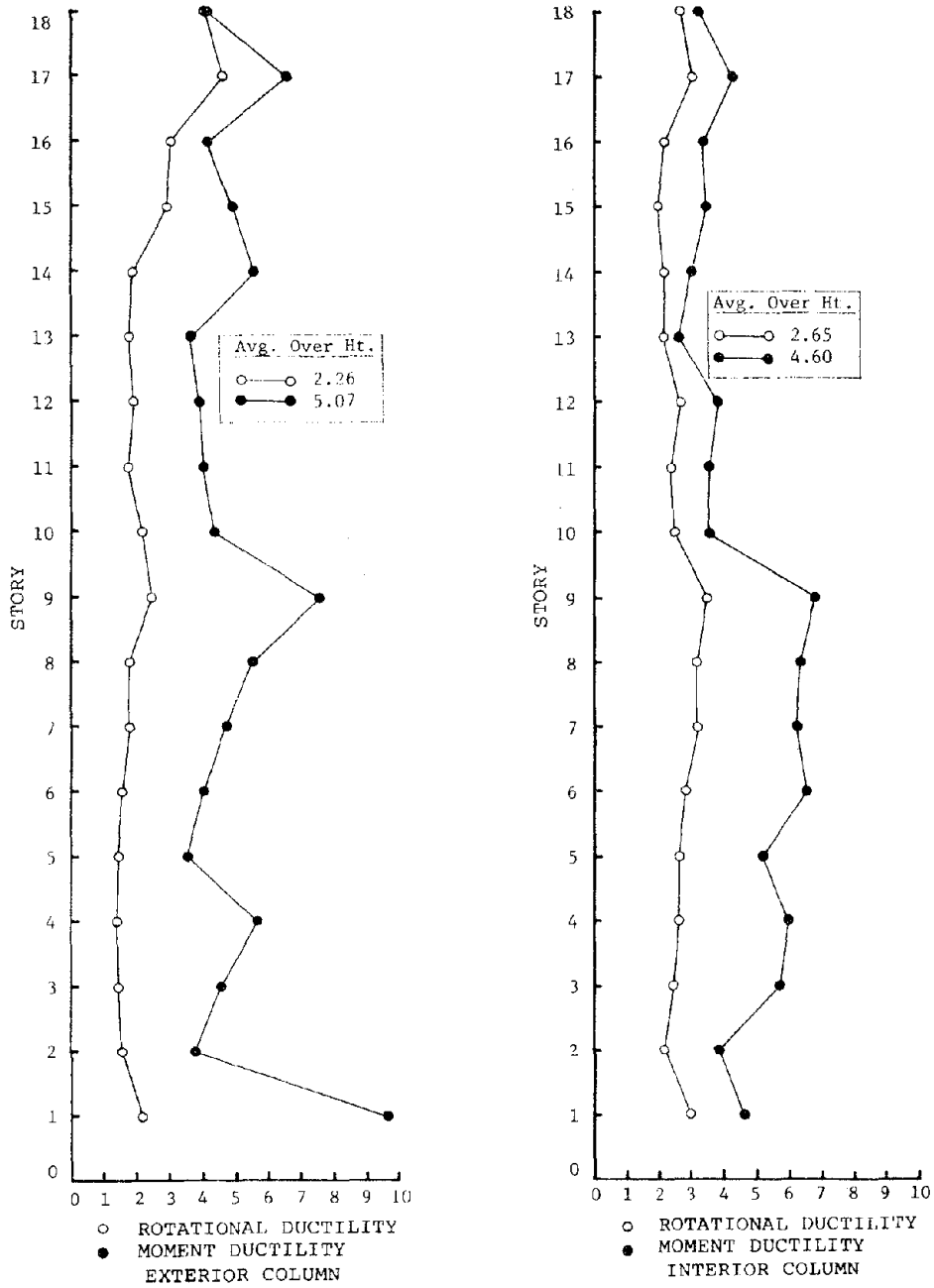


FIGURE 4.1.7 - MAXIMUM COLUMN DUCTILITY FACTORS FOR GRAVITY AND EARTHQUAKE DESIGN

$\mu = 4$; 18-Story Frame; Motion 2

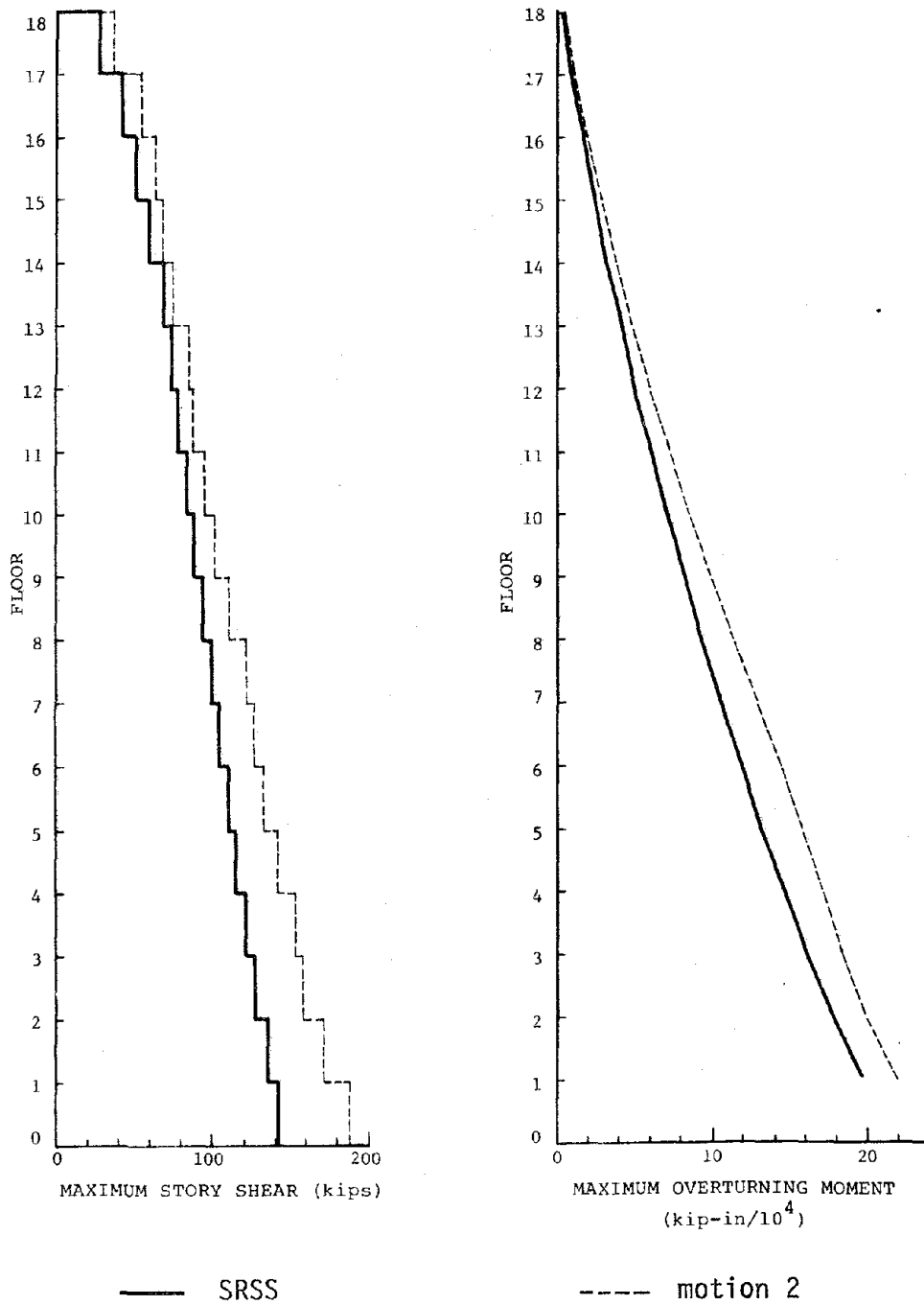


FIGURE 4.1.8 - MAXIMUM FORCES FOR GRAVITY AND EARTHQUAKE DESIGN
 $\mu = 4$; 18-Story Frame; Motion 2

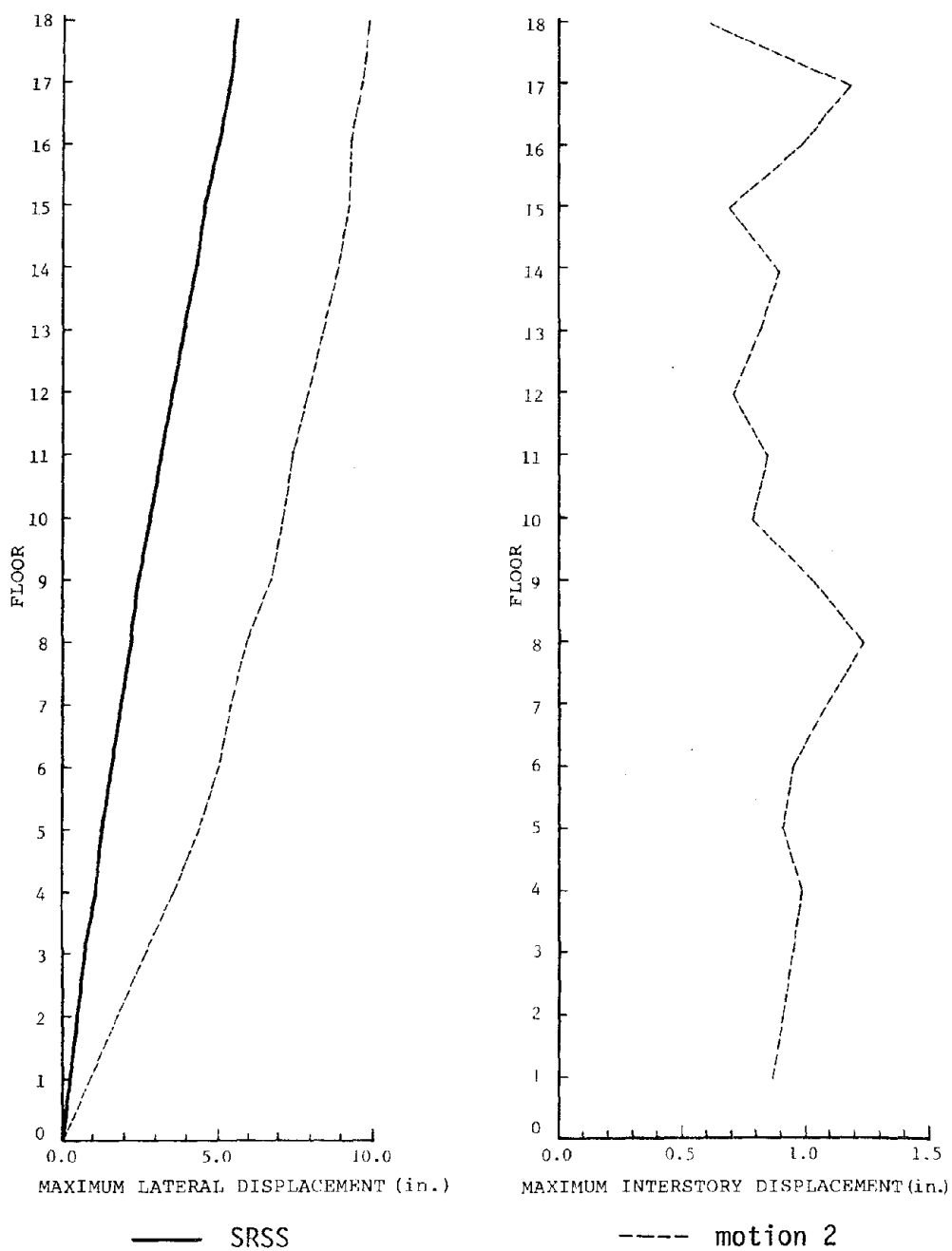


FIGURE 4.1.9 - MAXIMUM DISPLACEMENTS FOR GRAVITY AND EARTHQUAKE DESIGN
 $\mu = 4$; 18-Story Frame; Motion 2

TABLE 4.1.1 - AVERAGE DUCTILITY FACTORS FOR GRAVITY AND EARTHQUAKE DESIGN
 $\mu = 4$; 4-Story Frame; Motions 1, 2, 3

LEVEL	ROTATIONAL DUCTILITY		MOMENT DUCTILITY	
	GIRDERS	COLUMNS	GIRDERS	COLUMNS
MOTION 1				
1	6.73	4.27	6.64	4.67
2	4.45	4.53	4.13	4.58
3	4.20	3.20	3.13	2.69
4	2.56	4.23	1.26	3.57
MOTION 2				
1	5.69	3.53	5.57	3.75
2	4.36	3.88	4.12	3.32
3	4.66	4.00	4.02	4.26
4	2.74	5.51	1.24	4.87
MOTION 3				
1	5.21	3.16	5.21	3.57
2	2.95	3.69	2.31	3.29
3	3.83	2.69	2.87	2.33
4	2.69	4.15	1.26	4.22

TABLE 4.1.2 - STORY DUCTILITY FACTORS FOR GRAVITY AND EARTHQUAKE DESIGN
 $\mu = 4$; 4-Story Frame; Motions 1, 2, 3

STORY	DUCTILITY FACTOR		
	MOTION 1	MOTION 2	MOTION 3
1	5.3	4.2	3.8
2	5.1	4.1	3.7
3	3.0	3.8	1.9
4	2.9	3.9	3.2

TABLE 4.1.3 - AVERAGE DUCTILITY FACTORS FOR GRAVITY AND EARTHQUAKE DESIGN
 $\mu = 4$; 10-Story Frame; Motions 1, 2, 3

LEVEL	ROTATIONAL DUCTILITY		MOMENT DUCTILITY	
	GIRDERS	COLUMNS	GIRDERS	COLUMNS
MOTION 1				
1	5.23	2.39	5.11	5.78
2	4.74	2.66	4.44	4.87
3	4.52	2.60	4.06	4.38
4	4.94	2.91	4.49	4.36
5	5.03	2.96	4.78	4.56
6	4.57	3.23	4.23	4.94
7	4.45	2.80	4.00	4.12
8	5.33	3.29	4.65	3.97
9	2.21	3.44	1.48	4.51
10	1.46	4.89	1.00	5.40
MOTION 2				
1	6.04	2.64	5.73	4.73
2	5.46	2.70	5.16	4.51
3	5.40	2.88	5.07	5.03
4	5.01	2.99	4.83	5.34
5	3.99	2.75	3.67	4.55
6	3.78	2.61	3.40	3.64
7	4.64	3.03	4.40	4.02
8	4.80	3.36	3.97	4.42
9	2.19	3.48	1.51	4.43
10	1.60	4.37	0.98	4.81
MOTION 3				
1	7.00	3.26	6.96	5.46
2	6.33	3.11	6.27	5.32
3	6.90	3.45	6.69	5.58
4	5.88	3.81	5.82	5.86
5	3.96	3.04	3.85	5.56
6	3.20	2.69	2.77	4.07
7	3.45	2.23	2.98	2.70
8	4.65	2.97	4.01	3.52
9	2.20	3.29	1.67	3.84
10	1.35	5.03	0.96	5.30

TABLE 4.1.4 - STORY DUCTILITY FACTORS FOR GRAVITY AND EARTHQUAKE DESIGN
 $\mu = 4$; 10-Story Frame; Motions 1, 2, 3

STORY	DUCTILITY FACTOR		
	MOTION 1	MOTION 2	MOTION 3
1	3.9	4.5	5.8
4	3.9	4.5	6.1
7	3.2	3.7	2.6
10	3.7	2.9	3.5

TABLE 4.1.5 - AVERAGE DUCTILITY FACTORS FOR GRAVITY AND EARTHQUAKE DESIGN
 $\mu = 4$; 18-Story Frame; Motion 2

LEVEL	ROTATIONAL DUCTILITY		MOMENT DUCTILITY	
	GIRDERS	COLUMNS	GIRDERS	COLUMNS
MOTION 2				
1	5.52	1.82	4.69	3.57
2	5.15	1.66	4.20	3.07
3	4.99	1.91	4.16	4.19
4	5.37	1.88	4.36	4.37
5	4.75	1.83	3.88	3.88
6	4.47	2.01	3.88	4.37
7	4.58	1.83	4.39	3.93
8	4.64	1.97	4.48	4.39
9	3.94	2.17	2.99	4.60
10	3.94	1.81	2.79	3.22
11	3.88	1.83	2.72	2.95
12	4.12	2.12	2.93	3.41
13	3.87	1.73	2.56	2.32
14	3.23	1.75	2.03	3.14
15	2.43	2.22	1.76	3.61
16	2.37	2.51	1.68	3.52
17	1.63	3.33	1.27	4.52
18	1.20	3.10	0.92	3.47

TABLE 4.1.6 - STORY DUCTILITY FACTORS FOR GRAVITY AND EARTHQUAKE DESIGN
 $\mu = 4$; 18-Story Frame; Motion 2

STORY	DUCTILITY FACTOR
	MOTION 2
1	3.4
3	3.8
5	3.7
7	3.7
11	2.8
13	2.0
15	2.1
18	—

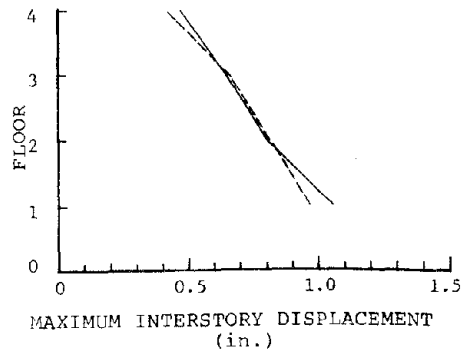
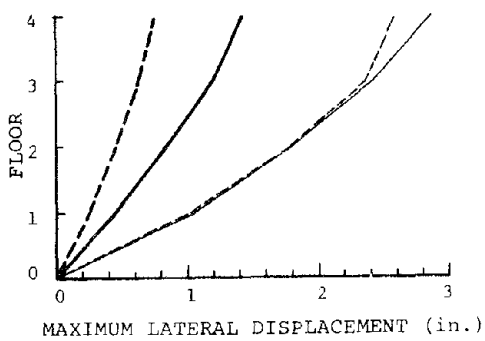
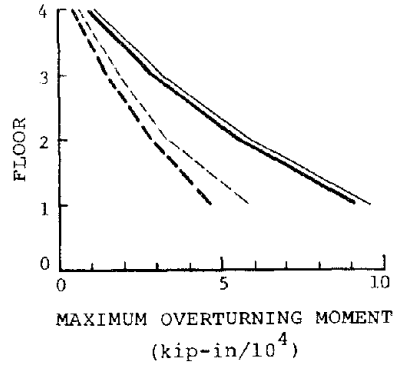
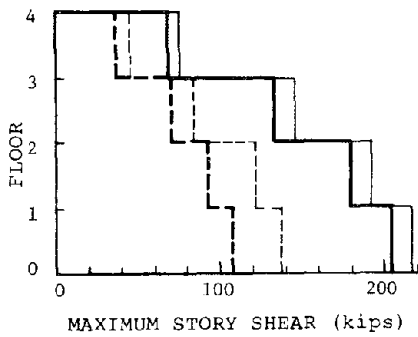
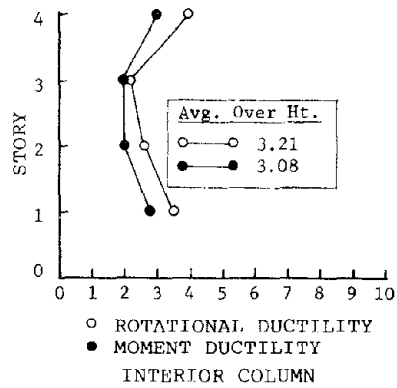
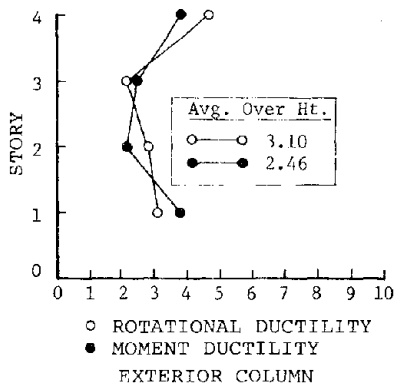
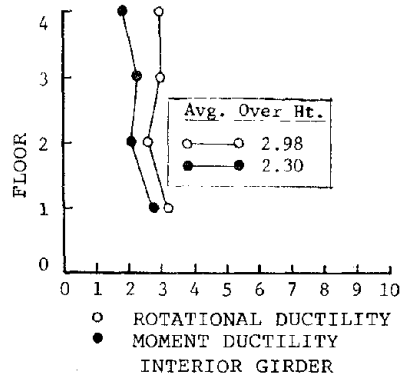
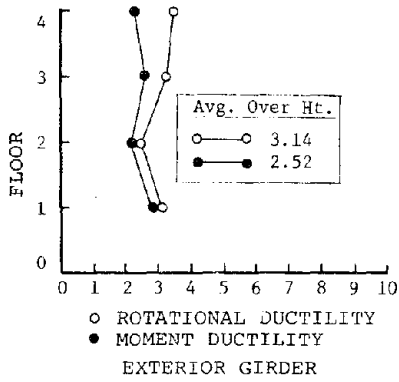
4.2 Results for Designs at a Ductility Level of 2, Including Gravity Effects

The 4-, 10- and 18-story frames were designed according to Section 2.4 for a ductility level of 2 and subsequently analyzed with motion 2. This permits investigation of the effect of the design level of ductility. The format of results are similar to those of Section 4.1. Some pertinent observations follow.

- 1) The maximum member ductility, average of the maximum over height and average for all column or girder cross-sections at a given height exceed the design level of 2 (see Figures 4.2.1, 4.2.2, 4.2.4, 4.2.5, and Tables 4.2.1, 4.2.3 and 4.2.5).
- 2) The maximum local ductility factors have been normalized by the respective design values in Tables 4.2.7 to 4.2.9 for the 3 frames. These indicate that the ratios of maximum to design value are within the same range regardless of the design level.
- 3) The story ductility factor is close to the design value at all locations; it ranges from 1.5 to 2.6 for the 3 frames (see Tables 4.2.2, 4.2.4, and 4.2.6).
- 4) Local concentrations of yielding several times greater than the design ductility occur even though the overall story response satisfies the nonlinear deformation criteria.

A major effect of the different design level is the change in distribution of ductility throughout the frame.

Lateral displacements are less in the top floors of the 3 frames for $\mu=4$ than for $\mu=2$ (see Figures 4.2.1, 4.2.3 and 4.2.7). This change in response may be due to the fact that the girders within the top floors in which the $wl^2/8$ condition controls are overdesigned by a larger degree for the higher ductility level due to the smaller earthquake forces.



— SRSS ($\mu = 2$) - - - SRSS ($\mu = 4$) — motion 2 ($\mu = 2$) - - - motion 2 ($\mu = 4$)

FIGURE 4.2.1 - MAXIMUM RESPONSE PARAMETERS FOR GRAVITY AND EARTHQUAKE DESIGN - $\mu = 2$; 4-Story Frame; Motion 2

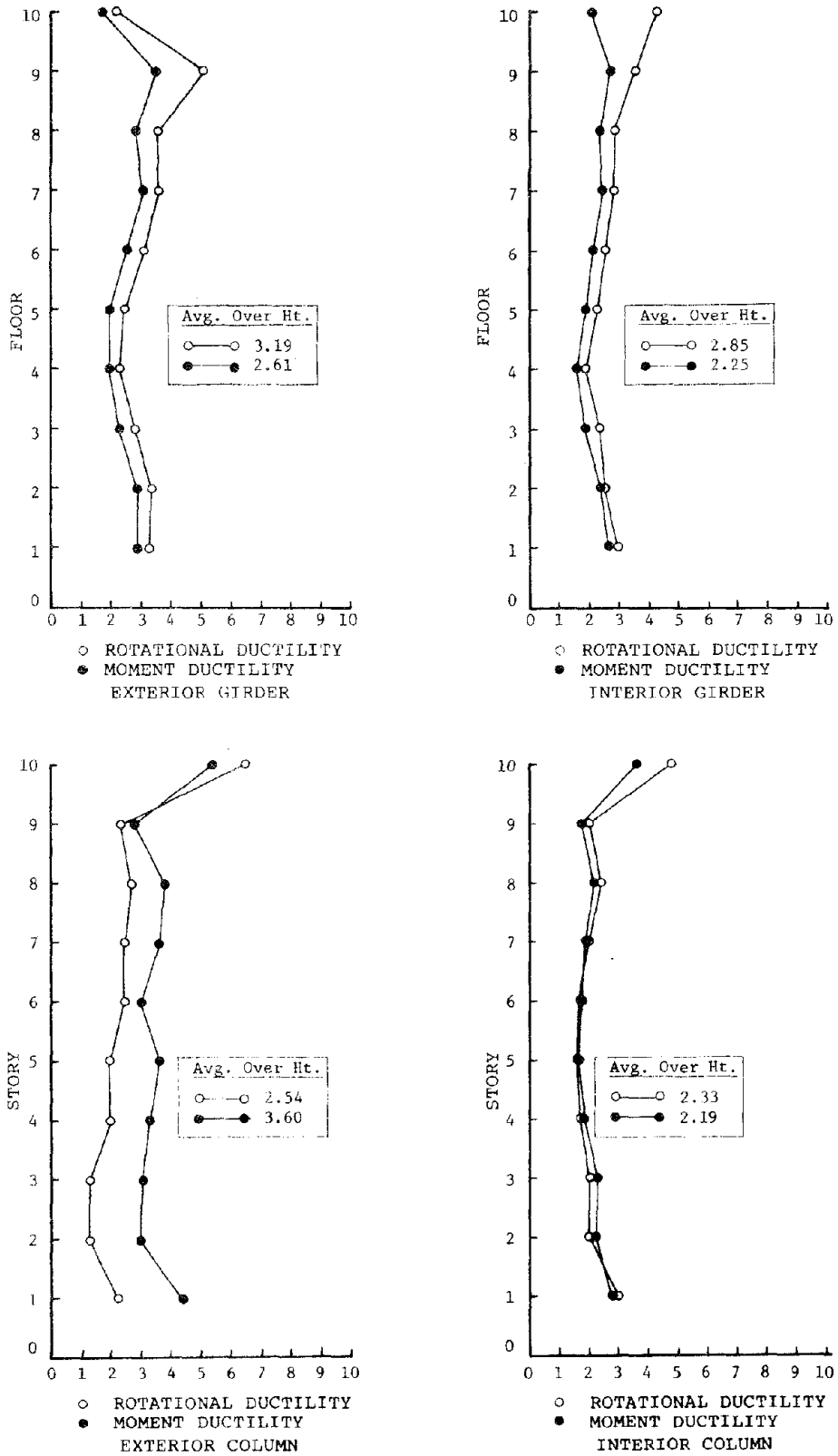
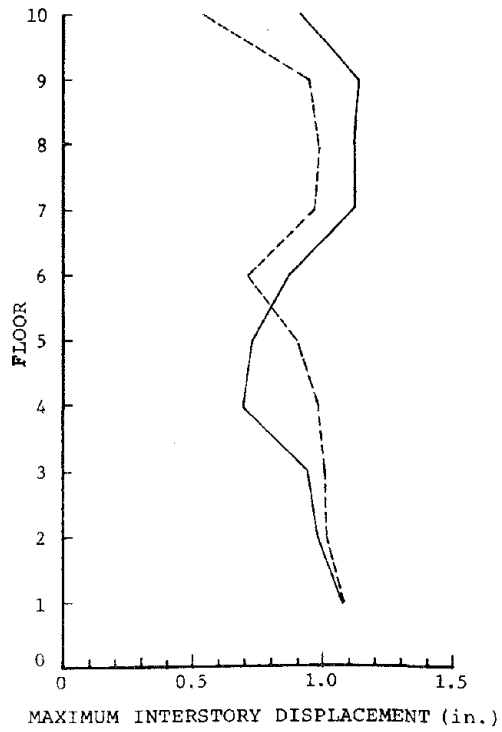
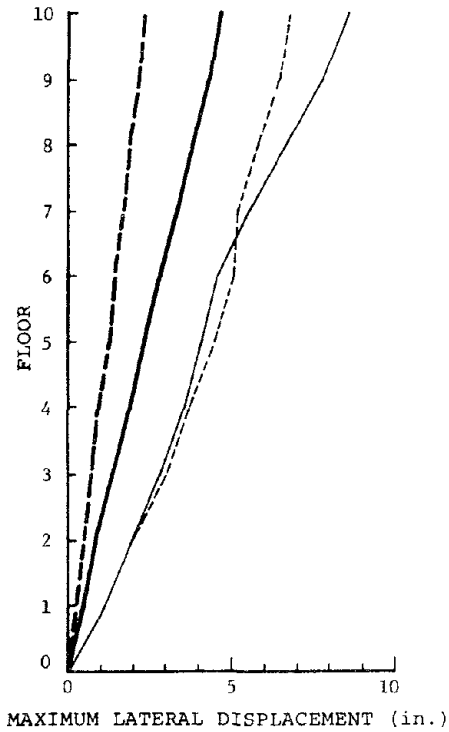
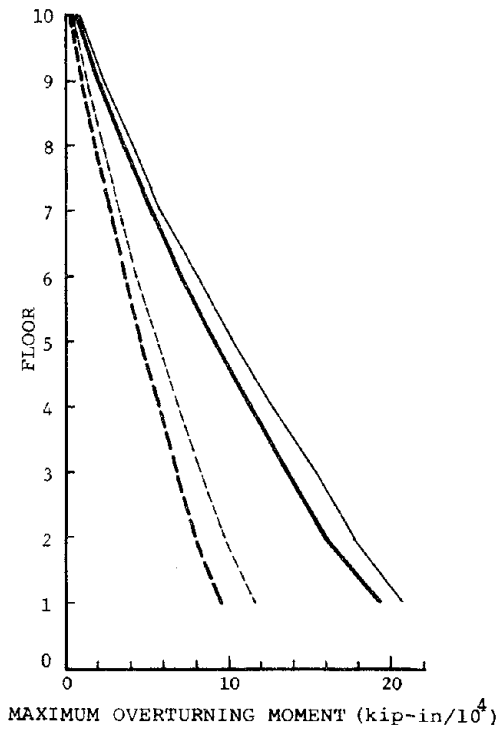
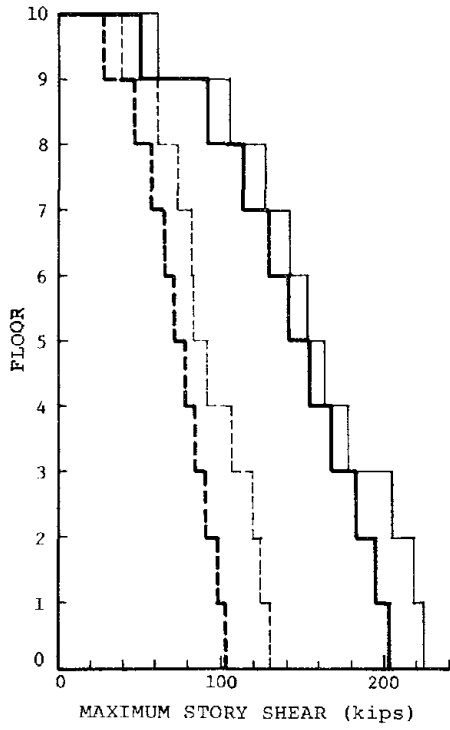


FIGURE 4.2.2 - MAXIMUM DUCTILITY FACTORS FOR GRAVITY AND EARTHQUAKE DESIGN
 $\mu = 2$; 10-Story Frame; Motion 2



— SRSS ($\mu = 2$) - - - SRSS ($\mu = 4$) ——— motion 2 ($\mu = 2$) - - - - motion 2 ($\mu = 4$)

FIGURE 4.2.3 - MAXIMUM STORY LEVEL PARAMETERS FOR GRAVITY AND EARTHQUAKE DESIGN
 $\mu = 2$; 10-Story Frame; Motion 2

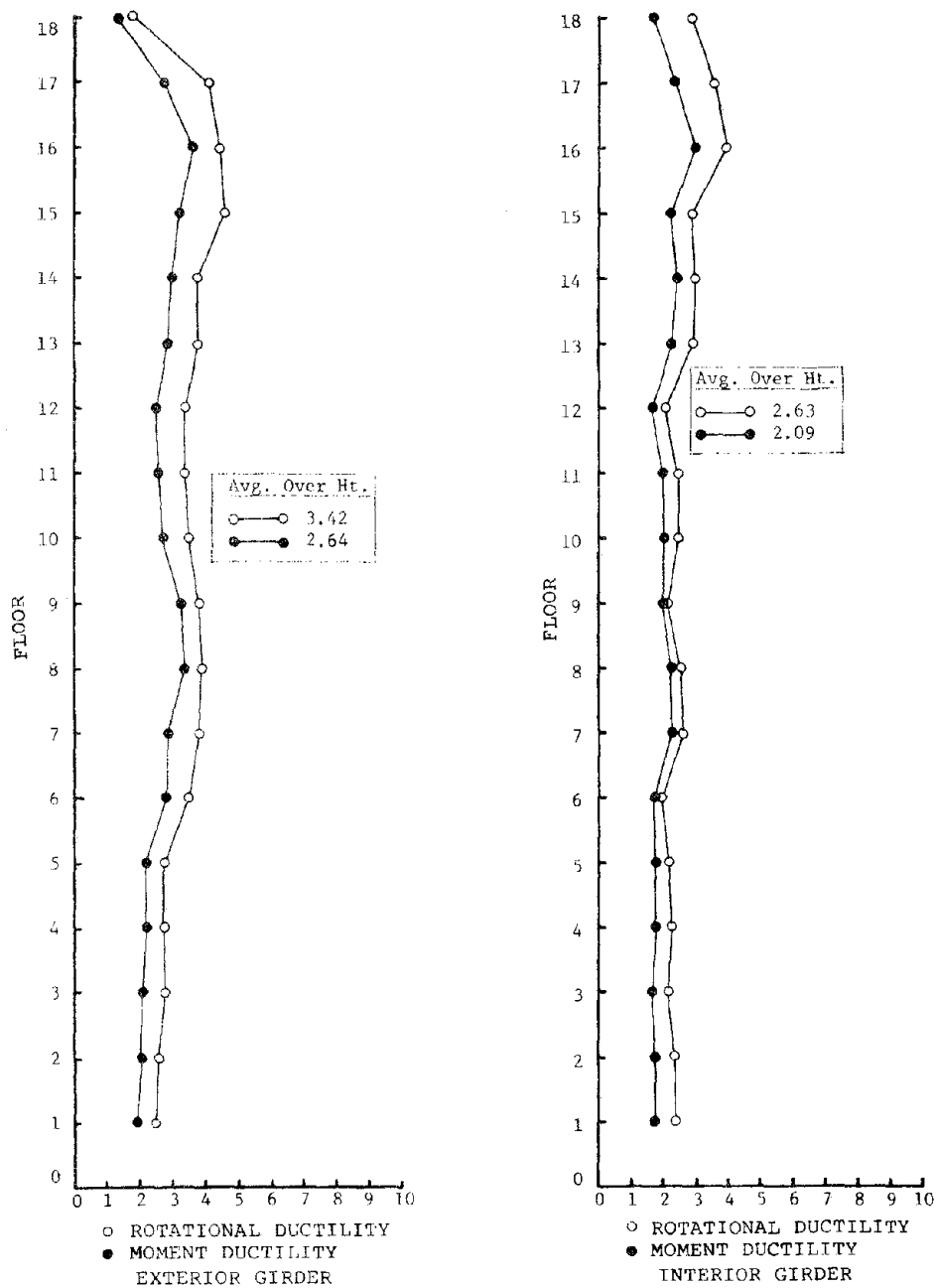


FIGURE 4.2.4 - MAXIMUM GIRDER DUCTILITY FACTORS FOR GRAVITY AND EARTHQUAKE DESIGN
 $\mu = 2$; 18-Story Frame; Motion 2

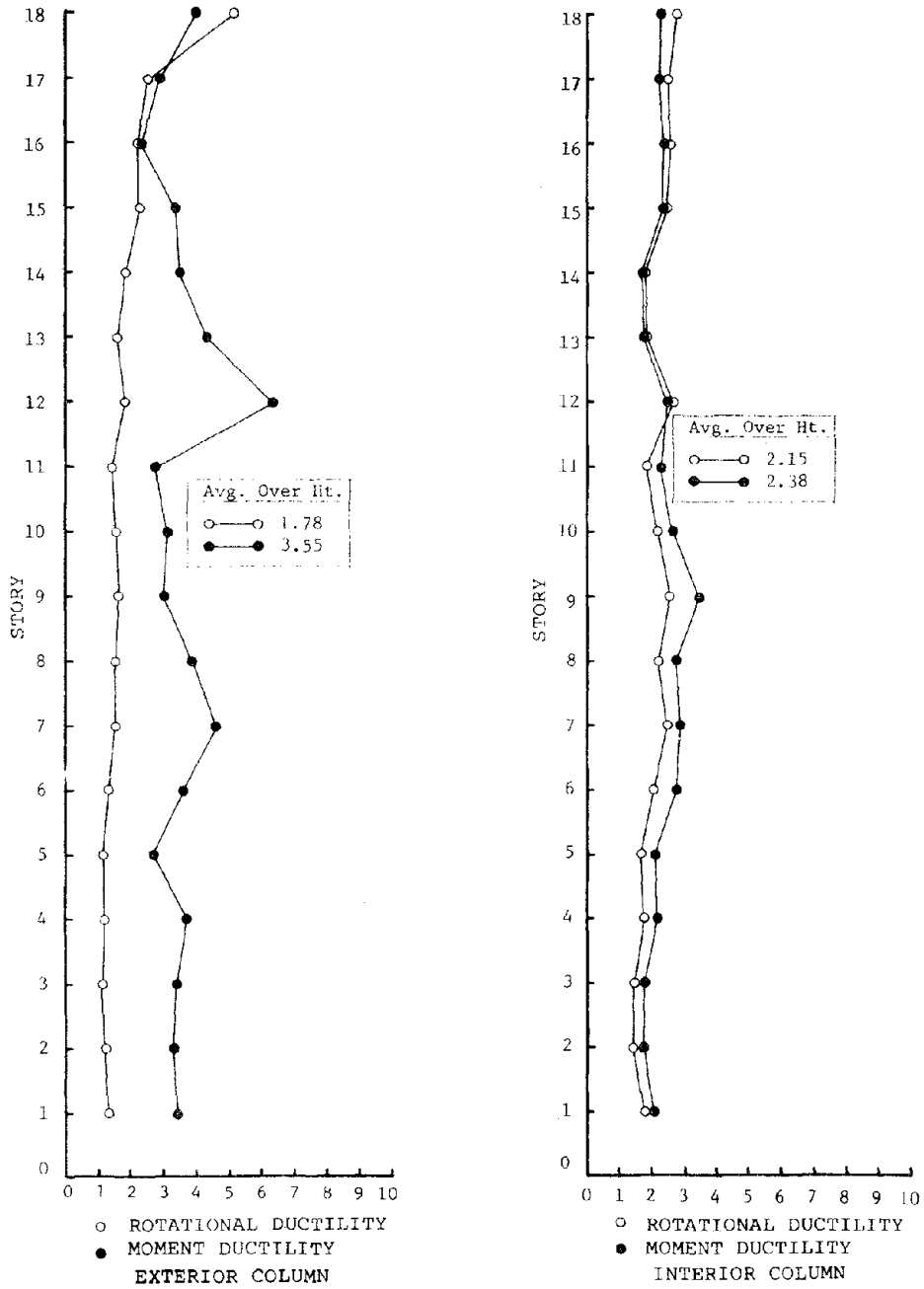
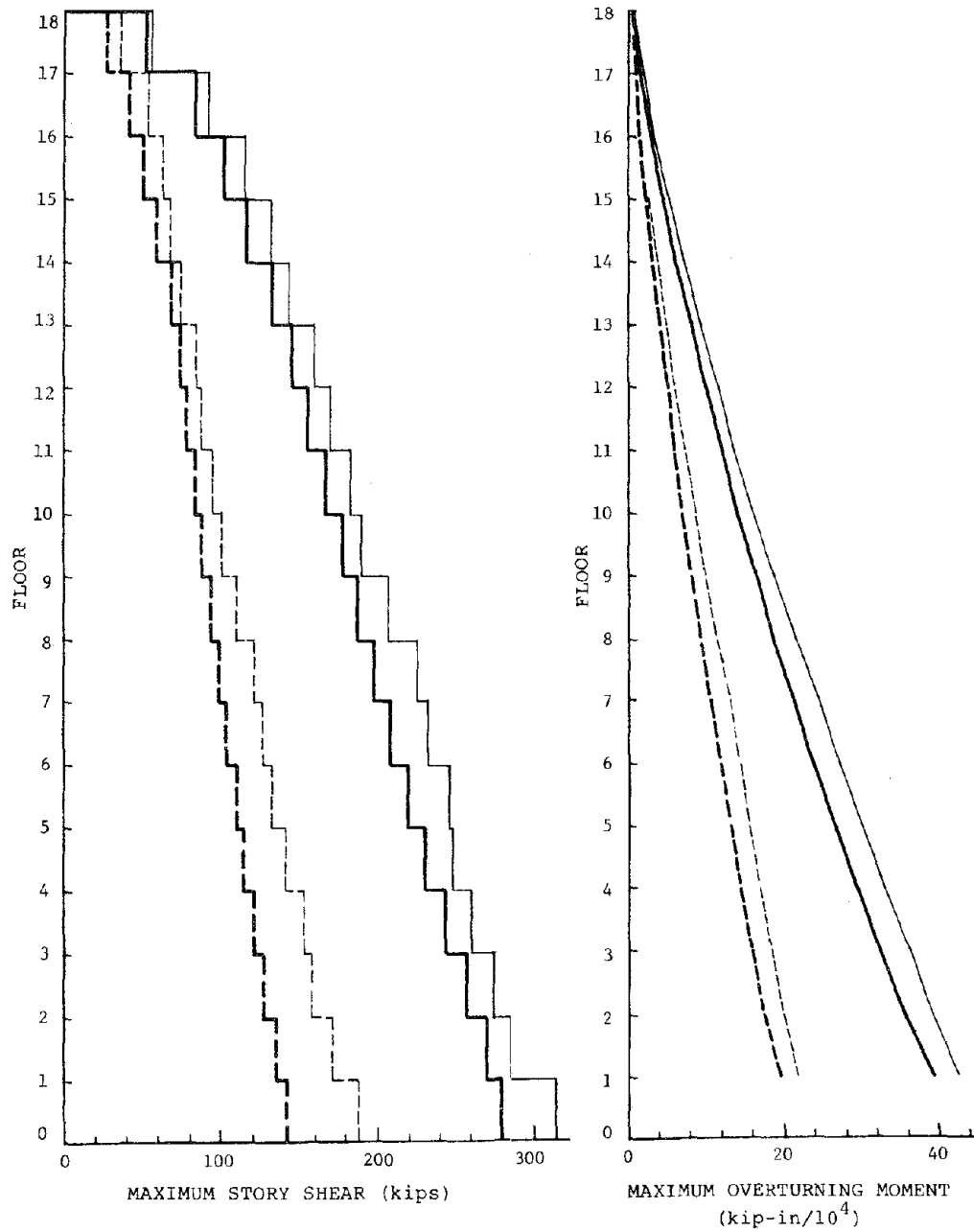
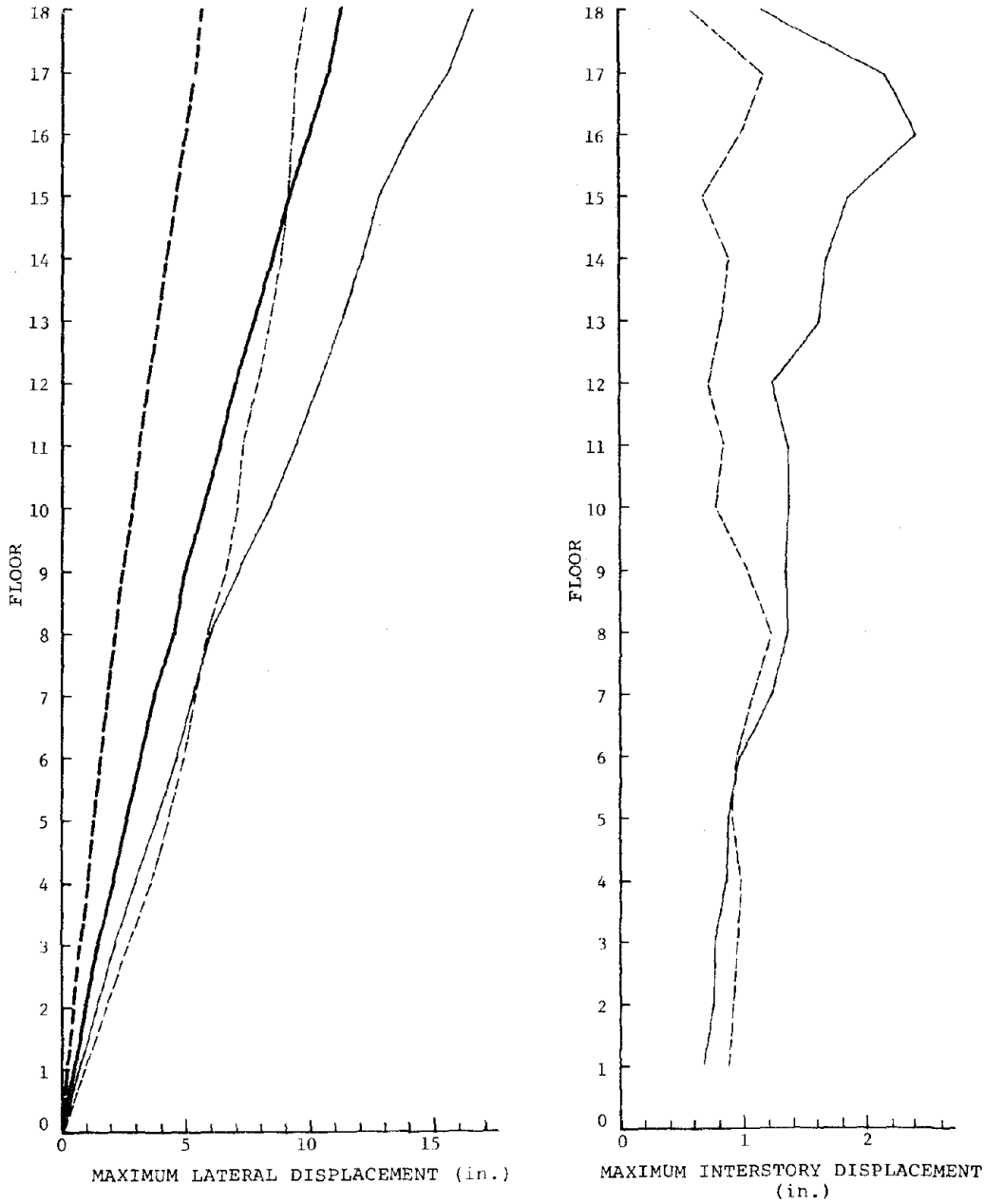


FIGURE 4.2.5 - MAXIMUM COLUMN DUCTILITY FACTORS FOR GRAVITY AND EARTHQUAKE DESIGN
 $\mu = 2$; 18-Story Frame; Motion 2



— SRSS ($\mu = 2$) - - - - SRSS ($\mu = 4$) - - - - motion 2 ($\mu = 2$) - - - - motion 2 ($\mu = 4$)

FIGURE 4.2.6 - MAXIMUM FORCES FOR GRAVITY AND EARTHQUAKE DESIGN
 $\mu = 2$; 18-Story Frame; Motion 2



— SRSS ($\mu = 2$) ---- SRSS ($\mu = 4$) — motion 2 ($\mu = 2$) ---- motion 2 ($\mu = 4$)

FIGURE 4.2.7 - MAXIMUM DISPLACEMENTS FOR GRAVITY AND EARTHQUAKE DESIGN
 $\mu = 2$; 18-Story Frame; Motion 2

TABLE 4.2.1 - AVERAGE DUCTILITY FACTORS FOR GRAVITY AND EARTHQUAKE DESIGN
 $\mu = 2$; 4-Story Frame; Motion 2

LEVEL	ROTATIONAL DUCTILITY		MOMENT DUCTILITY	
	GIRDERS	COLUMNS	GIRDERS	COLUMNS
MOTION 2				
1	2.81	2.10	2.76	1.89
2	2.09	1.74	1.98	1.71
3	2.31	1.90	2.20	1.86
4	2.49	2.70	1.65	2.57

TABLE 4.2.2 - STORY DUCTILITY FACTORS FOR GRAVITY AND EARTHQUAKE DESIGN
 $\mu = 2$; 4-Story Frame; Motion 2

STORY	DUCTILITY FACTOR
MOTION 2	
1	2.5
2	2.3
3	1.9
4	2.2

TABLE 4.2.3 - AVERAGE DUCTILITY FACTORS FOR GRAVITY AND EARTHQUAKE DESIGN
 $\mu = 2$; 10-Story Frame; Motion 2

LEVEL	ROTATIONAL DUCTILITY		MOMENT DUCTILITY	
	GIRDERS	COLUMNS	GIRDERS	COLUMNS
MOTION 2				
1	2.76	1.72	2.71	2.13
2	2.55	1.49	2.51	1.96
3	2.04	1.47	1.99	1.92
4	2.01	1.54	1.67	1.92
5	2.21	1.52	1.85	1.98
6	2.39	1.68	2.19	1.94
7	2.62	1.64	2.49	1.89
8	2.49	1.95	2.40	2.03
9	3.23	1.68	2.78	1.81
10	2.09	3.04	1.30	3.04

TABLE 4.2.4 - STORY DUCTILITY FACTORS FOR GRAVITY AND EARTHQUAKE DESIGN
 $\mu = 2$; 10-Story Frame; Motion 2

STORY	DUCTILITY FACTOR
	MOTION 2
1	2.2
2	2.3
3	2.2
5	1.5
6	1.9
7	2.2
9	2.0
10	—

TABLE 4.2.5 - AVERAGE DUCTILITY FACTORS FOR GRAVITY AND EARTHQUAKE DESIGN
 $\mu = 2$; 18-Story Frame; Motion 2

LEVEL	ROTATIONAL DUCTILITY		MOMENT DUCTILITY	
	GIRDERS	COLUMNS	GIRDERS	COLUMNS
MOTION 2				
1	2.16	1.26	1.63	1.72
2	1.95	1.19	1.65	1.63
3	1.96	1.17	1.70	1.59
4	2.00	1.25	1.76	2.00
5	2.17	1.34	1.84	2.01
6	2.46	1.52	2.09	2.52
7	2.74	1.50	2.41	2.52
8	2.87	1.60	2.63	2.60
9	2.81	1.79	2.46	2.73
10	2.52	1.55	2.24	2.14
11	2.44	1.44	2.16	1.86
12	2.46	1.67	1.89	2.59
13	2.79	1.43	2.30	2.08
14	3.04	1.54	2.47	1.83
15	2.91	1.93	2.48	2.16
16	3.08	1.63	2.85	1.71
17	2.94	1.62	1.96	1.70
18	1.72	2.43	0.99	2.31

TABLE 4.2.6 - STORY DUCTILITY FACTORS FOR GRAVITY AND EARTHQUAKE DESIGN
 $\mu = 2$; 18-Story Frame; Motion 2

STORY	DUCTILITY FACTOR
	MOTION 2
1	1.7
3	1.8
5	1.8
7	2.1
11	1.9
13	1.9
15	2.6
18	

TABLE 4.2.7 - NORMALIZED MAXIMUM DUCTILITY FACTORS FOR 4-STORY FRAME

LEVEL	ROTATIONAL DUCTILITY				MOMENT DUCTILITY			
	$\mu = 2$		$\mu = 4$		$\mu = 2$		$\mu = 4$	
	EXT.	INT.	EXT.	INT.	EXT.	INT.	EXT.	INT.
	GIRDERS							
1	1.65	1.62	1.67	1.65	1.47	1.43	1.48	1.46
2	1.25	1.31	1.39	1.31	1.12	1.07	1.17	1.06
3	1.64	1.50	1.54	1.44	1.28	1.17	1.19	1.08
4	1.74	1.53	1.21	1.00	1.15	0.94	0.45	0.47
	COLUMNS							
1	1.57	1.74	1.14	1.51	1.91	1.38	1.63	1.26
2	1.42	1.31	1.65	1.03	1.09	1.02	1.23	0.97
3	1.08	1.11	1.68	1.31	1.23	1.01	1.68	1.06
4	2.35	2.03	2.27	1.76	1.93	1.51	1.95	1.51

TABLE 4.2.8 - NORMALIZED MAXIMUM DUCTILITY FACTORS FOR 10-STORY FRAME

LEVEL	ROTATIONAL DUCTILITY				MOMENT DUCTILITY			
	$\mu = 2$		$\mu = 4$		$\mu = 2$		$\mu = 4$	
	EXT.	INT.	EXT.	INT.	EXT.	INT.	EXT.	INT.
	GIRDERS							
1	1.66	1.51	1.62	1.54	1.30	1.33	1.54	1.40
2	1.70	1.31	1.67	1.25	1.44	1.18	1.44	1.11
3	1.43	1.18	1.70	1.25	1.16	0.97	1.58	1.10
4	1.13	0.97	1.66	1.27	0.98	0.78	1.54	1.07
5	1.23	1.14	1.11	0.99	1.02	0.95	1.20	0.76
6	1.53	1.30	1.29	0.95	1.32	1.11	1.07	0.80
7	1.79	1.44	1.49	1.23	1.53	1.24	1.42	0.99
8	1.81	1.49	1.64	1.27	1.47	1.22	1.32	0.92
9	2.55	1.78	0.75	0.88	1.77	1.40	0.51	0.43
10	1.11	2.13	0.83	0.31	0.86	1.07	0.27	0.35
	COLUMNS							
1	1.10	1.51	0.99	1.17	2.20	1.38	2.58	1.38
2	0.63	1.02	0.74	0.87	1.52	1.12	1.27	1.20
3	0.67	1.02	0.81	0.82	1.53	1.13	1.52	1.27
4	1.02	0.86	0.75	0.89	1.66	0.90	2.23	1.26
5	1.06	0.80	0.92	0.82	1.82	0.79	1.55	1.09
6	1.23	0.85	0.96	0.67	1.51	0.83	1.24	0.81
7	1.24	1.01	1.10	0.98	1.78	0.95	1.56	1.21
8	1.34	1.20	1.13	0.93	1.89	1.11	1.53	1.14
9	1.15	1.02	1.42	1.11	1.39	0.91	1.55	1.24
10	3.25	2.38	1.48	1.12	2.68	1.81	1.69	1.34

TABLE 4.2.9 - NORMALIZED MAXIMUM DUCTILITY FACTORS FOR 18-STORY FRAME

LEVEL	ROTATIONAL DUCTILITY				MOMENT DUCTILITY			
	$\mu = 2$		$\mu = 4$		$\mu = 2$		$\mu = 4$	
	EXT.	INT.	EXT.	INT.	EXT.	INT.	EXT.	INT.
GIRDERS								
1	1.27	1.20	1.50	1.37	0.94	0.85	1.26	1.13
2	1.33	1.19	1.52	1.26	0.99	0.89	1.23	0.99
3	1.40	1.11	1.55	1.13	1.05	0.86	1.25	0.92
4	1.43	1.15	1.54	1.17	1.09	0.89	1.22	0.94
5	1.40	1.11	1.61	1.00	1.12	0.88	1.20	0.82
6	1.75	1.01	1.64	0.88	1.40	0.92	1.28	0.78
7	1.90	1.30	1.83	1.13	1.45	1.14	1.40	0.95
8	1.96	1.29	1.84	1.01	1.68	1.17	1.44	0.91
9	1.91	1.09	1.39	0.75	1.64	1.04	0.98	0.62
10	1.74	1.26	1.32	0.86	1.37	1.06	0.94	0.68
11	1.71	1.19	1.16	0.82	1.31	1.03	0.81	0.61
12	1.22	1.07	1.30	0.84	1.27	0.86	0.95	0.64
13	1.88	1.49	1.26	0.84	1.49	1.17	0.82	0.63
14	1.89	1.48	0.95	0.75	1.50	1.26	0.61	0.55
15	2.33	1.46	0.62	0.74	1.58	1.14	1.45	0.50
16	2.25	1.98	0.71	0.66	1.79	1.54	0.53	0.45
17	2.05	1.80	0.49	0.57	1.38	1.21	0.39	0.37
18	0.89	1.44	0.35	0.36	0.71	0.87	0.31	0.30
COLUMNS								
1	0.66	0.90	0.56	0.76	1.71	1.07	2.43	1.17
2	0.58	0.71	0.40	0.55	1.66	0.93	0.96	0.98
3	0.56	0.73	0.38	0.62	1.69	0.90	1.15	1.41
4	0.59	0.90	0.38	0.67	1.84	1.11	1.43	1.51
5	0.57	0.86	0.37	0.68	1.33	1.06	0.91	1.31
6	0.66	1.06	0.40	0.72	1.82	1.42	1.01	1.64
7	0.74	1.27	0.44	0.79	2.32	1.48	1.20	1.54
8	0.75	1.09	0.44	0.80	1.94	1.39	1.39	1.61
9	0.82	1.28	0.62	0.86	1.49	1.77	1.89	1.70
10	0.75	1.12	0.56	0.64	1.56	1.35	1.10	0.89
11	0.68	0.96	0.47	0.60	1.36	1.15	1.03	0.90
12	0.91	1.35	0.48	0.67	3.18	1.28	0.99	0.94
13	0.81	0.99	0.44	0.55	2.15	0.90	0.92	0.68
14	0.90	0.92	0.49	0.54	1.76	0.90	1.40	0.76
15	1.12	1.25	0.76	0.50	1.64	1.19	1.26	0.87
16	1.11	1.33	0.78	0.54	1.06	1.18	1.04	0.85
17	1.27	1.25	1.17	0.77	1.44	1.11	1.64	1.09
18	2.56	1.40	1.04	0.68	2.02	1.16	1.03	0.83

4.3 Results for Analyses Ignoring Gravity Effects

Several studies have been performed on the inelastic behavior of tall buildings which have neglected the presence of static gravity loads in the analysis of member systems (14, 15, 17, 23). This section compares the results of analyses with and without gravity for the same frame design.

The 4- and 10-story frames tested are those designed in Section 4.1 for gravity and seismic loads at a ductility of 4. Strength properties are listed in Appendix B.

Comparisons of the maximum moment and rotational ductility factors for columns and girders are shown in Figures 4.3.1 to 4.3.4, 4.3.6, and 4.3.8 for the three motions.

Column ductilities decrease at nearly every location without gravity. The largest difference occurs at the bottom of the 10-story frame and is about 12 for μ_M . The pattern of yielding alters significantly in both frames. Columns remain elastic over much of the height in the 10-story frame. Yielding in the girders is generally less at the top and bottom floors in the absence of gravity, but the effect is much less than in the case of columns.

Both definitions of member ductility give similar results without gravity. The two factors contributing to these observations are: the frame tends to deform symmetrically under lateral load alone which improves the accuracy of the approximation for the yield rotation in the definition of μ_R ; secondly, the effects of axial-flexural interaction, only considered for μ_M , decrease in importance. These deficiencies in the definition of μ_R (i.e., does not include interaction and has arbitrary yield rotation) suggest that μ_M may provide a better index

of inelastic deformation.

The story shears and overturning moments increase without gravity due to the reduction of inelastic action, as seen in Figures 4.3.1 to 4.3.3, 4.3.5, 4.3.7 and 4.3.9. Lateral and interstory displacements illustrate the importance of the distribution of ductility in determining the overall structural deformation. There is a decrease in lateral displacement corresponding to the large change in column ductility in the lower levels of the frames, emphasizing the importance of local column deformations in controlling response at the story level.

The average ductility for all column cross-sections in a story and all girder cross-sections in a floor further points out the shift in location of yielding throughout the frames, as indicated by comparing Tables 4.3.1 to 4.1.1 and 4.3.3 to 4.1.3.

Comparison of Tables 4.3.2 to 4.1.2 and 4.3.4 to 4.1.4, which summarize the story ductility factors with and without gravity, demonstrate a similar shift in location of nonlinear deformation at the story level.

All of these results serve to indicate the importance of including gravity effects in non-linear analysis.

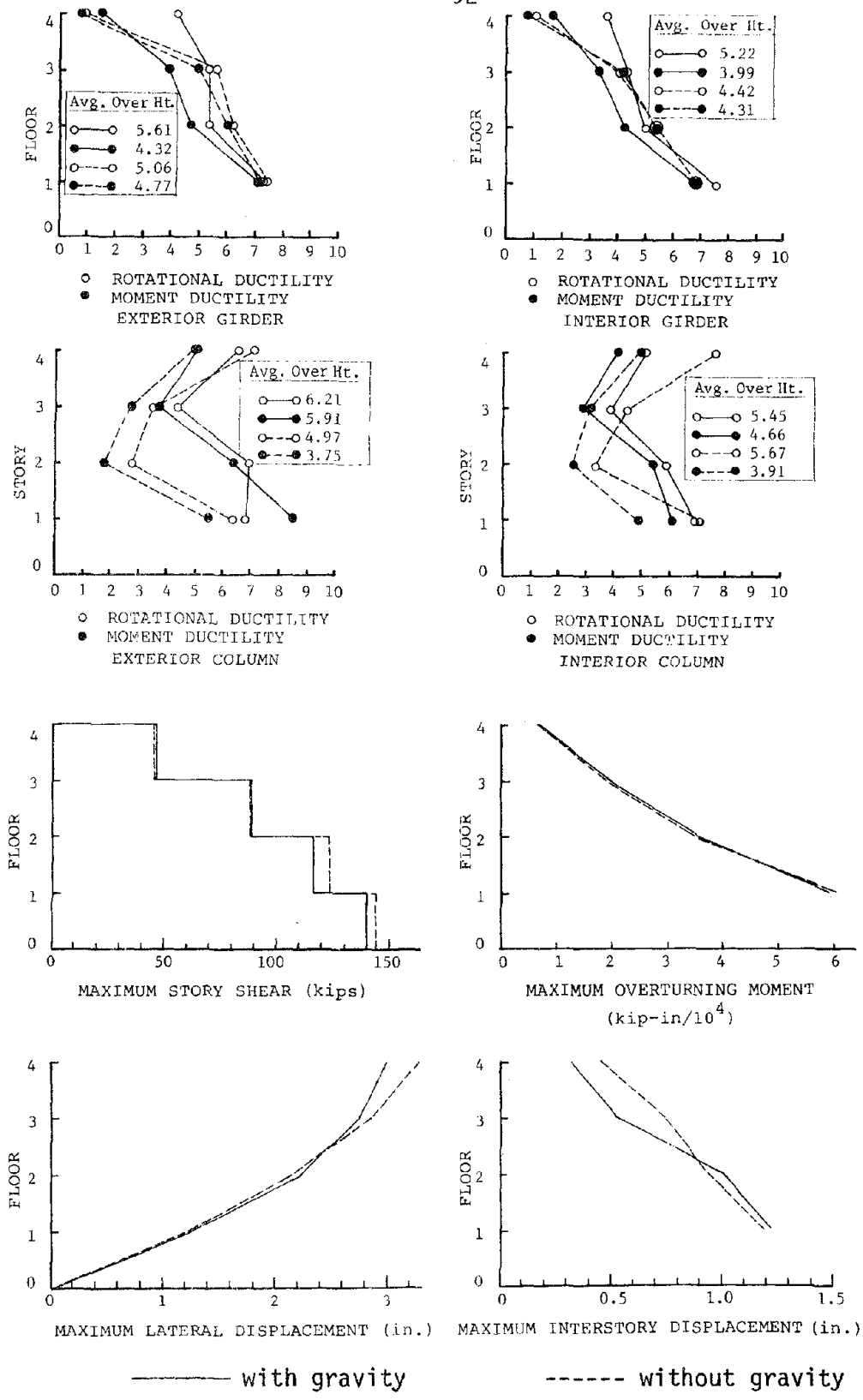


FIGURE 4.3.1 - MAXIMUM RESPONSE PARAMETERS FOR ANALYSIS WITHOUT GRAVITY
 $\mu = 4$; 4-Story Frame; Motion 1

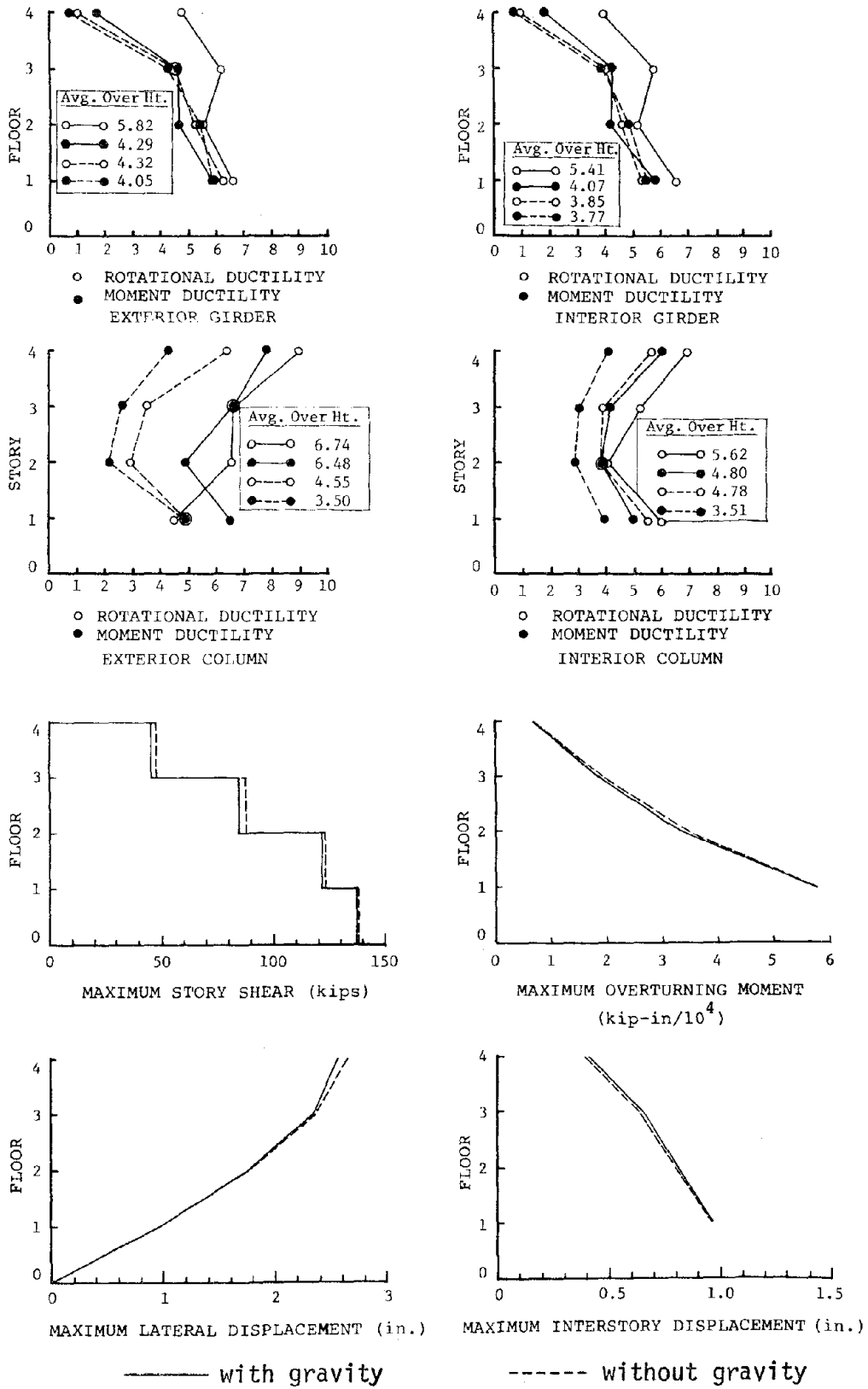
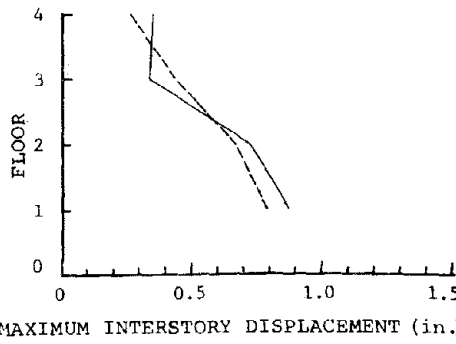
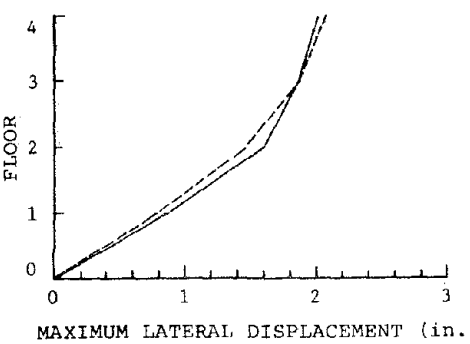
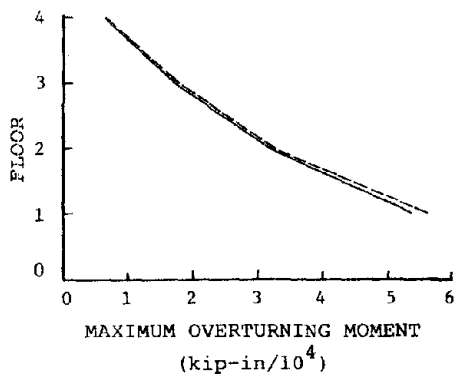
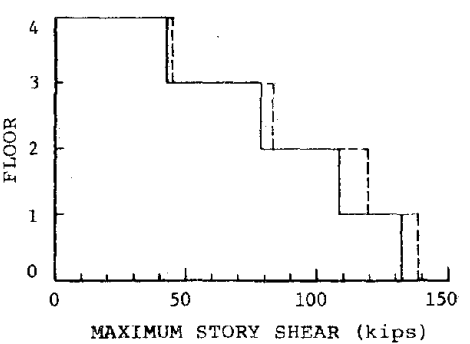
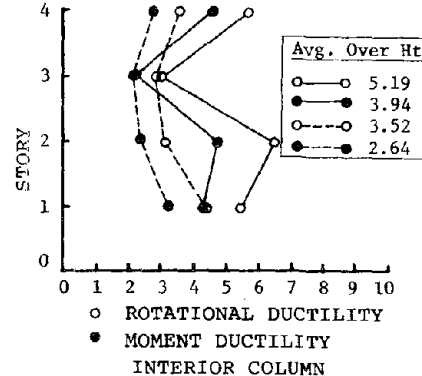
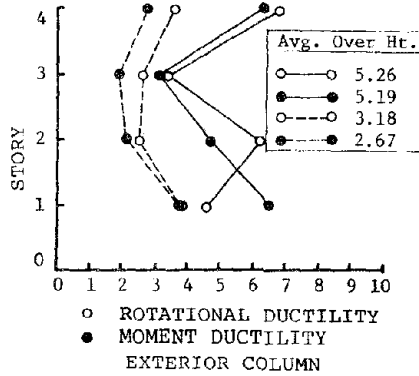
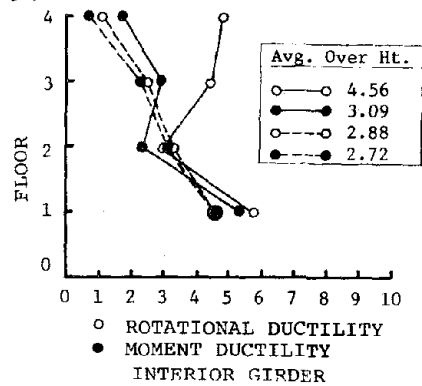
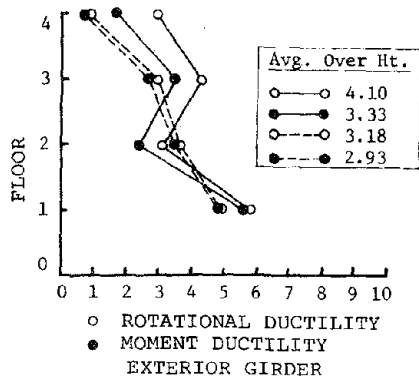
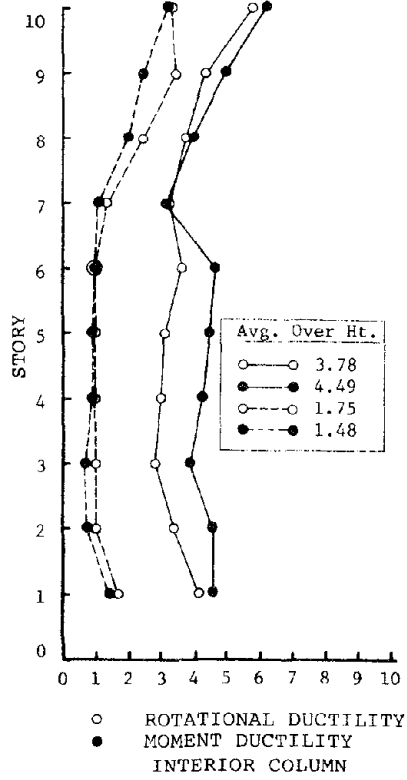
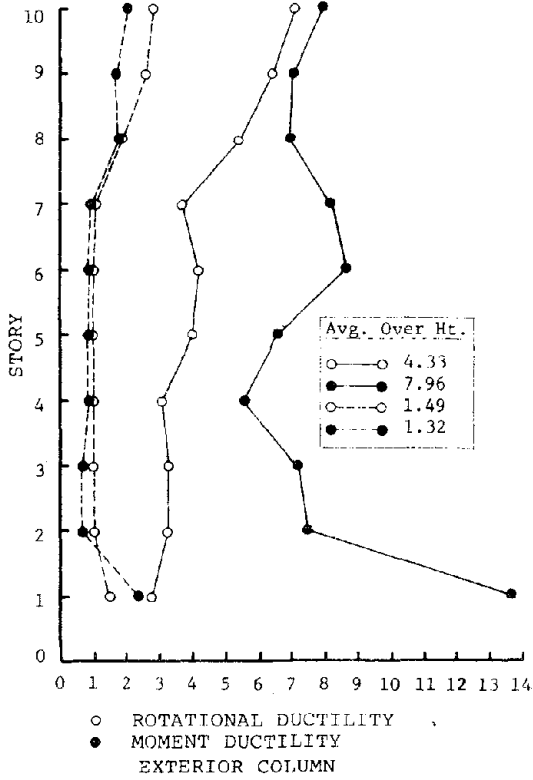
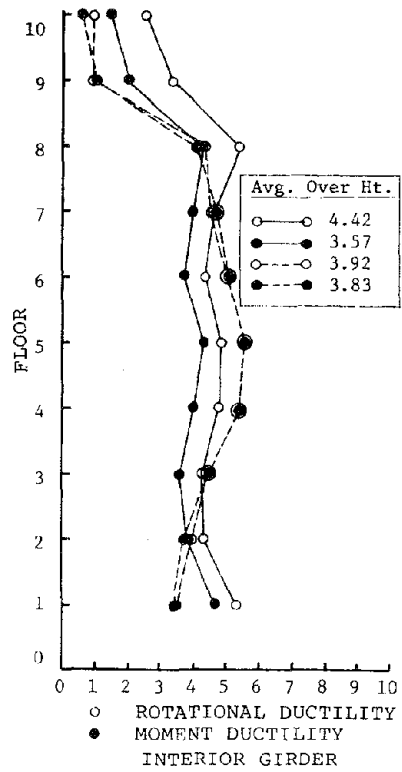
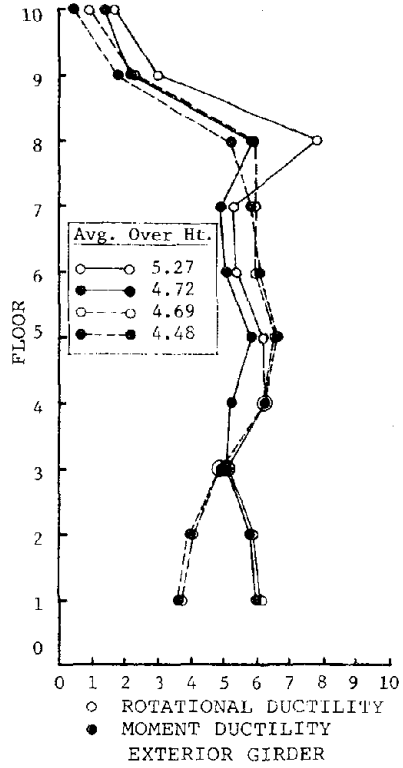


FIGURE 4.3.2 - MAXIMUM RESPONSE PARAMETERS FOR ANALYSIS WITHOUT GRAVITY
 $\mu = 4$; 4-Story Frame; Motion 2



— with gravity - - - - - without gravity

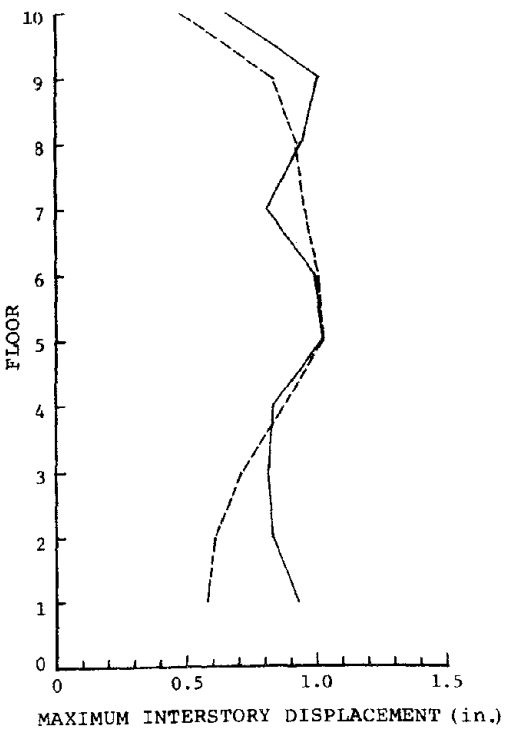
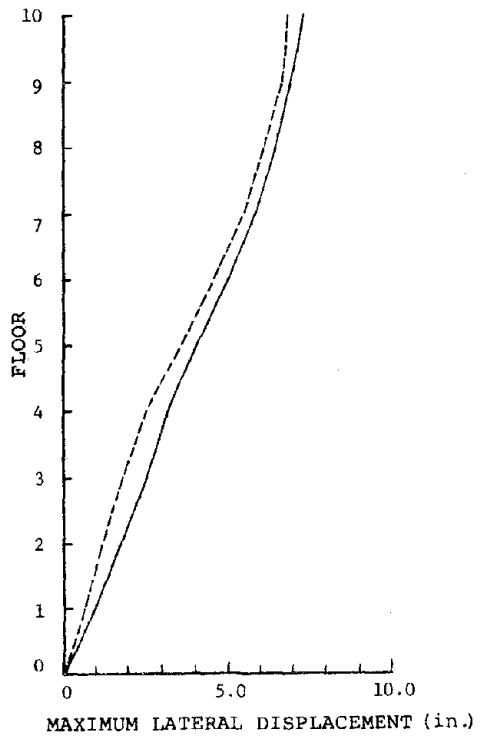
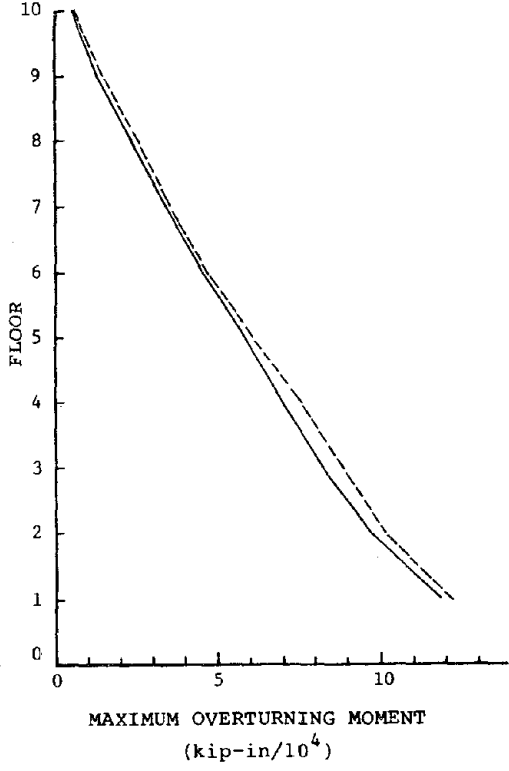
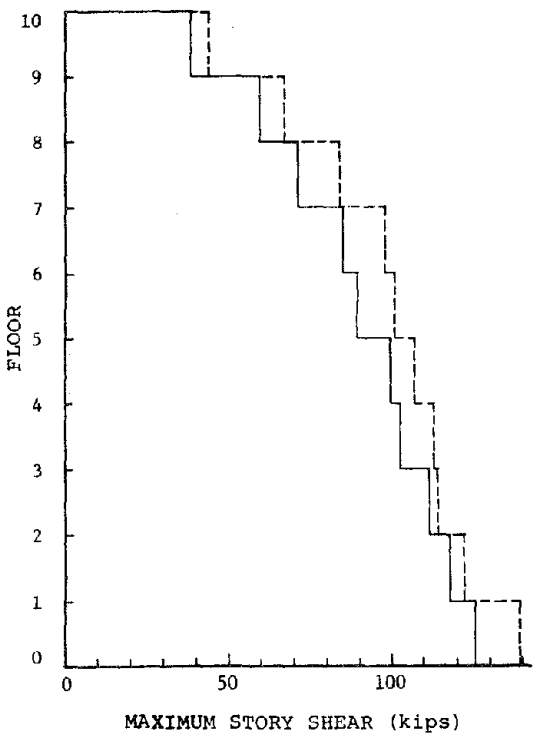
FIGURE 4.3.3 - MAXIMUM RESPONSE PARAMETERS FOR ANALYSIS WITHOUT GRAVITY
 $\mu = 4$; 4-Story Frame; Motion 3



———— with gravity

----- without gravity

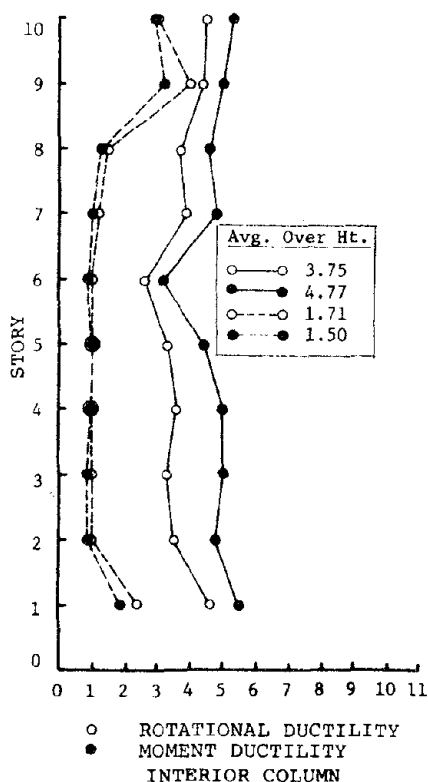
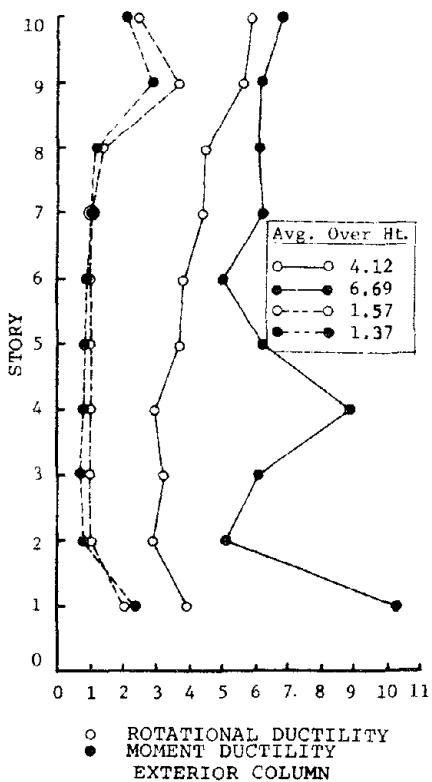
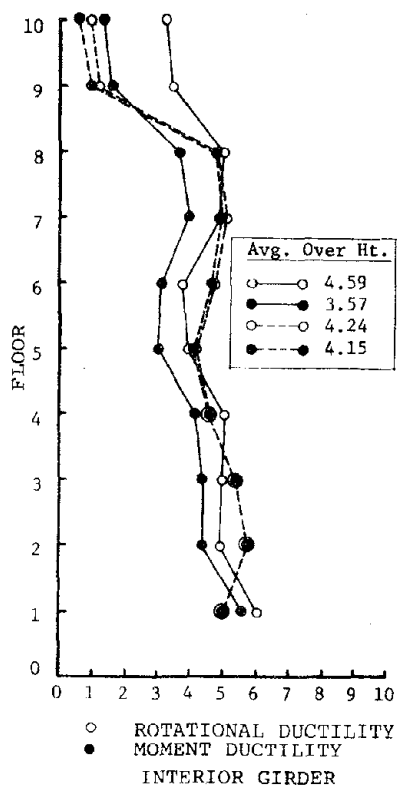
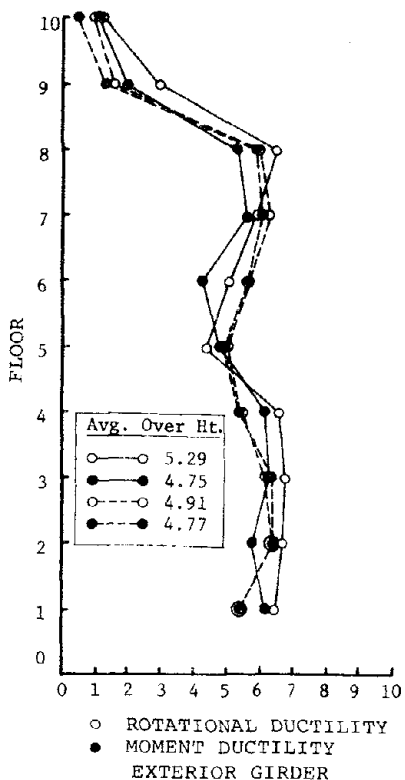
FIGURE 4.3.4 - MAXIMUM DUCTILITY FACTORS FOR ANALYSIS WITHOUT GRAVITY
 $\mu = 4$; 10-Story Frame; Motion 1



———— with gravity

----- without gravity

FIGURE 4.3.5 - MAXIMUM STORY LEVEL PARAMETERS FOR ANALYSIS WITHOUT GRAVITY
 $\mu = 4$; 10-Story Frame; Motion 1



———— with gravity

----- without gravity

FIGURE 4.3.6 - MAXIMUM DUCTILITY FACTORS FOR ANALYSIS WITHOUT GRAVITY
 $\mu = 4$; 10-Story Frame; Motion 2

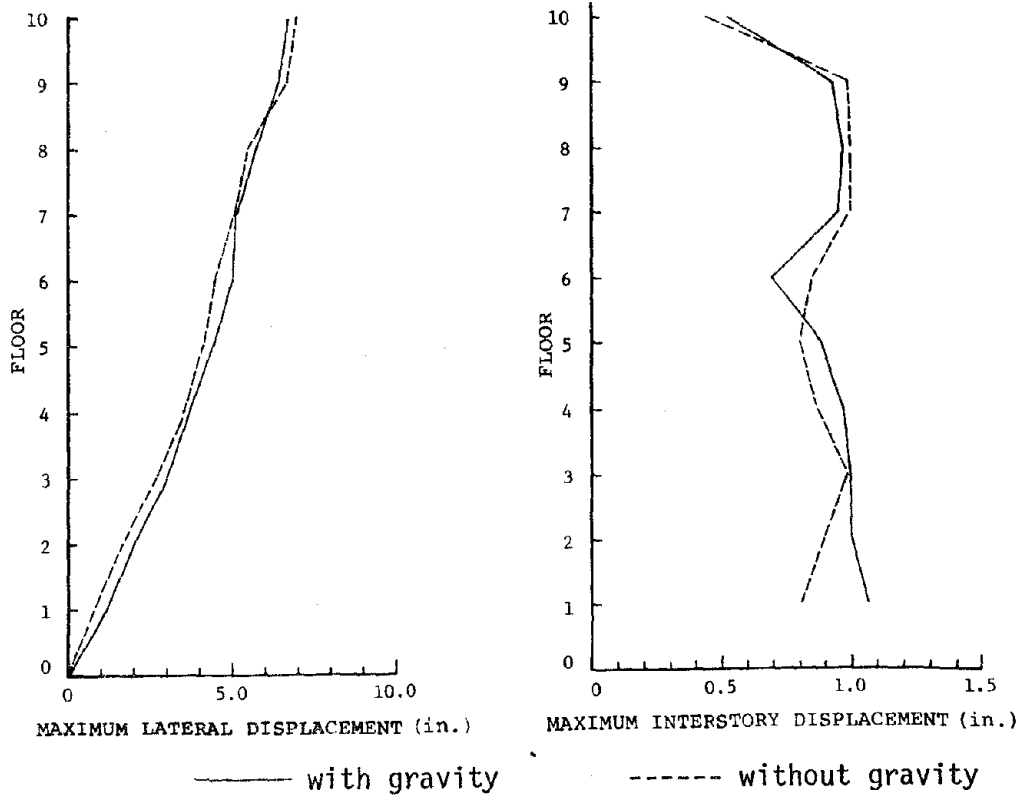
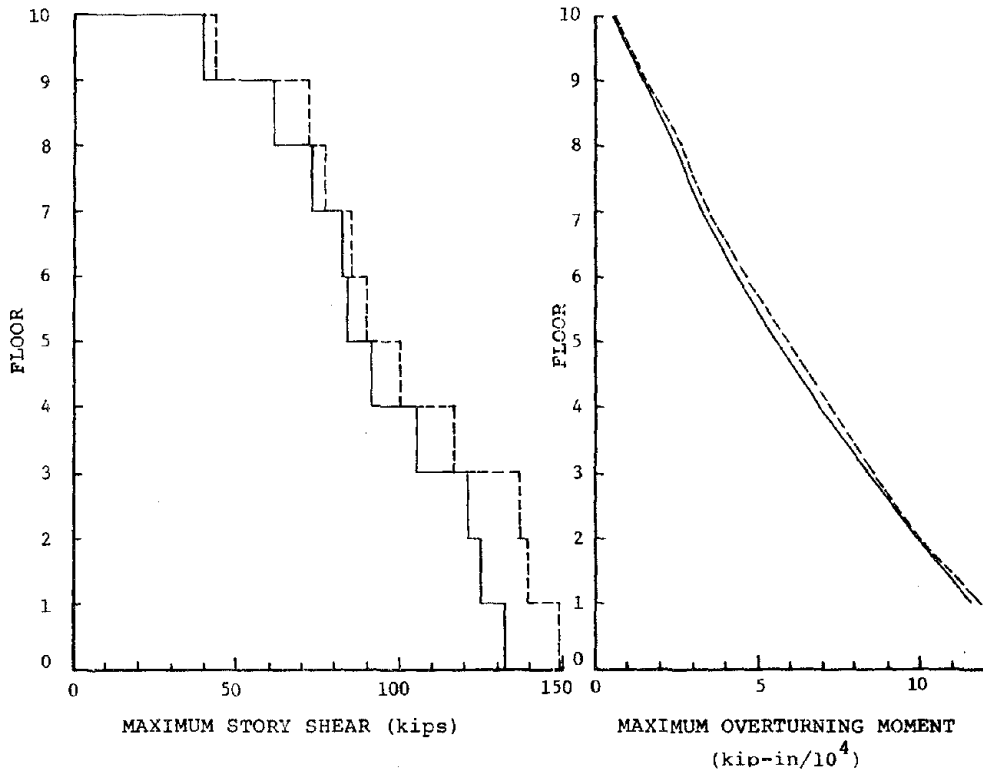
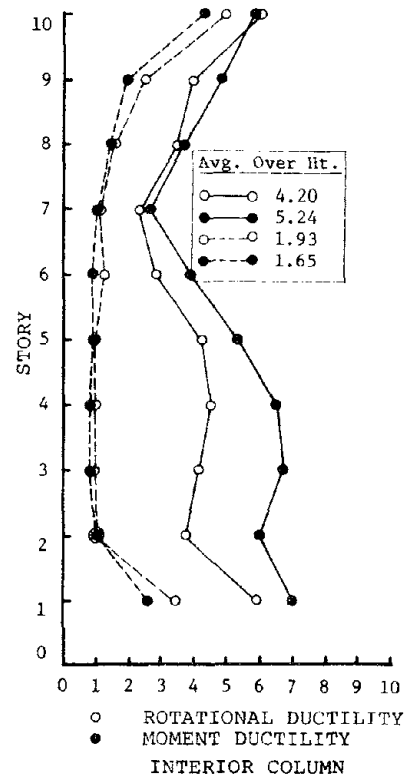
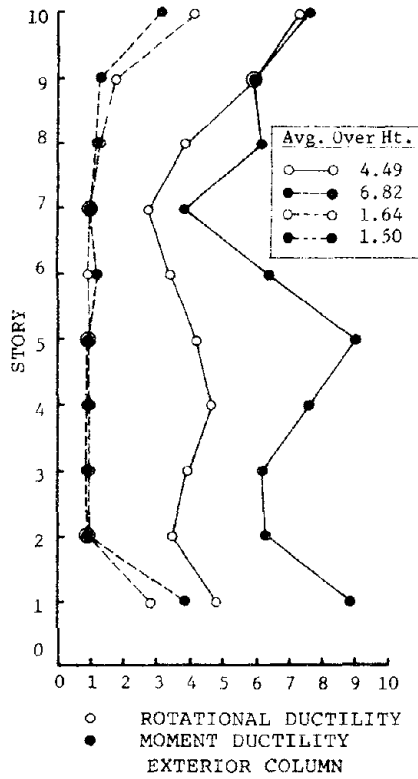
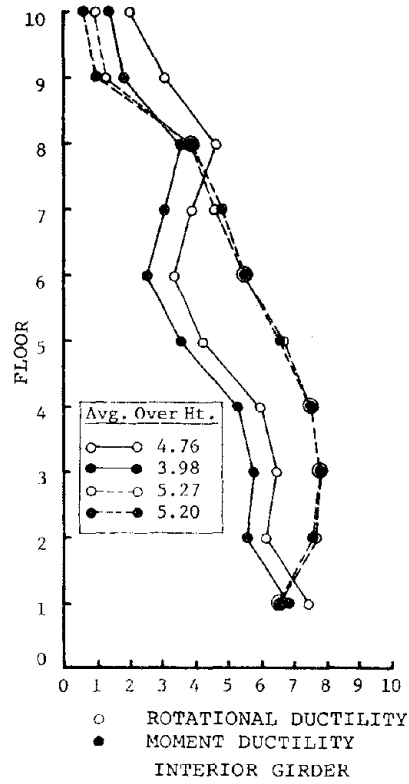
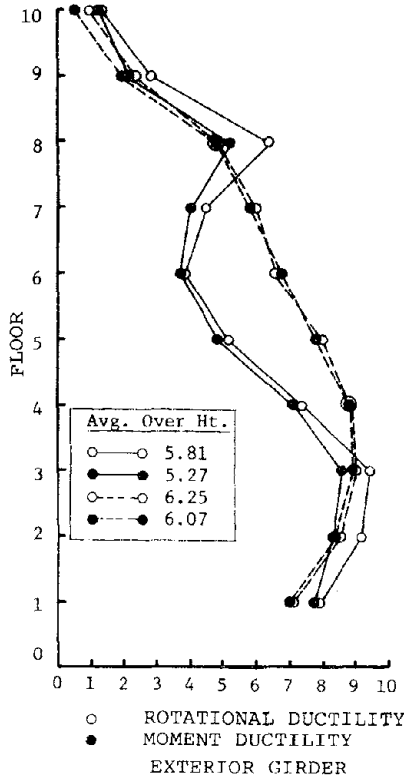


FIGURE 4.3.7 - MAXIMUM STORY LEVEL PARAMETERS FOR ANALYSIS WITHOUT GRAVITY
 $\mu = 4$; 10-Story Frame; Motion 2



———— with gravity

----- without gravity

FIGURE 4.3.8 - MAXIMUM DUCTILITY FACTORS FOR ANALYSIS WITHOUT GRAVITY
 $\mu = 4$; 10-Story Frame; Motion 3

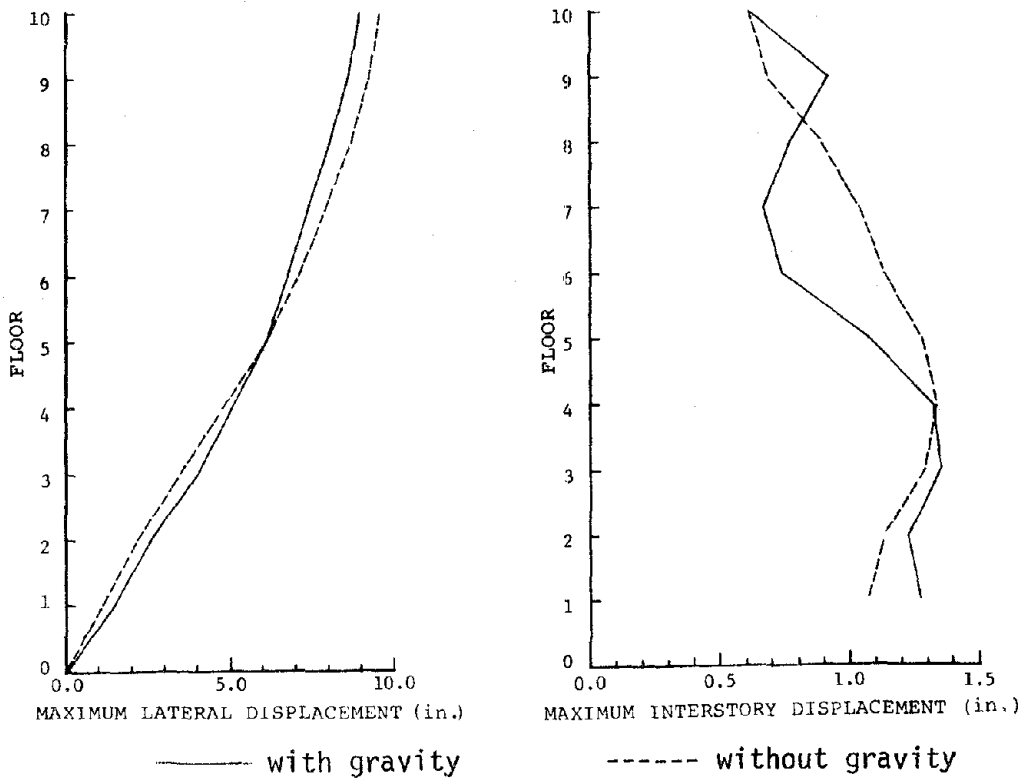
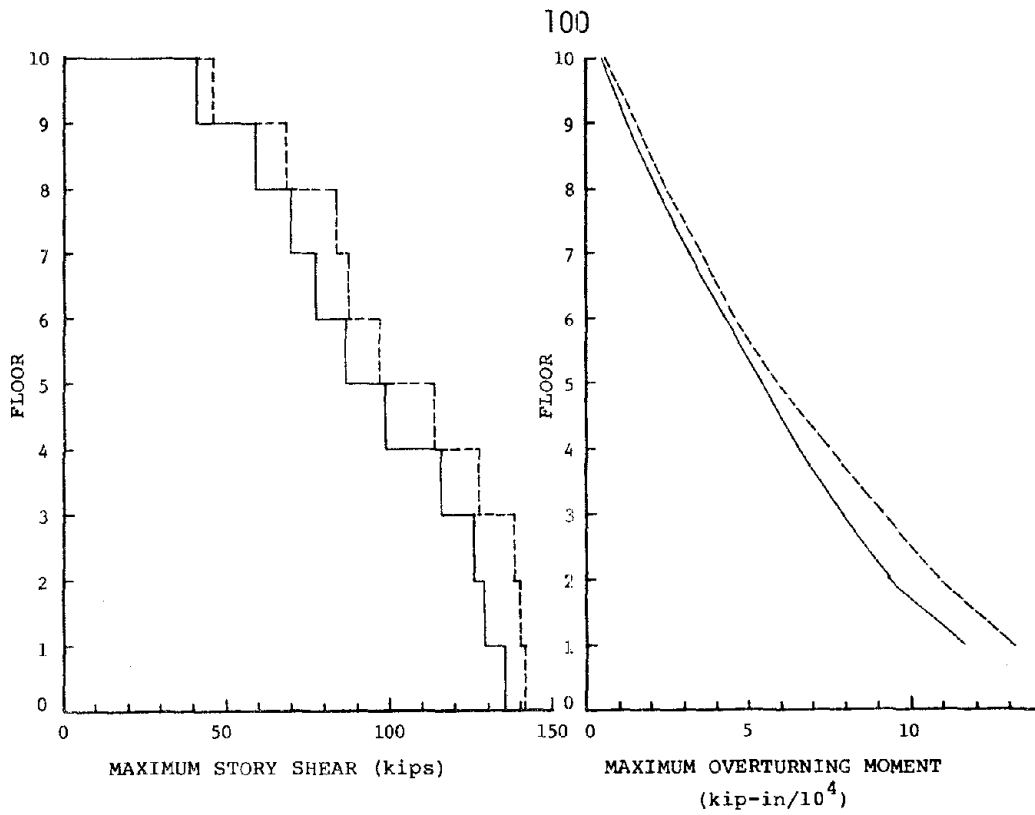


FIGURE 4.3.9 - MAXIMUM STORY LEVEL PARAMETERS FOR ANALYSIS WITHOUT GRAVITY
 $\mu = 4$; 10-Story Frame; Motion 3

TABLE 4.3.1 - AVERAGE DUCTILITY FACTORS FOR ANALYSIS WITHOUT GRAVITY
 $\mu = 4$; 4-Story Frame; Motions 1, 2, 3

LEVEL	ROTATIONAL DUCTILITY		MOMENT DUCTILITY	
	GIRDERS	COLUMNS	GIRDERS	COLUMNS
MOTION 1				
1	7.14	3.88	7.02	3.31
2	5.89	2.09	5.79	1.69
3	4.82	2.94	4.71	2.52
4	1.00	4.59	0.76	3.99
MOTION 2				
1	5.80	3.19	5.73	2.72
2	5.15	2.45	5.19	2.07
3	4.41	3.11	4.13	2.51
4	1.00	4.06	0.72	3.37
MOTION 3				
1	4.84	2.56	4.75	2.19
2	3.47	1.99	3.38	1.65
3	2.75	1.95	2.52	1.76
4	1.00	2.62	0.72	2.38

TABLE 4.3.2 - STORY DUCTILITY FACTORS FOR ANALYSIS WITHOUT GRAVITY
 $\mu = 4$; 4-Story Frame; Motions 1, 2, 3

STORY	DUCTILITY FACTOR		
	MOTION 1	MOTION 2	MOTION 3
1	4.8	3.9	3.2
2	4.5	3.8	3.2
3	4.2	3.7	2.5
4	4.1	3.5	2.4

TABLE 4.3.3 - AVERAGE DUCTILITY FACTORS FOR ANALYSIS WITHOUT GRAVITY
 $\mu = 4$; 10-Story Frame; Motions 1, 2, 3

LEVEL	ROTATIONAL DUCTILITY		MOMENT DUCTILITY	
	GIRDERS	COLUMNS	GIRDERS	COLUMNS
MOTION 1				
1	3.62	1.30	3.56	1.26
2	4.04	1.00	3.97	0.72
3	4.90	1.00	4.80	0.72
4	5.99	1.00	5.94	0.83
5	6.21	1.00	6.26	0.85
6	5.71	1.01	5.75	0.94
7	5.40	1.17	5.40	1.04
8	5.16	1.65	4.78	1.55
9	1.43	2.04	1.27	1.70
10	1.00	2.69	0.55	2.35
MOTION 2				
1	5.26	1.64	5.25	1.42
2	6.18	1.00	6.20	0.79
3	5.90	1.00	5.91	0.79
4	5.09	1.00	5.12	0.81
5	4.72	1.00	4.63	0.82
6	5.40	1.00	5.34	0.87
7	5.86	1.04	5.78	0.93
8	5.68	1.25	5.55	1.16
9	1.32	2.84	1.17	2.56
10	1.00	2.39	0.52	2.35
MOTION 3				
1	6.97	2.11	6.88	1.92
2	8.11	1.00	8.05	0.83
3	8.58	1.00	8.56	0.83
4	8.45	1.00	8.34	0.83
5	7.44	1.00	7.44	0.86
6	6.21	1.09	6.30	0.94
7	5.49	1.06	5.49	1.02
8	4.45	1.27	4.52	1.16
9	1.56	1.61	1.38	1.29
10	1.00	4.00	0.52	3.45

TABLE 4.3.4 - STORY DUCTILITY FACTORS FOR ANALYSIS WITHOUT GRAVITY
 $\mu = 4$; 10-Story Frame; Motions 1, 2, 3

STORY	DUCTILITY FACTOR		
	MOTION 1	MOTION 2	MOTION 3
1	2.1	2.9	3.9
4	3.8	3.8	5.8
7	3.4	3.6	3.7
10	2.4	2.2	3.0

4.4 Results for Designs Ignoring Gravity Effects

The 4- and 10-story frames were designed and subsequently analyzed for the three motions without considering gravity effects. Resistances were proportioned, as discussed in Section 2.4, with the following exceptions: the $wl^2/8$ condition did not apply for the girders, the gravity axial load was not added to increase column strength, and only spectral end moments were used in the interaction equation. A design ductility level of 4 was used to relate the results with those of Section 4.1. Strength properties for the 2 frames are given in Appendix B.

Some shift in the pattern of yielding is observed for each motion. This can be seen by comparison of the maximum local ductility vs. height. (See Figures 4.4.1 vs. 4.1.1, 4.4.3 vs. 4.1.3, 4.4.4 vs. 4.1.4). This is anticipated due to the following: girders are not controlled by $wl^2/8$ which eliminates the sharp decrease in ductility within the top floors, and gravity loads alter the time to first yield. With the exception of the top floors, the distribution of ductility remains fairly even between columns and girders; neither type of element has been penalized due to gravity considerations. The mean value over height of the maximum ductility factors and the variation due to the motion is similar in both cases.

The local ductility factors averaged at all girder or column cross-sections at a given level (see Tables 4.4.1 vs. 4.1.1 and 4.4.3 vs. 4.1.3) and the story ductility factors (see Tables 4.4.2 vs. 4.1.2 and 4.4.4 vs. 4.1.4) are within the same range of values; differences observed at any particular level emphasize the change in yielding pattern. Maximum lateral displacements (see Figures 4.4.2 vs. 4.1.2 and 4.4.5 vs. 4.1.5) vary only

slightly for the same motion.

The lack of significant change in response observed when gravity is completely ignored suggests that the procedure for handling gravity loads in design and in analysis (as in Sections 4.1 and 4.2) is consistent.

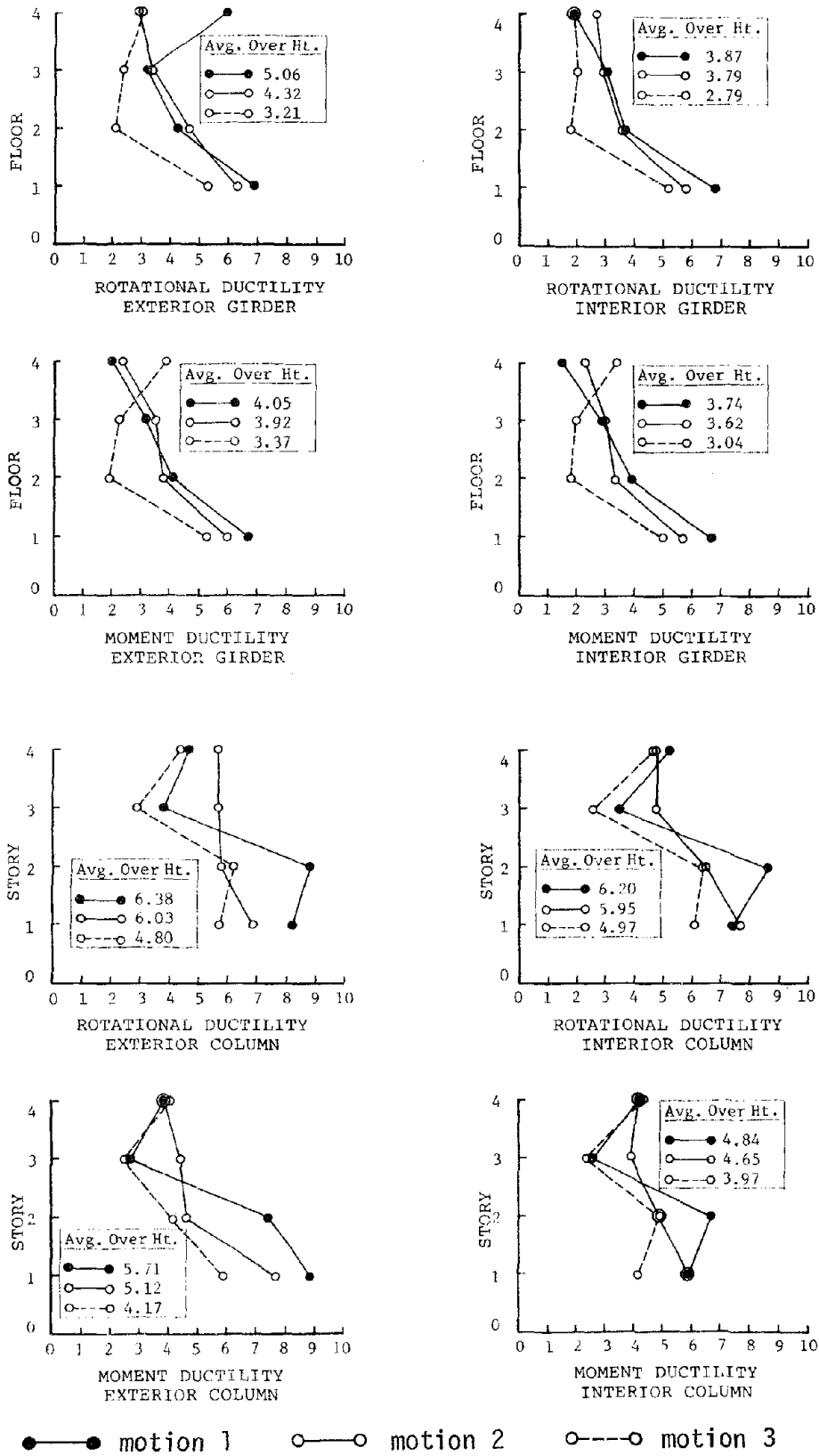


FIGURE 4.4.1 - MAXIMUM DUCTILITY FACTORS FOR EARTHQUAKE DESIGN $\mu=4$; 4-Story Frame; Motions 1, 2, 3

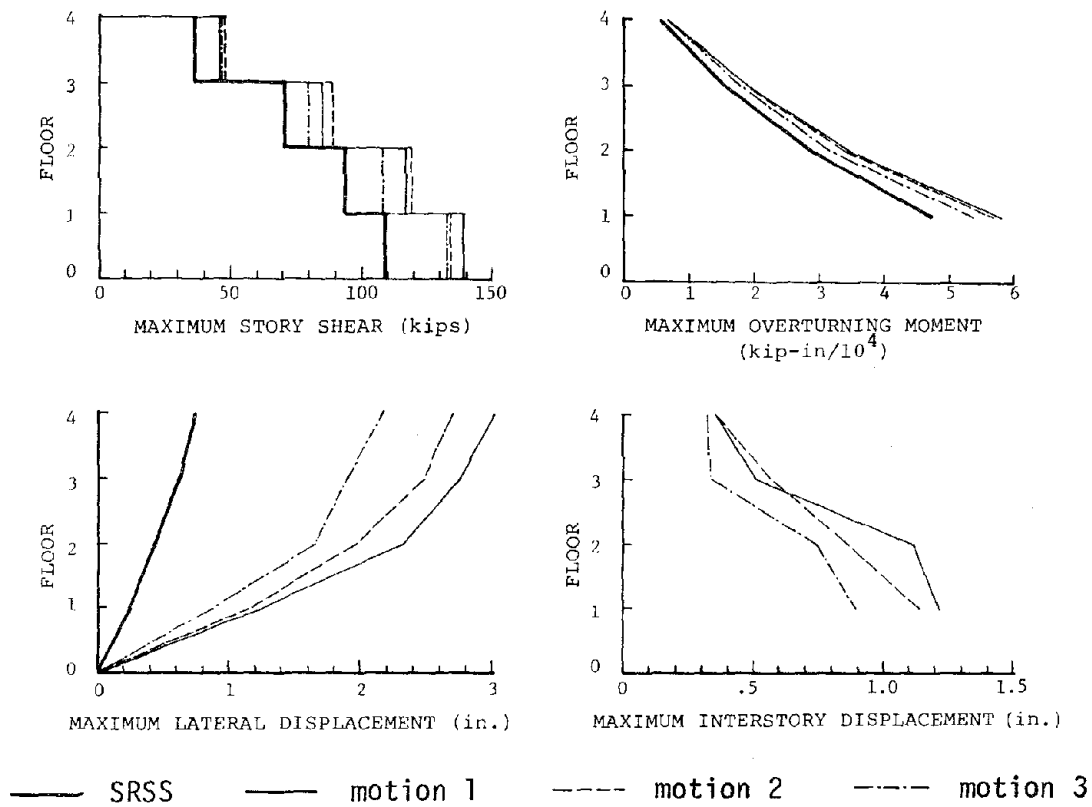
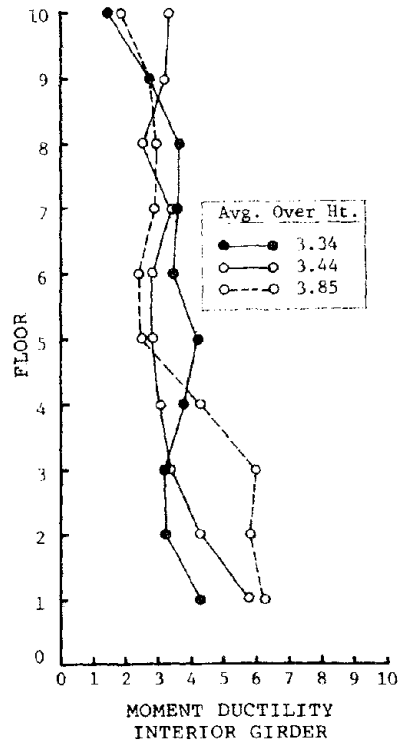
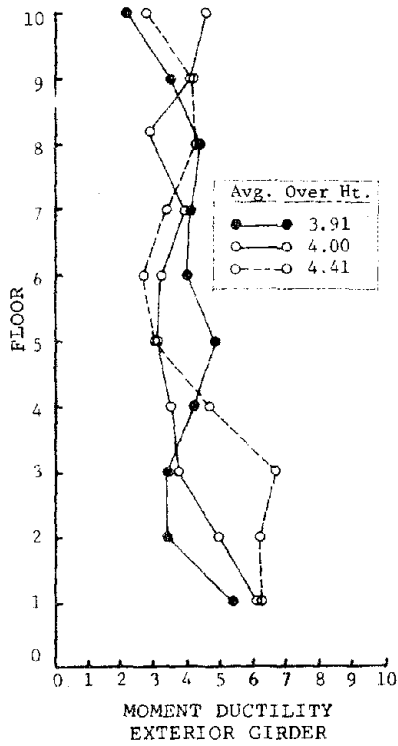
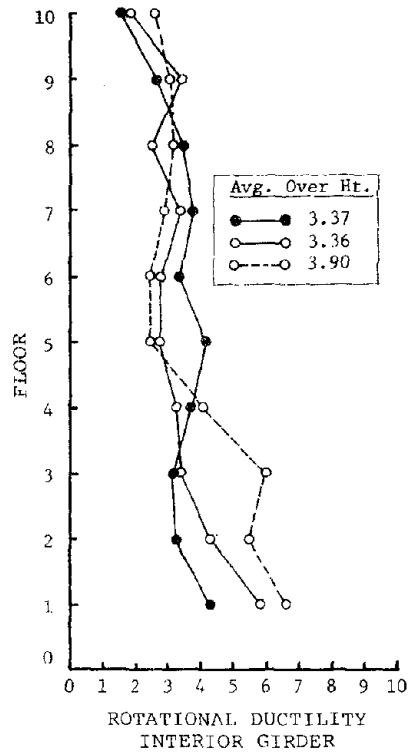
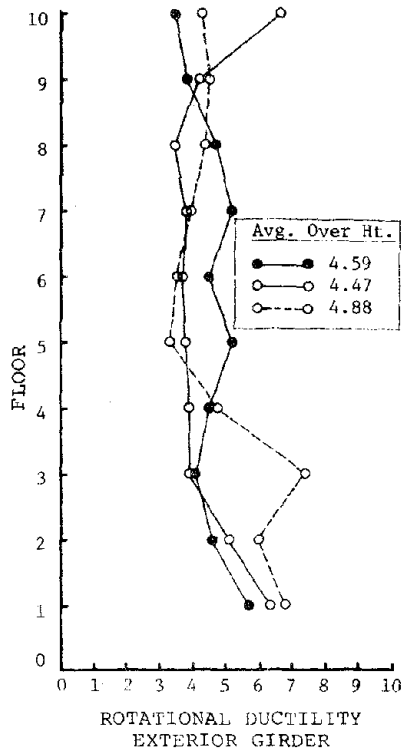


FIGURE 4.4.2 - MAXIMUM STORY LEVEL PARAMETERS FOR EARTHQUAKE DESIGN
 $\mu = 4$; 4-Story Frame; Motions 1, 2, 3



●—● Motion 1 ○—○ Motion 2 ○—○ Motion 3

FIGURE 4.4.3 - MAXIMUM GIRDER DUCTILITY FACTORS FOR EARTHQUAKE DESIGN
 $\mu = 4$; 10-Story Frame; Motions 1, 2, 3

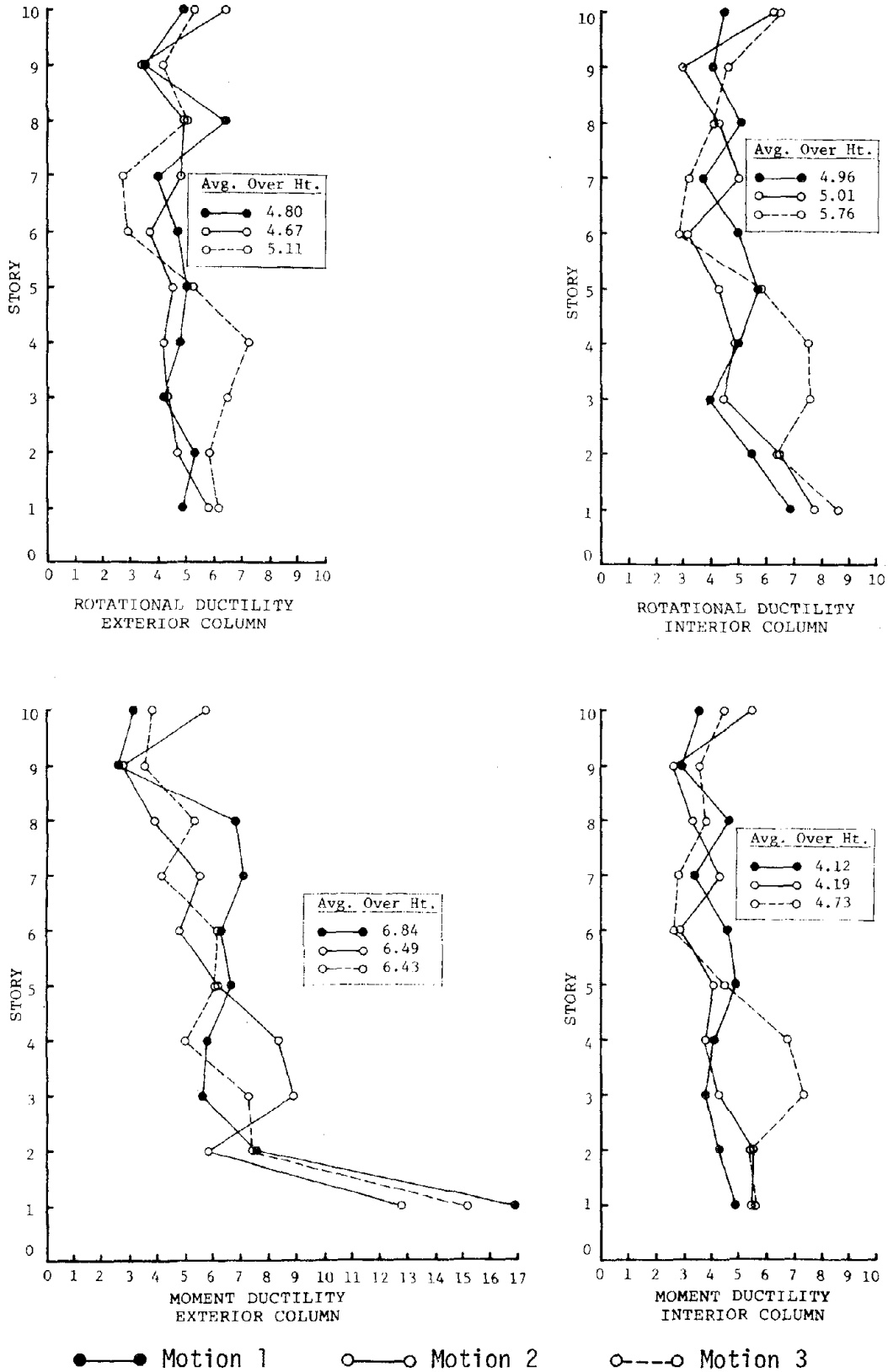
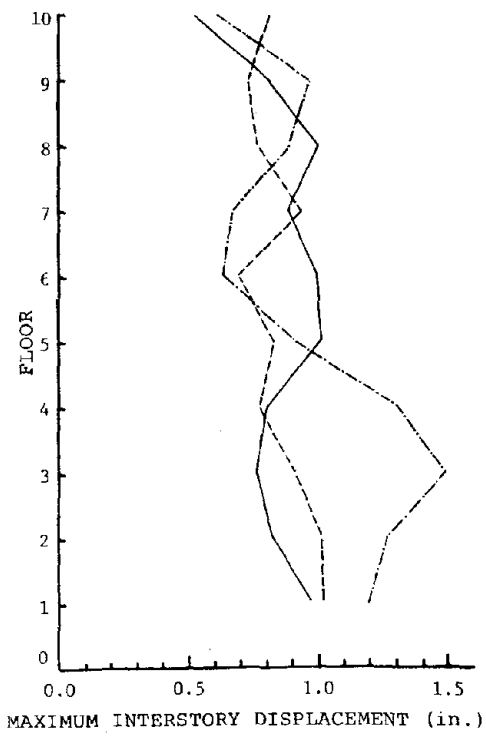
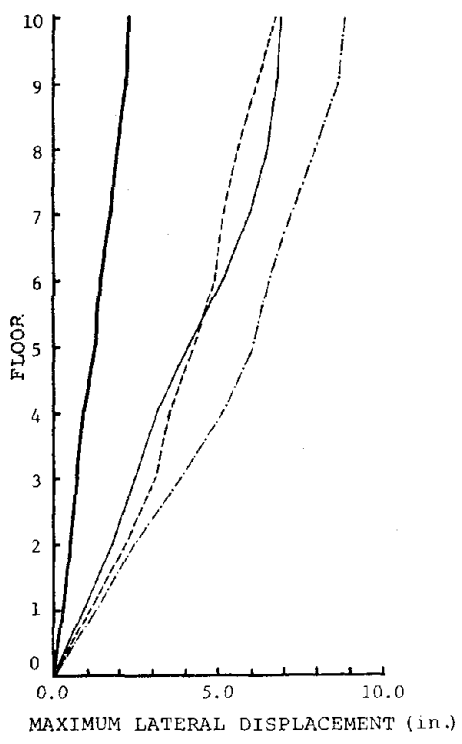
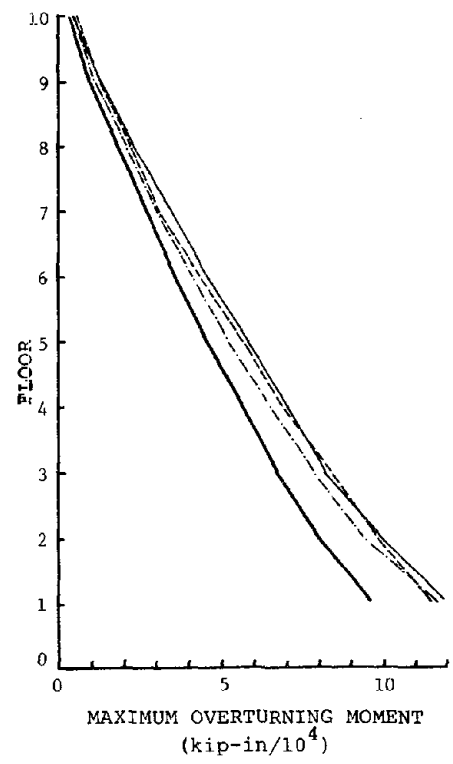
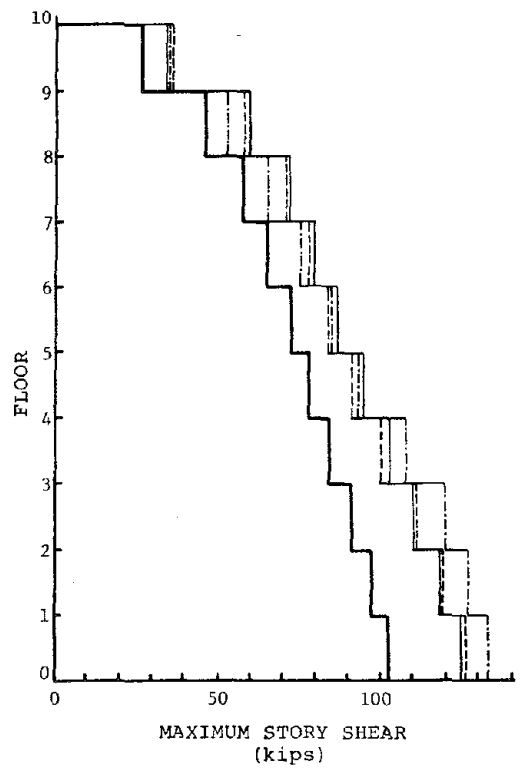


FIGURE 4.4.4 - MAXIMUM COLUMN DUCTILITY FACTORS FOR EARTHQUAKE DESIGN $\mu = 4$; 10-Story Frame; Motions 1, 2, 3



— SRSS — motion 1 - - - motion 2 - · - motion 3

FIGURE 4.4.5 - MAXIMUM STORY LEVEL PARAMETERS FOR EARTHQUAKE DESIGN
 $\mu = 4$; 10-Story Frame; Motions 1, 2, 3

TABLE 4.4.1 - AVERAGE DUCTILITY FACTORS FOR EARTHQUAKE DESIGN
 $\mu = 4$; 4-Story Frame; Motions 1, 2, 3

LEVEL	ROTATIONAL DUCTILITY		MOMENT DUCTILITY	
	GIRDERS	COLUMNS	GIRDERS	COLUMNS
MOTION 1				
1	6.77	4.78	6.67	5.73
2	3.95	6.98	4.05	6.22
3	3.04	3.05	3.11	2.29
4	4.07	4.42	1.75	3.52
MOTION 2				
1	6.02	4.76	5.88	5.31
2	3.97	5.43	3.65	4.21
3	3.15	4.00	3.29	3.64
4	2.79	4.35	2.22	3.49
MOTION 3				
1	5.24	3.79	5.18	3.60
2	1.97	4.44	1.84	3.91
3	2.25	2.48	2.15	2.41
4	2.62	4.16	3.75	3.89

TABLE 4.4.2 - STORY DUCTILITY FACTORS FOR EARTHQUAKE DESIGN
 $\mu = 4$; 4-Story Frame; Motions 1, 2, 3

STORY	DUCTILITY FACTOR		
	MOTION 1	MOTION 2	MOTION 3
1	5.3	5.0	3.8
2	5.6	4.4	3.7
3	2.8	3.1	1.8
4	3.5	3.5	3.2

TABLE 4.4.3 - AVERAGE DUCTILITY FACTORS FOR EARTHQUAKE DESIGN
 $\mu = 4$; 10-Story Frame; Motions 1, 2, 3

LEVEL	ROTATIONAL DUCTILITY		MOMENT DUCTILITY	
	GIRDERS	COLUMNS	GIRDERS	COLUMNS
MOTION 1				
1	4.92	3.81	4.85	7.56
2	3.66	4.25	3.28	5.55
3	3.56	3.80	3.28	4.61
4	4.10	4.35	4.01	4.90
5	4.69	4.50	4.63	2.90
6	3.86	4.51	3.76	4.93
7	4.31	3.82	3.87	4.38
8	4.10	5.32	4.08	5.35
9	3.23	3.24	3.18	2.55
10	2.38	3.65	1.78	2.89
MOTION 2				
1	6.02	4.22	3.36	6.84
2	4.67	4.65	4.70	5.53
3	3.67	4.06	3.57	5.62
4	3.63	4.34	3.32	5.35
5	3.33	4.30	2.96	5.44
6	3.18	3.27	3.02	3.76
7	3.66	4.30	3.72	4.36
8	2.93	3.96	2.73	3.44
9	3.85	2.81	3.69	2.68
10	3.62	5.64	3.90	5.27
MOTION 3				
1	6.36	4.64	6.17	7.25
2	5.76	5.59	5.99	6.28
3	6.68	6.60	6.42	7.09
4	4.55	6.04	4.50	5.78
5	2.85	4.54	2.79	4.38
6	2.82	2.83	2.61	3.67
7	3.32	2.68	3.18	2.95
8	3.89	4.19	3.94	4.22
9	3.82	3.46	3.71	3.36
10	3.54	4.31	2.21	3.55

TABLE 4.4.4 - STORY DUCTILITY FACTORS FOR EARTHQUAKE DESIGN
 $\mu = 4$; 10-Story Frame; Motions 1, 2, 3

STORY	DUCTILITY FACTOR		
	MOTION 1	MOTION 2	MOTION 3
1	4.2	5.0	5.2
4	3.8	3.7	6.1
7	3.5	3.6	2.6
10	3.2	5.1	3.8

4.5 Results for Designs Using Factored Spectral Forces

Use of the inelastic spectra constructed by the Newmark-Hall rules yields excessive nonlinear member deformations above the two levels of design ductility considered (Section 4.1 and 4.2). In order to reduce the local ductility, some conservatism is introduced by factoring the spectral forces obtained from the elastic modal analysis as follows: 1.5 for exterior columns, 1.2 for interior columns, 1.2 for girders. Justification for a different factor for the exterior columns is based on the observation, first, that the largest of the maximum, and average of the maximum local ductility over height, occur at exterior column sections and, second, that the exterior columns are more critical in terms of fluctuations in axial load due to the contribution of the story overturning moment. The increase in column strength which forces more yielding into the girders must be compensated for by some increase in girder resistance. These factors were determined empirically by iterations of a time history analysis with the point hinge model.

The 4- and 10-story frames were designed following the procedure of Section 2.4 for $\mu = 4$, modified by using factored spectral forces. Corresponding strength properties are listed in Appendix B. The designs were subjected to motion 2.

The maximum local ductility values decrease at nearly every location along the height for both girders and columns in the factored design (see Figures 4.5.1, 4.5.3, 4.5.4). The amount of change is less for girders and interior columns than that for exterior columns, which is consistent with the factors applied. Based on μ_M alone, the factoring process has

successfully limited the average of the maximum ductility over height to less than the design level of 4 for columns and girders in the 4- and 10-story frames. Generally the shape of the maximum ductility vs. height is the same for the factored and unfactored cases. However, the fact that the ductility ratios are less uniform over height than is desirable suggests that the factors might be varied over the height.

The story ductility factors decrease in accordance with the reduction in yielding activity at the member level (see Tables 4.5.2 vs. 4.1.2 and 4.5.4 vs. 4.1.4). The largest value of μ_S is 3.4 in the 4-story frame and 3.2 in the 10-story frame. The story shear and overturning moment increase as the resistance increases (Figures 4.5.2 and 4.5.5). The lateral and interstory displacements do not change significantly (see Figures 4.5.2 and 4.5.5).

The concept of requiring the columns to remain elastic during strong motion earthquakes has been proposed on the basis of safety considerations (18). Such a philosophy could be incorporated in an inelastic spectrum procedure once appropriate factors were determined.

The numerical factors used herein may not be generally appropriate. They only serve to indicate a possible technique for controlling local yielding.

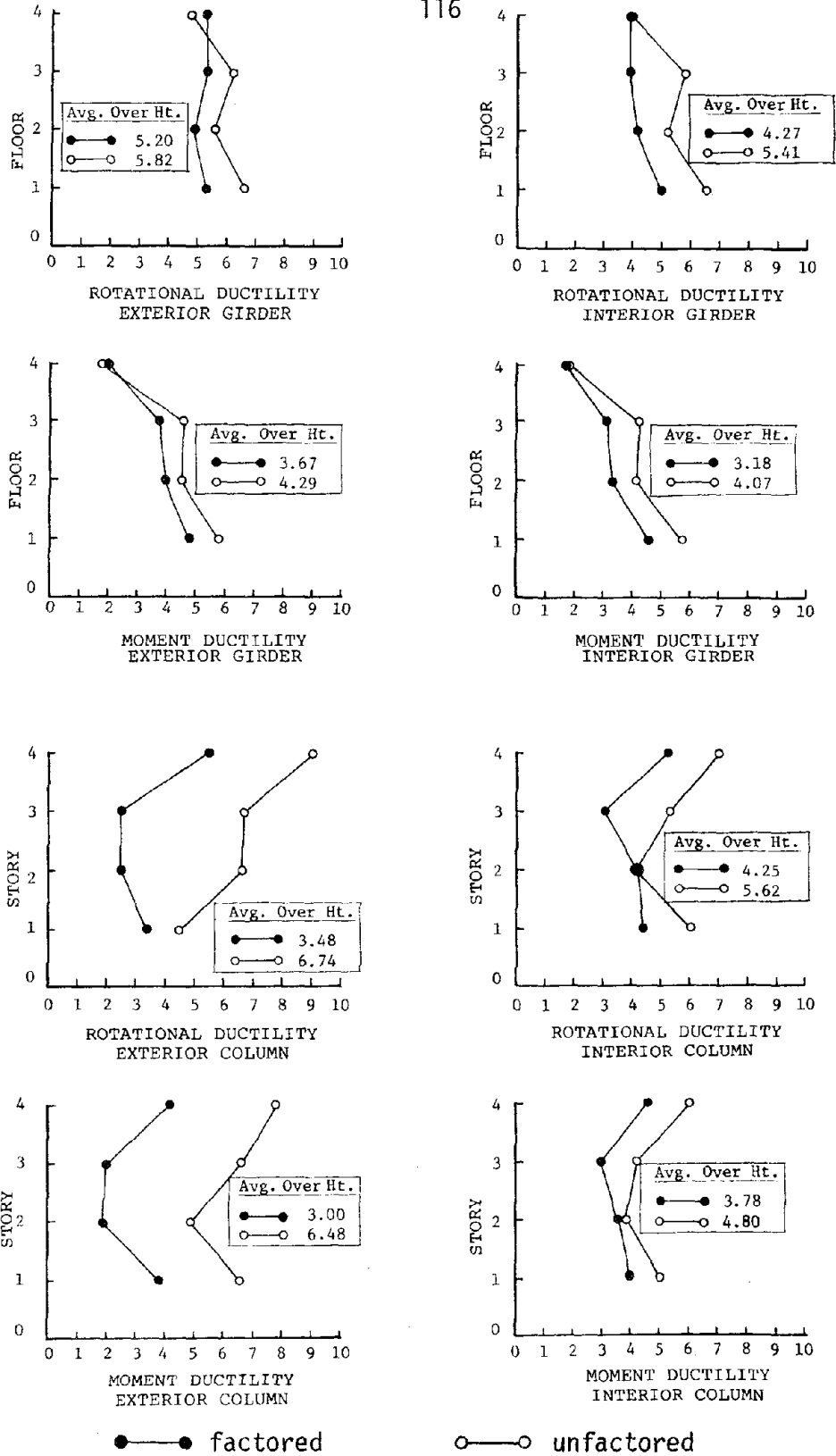


FIGURE 4.5.1 - MAXIMUM DUCTILITY FACTORS FOR GRAVITY AND FACTORED SPECTRAL DESIGN - $\mu = 4$; 4-Story Frame; Motion 2

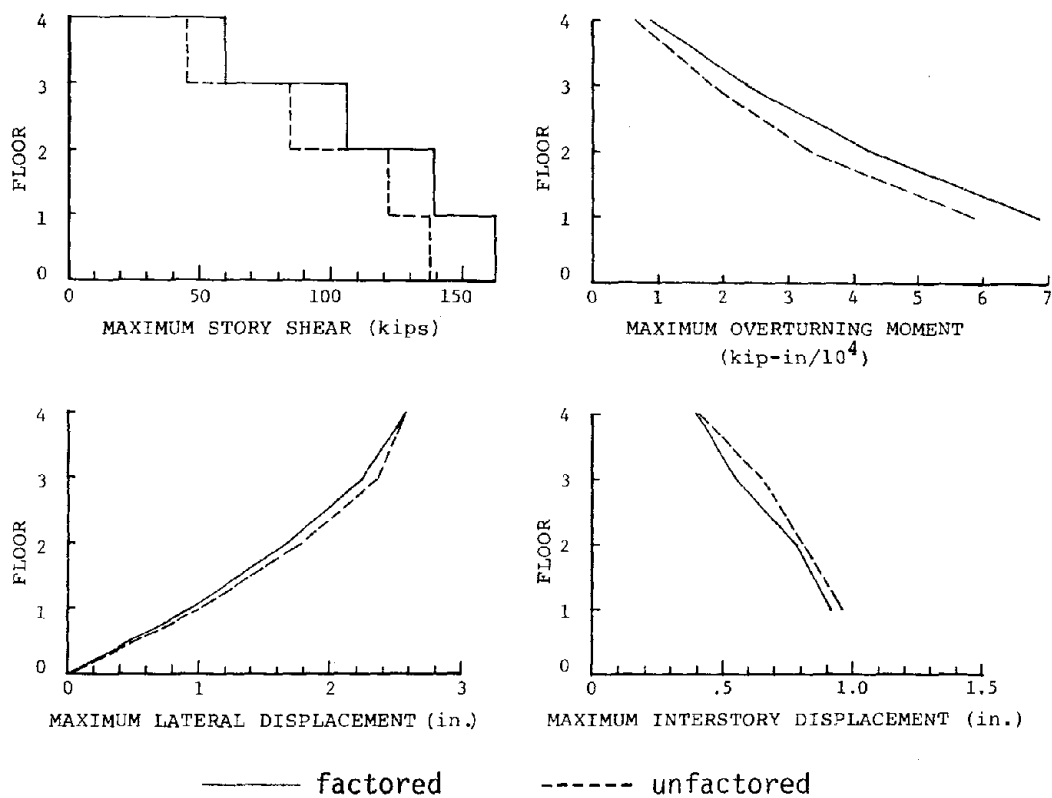
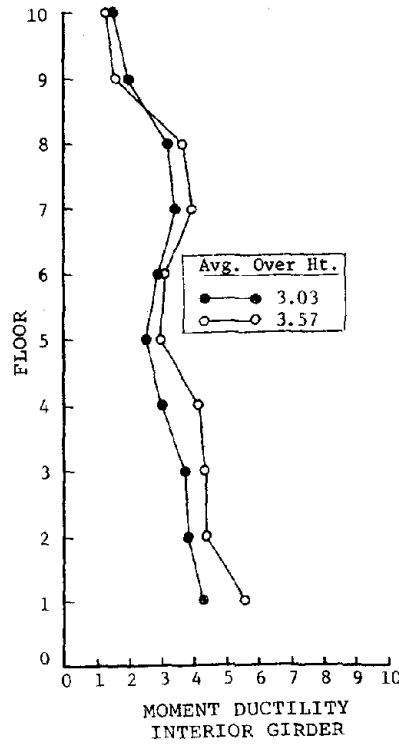
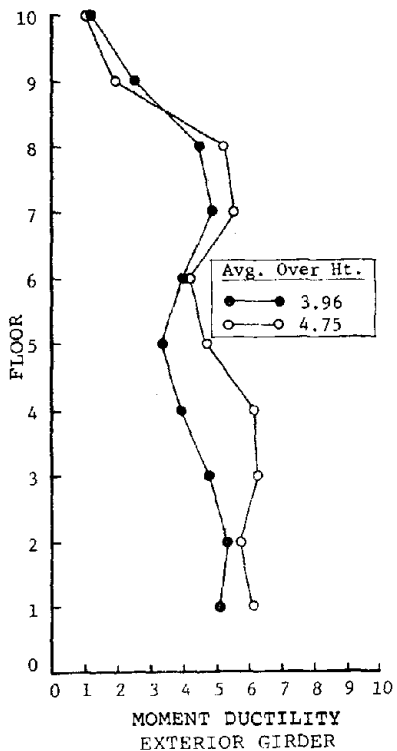
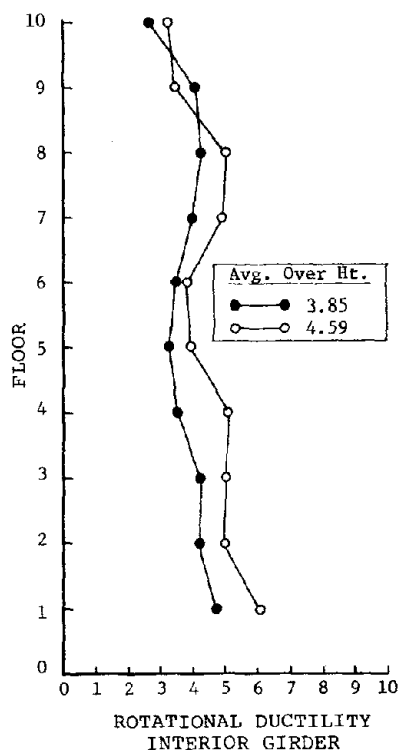
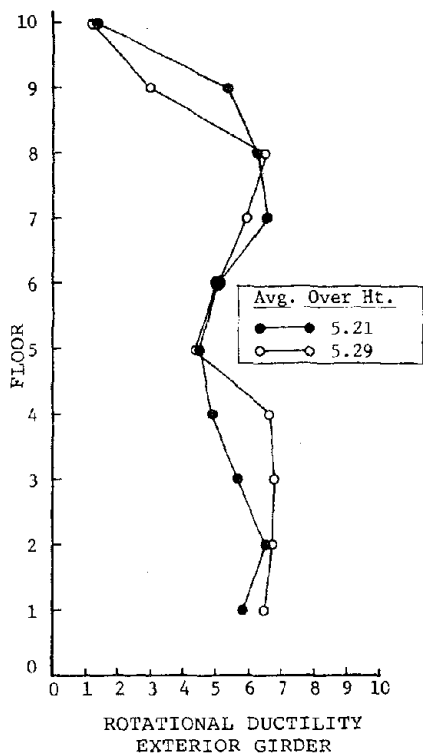
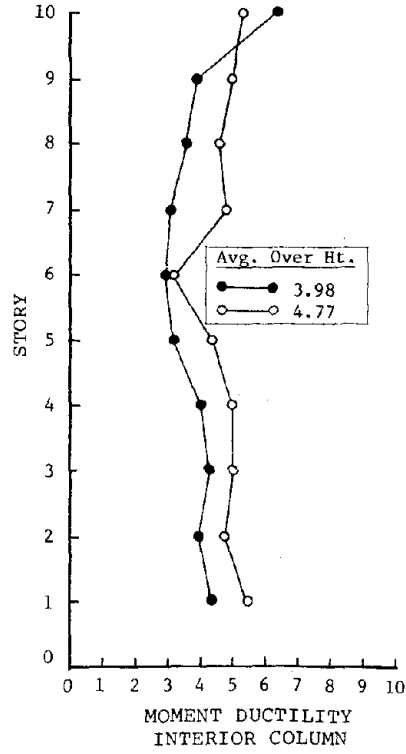
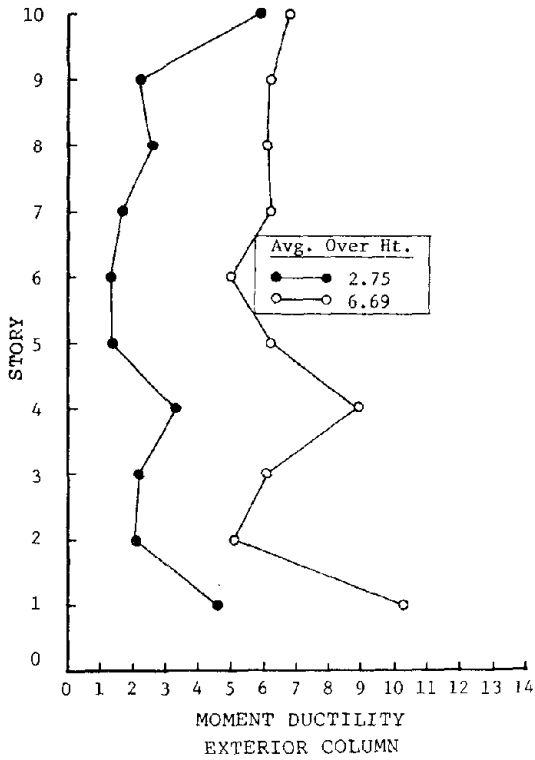
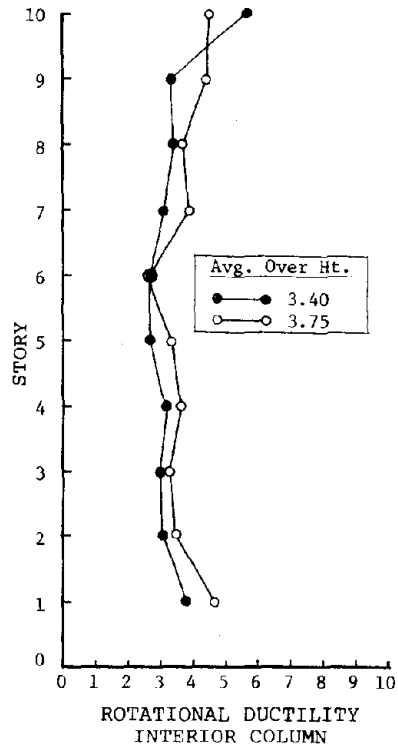
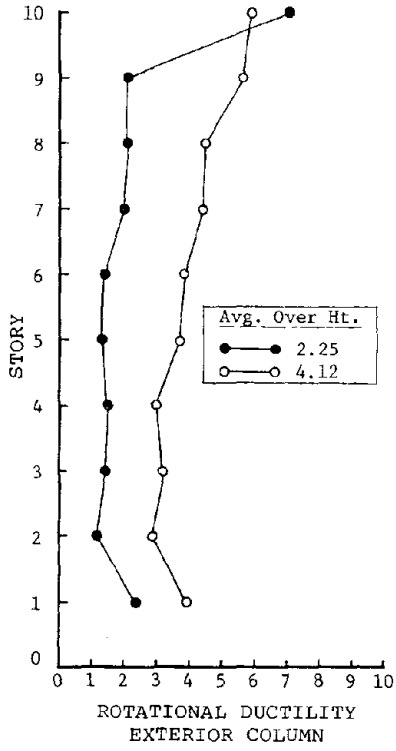


FIGURE 4.5.2 - MAXIMUM STORY LEVEL PARAMETERS FOR GRAVITY AND FACTORED SPECTRAL DESIGN - $\mu = 4$; 4-Story Frame; Motion 2



●—● Factored ○—○ Unfactored

FIGURE 4.5.3 - MAXIMUM GIRDER DUCTILITY FACTORS FOR GRAVITY AND FACTORED SPECTRAL DESIGN - $\mu = 4$; 10-Story Frame; Motion 2



●—● Factored ○—○ Unfactored

FIGURE 4.5.4 - MAXIMUM COLUMN DUCTILITY FACTORS FOR GRAVITY AND FACTORED SPECTRAL DESIGN - $\mu = 4$; 10-Story Frame; Motion 2

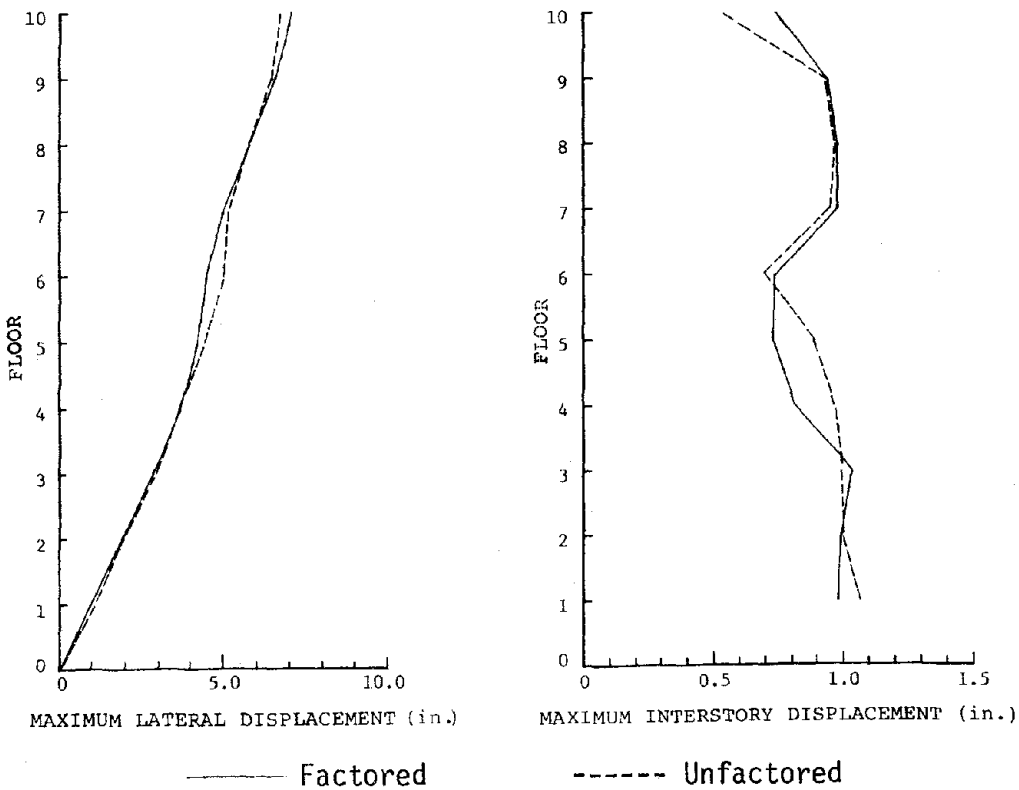
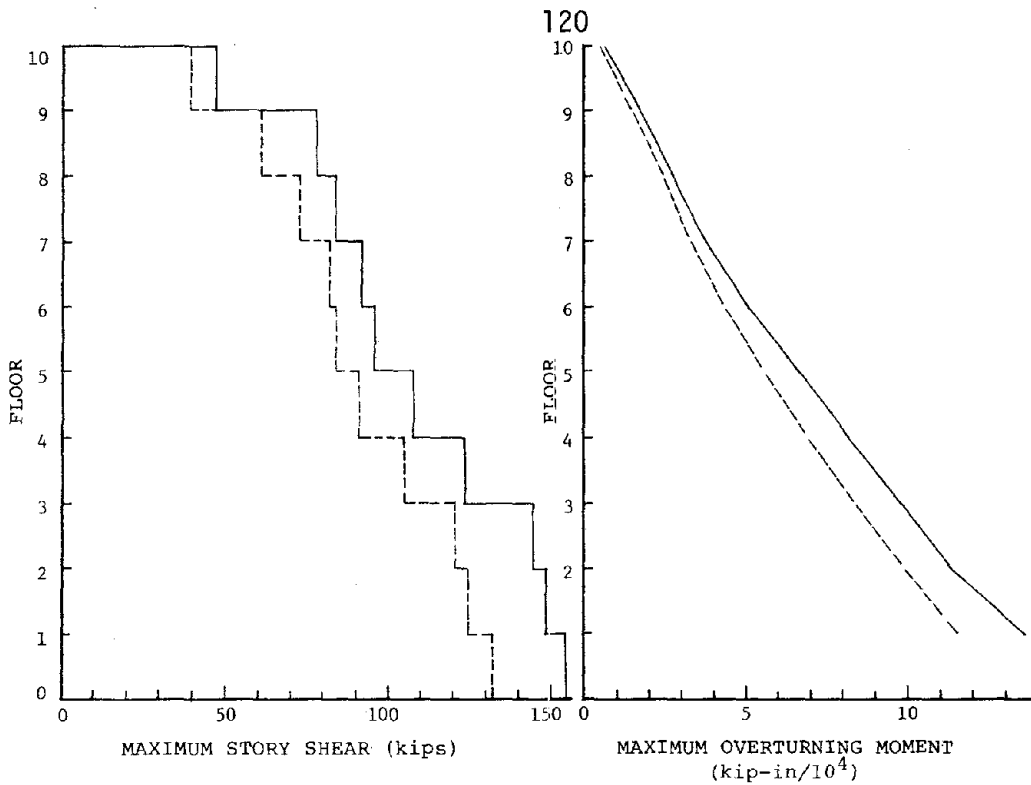


FIGURE 4.5.5 - MAXIMUM STORY LEVEL PARAMETERS FOR GRAVITY AND FACTORED SPECTRAL DESIGN - $\mu = 4$; 10-Story Frame; Motion 2

TABLE 4.5.1 - AVERAGE DUCTILITY FACTORS FOR GRAVITY AND FACTORED
SPECTRAL DESIGN - $\mu = 4$; 4-Story Frame; Motion 2

LEVEL	ROTATIONAL DUCTILITY		MOMENT DUCTILITY	
	GIRDERS	COLUMNS	GIRDERS	COLUMNS
MOTION 2				
1	4.46	2.43	4.49	2.23
2	3.55	2.24	3.42	2.09
3	3.49	2.26	3.01	2.03
4	2.89	3.65	1.53	3.26

TABLE 4.5.2 - STORY DUCTILITY FACTORS FOR GRAVITY AND FACTORED
SPECTRAL DESIGN - $\mu = 4$; 4-Story Frame; Motion 2

STORY	DUCTILITY FACTOR
	MOTION 2
1	3.3
2	3.4
3	2.5
4	2.9

TABLE 4.5.3 - AVERAGE DUCTILITY FACTORS FOR GRAVITY AND FACTORED SPECTRAL DESIGN - $\mu = 4$; 10-Story Frame; Motion 2

LEVEL	ROTATIONAL DUCTILITY		MOMENT DUCTILITY	
	GIRDERS	COLUMNS	GIRDERS	COLUMNS
MOTION 2				
1	4.79	2.02	4.48	2.58
2	4.78	1.97	4.40	2.63
3	4.58	1.95	4.07	2.58
4	3.81	1.99	3.29	2.52
5	3.45	1.72	2.73	2.05
6	3.47	1.72	3.20	1.76
7	4.06	1.86	3.85	1.97
8	4.05	2.09	3.41	2.44
9	3.38	2.31	2.25	2.54
10	1.57	4.28	1.05	4.66

TABLE 4.5.4 - STORY DUCTILITY FACTORS FOR GRAVITY AND FACTORED SPECTRAL DESIGN - $\mu = 4$; 10-Story Frame; Motion 2

STORY	DUCTILITY FACTOR
	MOTION 2
1	3.0
4	3.2
7	3.2
10	3.1

CHAPTER 5 - COMMENTARY5.1 Conclusions

The conclusions based on the results of Section 3.4 and Chapter 4 are summarized below. It should be emphasized that these observations are contingent on the modelling assumptions, analysis techniques, and methods of determining the frame properties.

- 1) A multistory frame can develop local ductility values (for both definitions) several times greater than the design ductility level, when the resistance is determined by an elastic modal analysis without load factors, using an inelastic response spectrum which has been constructed by the Newmark-Hall rules. The gross nonlinear deformation of a story, as measured by the story ductility factor, μ_S , is generally less than or only slightly in excess of the design ductility level. The largest values of μ_S for the designs including gravity are 6.1 for $\mu = 4$ and 2.6 for $\mu = 2$. Thus, inelastic action can be highly concentrated in hinges at the ends of members where the overall behavior of the story, in which the critical section is located, satisfies the deformation criteria.
- 2) For the basic spectral design (#1), there is a fairly even distribution of yielding between columns and girders as indicated by the maximum ductility factor at any cross-section in a given story, the average of the maximum over height, and the averages

for all column or girder cross-sections in a given story. Neither type of element is favored by the design philosophy.

- 3) Introducing conservatism into the calculation of member resistances, by factoring the forces obtained with a modal analysis using an inelastic spectrum, allows the control of local ductility values at critical sections. This capability provides the potential for implementing a design philosophy in which the columns are to remain elastic, once appropriate factors have been determined. The factors of 1.5 for exterior columns, 1.2 for interior columns, and 1.2 for girders restrict the non-linear member deformations for both definitions of ductility as follows: column values reduce to near or below the design level of 4; girder values do not decrease significantly but are generally less than 5; the distribution over height of the maximum local ductility in each story is similar for the factored and unfactored case. Sections cannot be factored at random due to the observation that altering the relationship of resistance causes more inelastic action to concentrate in the weaker (by contrast) parts of the frame. This is the motivation for strengthening girders even though for the unfactored situation their local deformations are not excessive. The process of including conservative factors for inelastic spectral forces yields a satisfactory design method for limiting local ductility.
- 4) The design ductility level does not have a significant effect on the performance of the basic spectral approach (#1). For

both cases (i.e., $\mu = 2$ or 4) the maximum local ductility values and the story ductility factors are within the same range of the design level. However, the distribution of the maximum local values occurring in a particular story changes over the height of the building for the same motion. The nature of the inelastic response is different but the output parameters are similar in terms of satisfying design criteria. Concerning practical applications, a three-fold increase in nonlinear deformation for a design ductility of 4 is more damaging than the same increase for $\mu = 2$ for actual steel sections. Therefore, safety standards may indicate the incorporation of a lower level of ductility.

- 5) Although the 3 motions generated to match the smoothed design elastic spectrum have similar characteristics in terms of frequency content and power spectral density function, the inelastic response varies significantly as a function of the input accelerogram. The two factors contributing to these differences are the degree of agreement between the computed and target spectra and the details of each motion.
- 6) Capabilities should be included to handle the presence of static gravity loads in nonlinear dynamic analyses with the point hinge model. Gravity loads influence the amount and pattern of yielding throughout a given frame.
- 7) The philosophy developed herein for considering the effects of elastic gravity end forces in determining member resistance appears adequate.

- 8) No significant improvement in performance is evident for a more flexible frame (i.e., 18-Story versus 10-Story and 10-Story versus 4-Story). This suggests that the height and fundamental natural period may not be important parameters in determining the ductility requirements of a frame. The practical implication is that the stiffness of the building may be adjusted to satisfy drift criteria within the framework of an inelastic spectrum based design procedure. It must be noted that the 3 frames in the study were selected with similar distributions of stiffness, tapering from bottom to top. Changing the period of vibration by altering the stiffness distribution (e.g., uniform from bottom to top) may produce differences in response, a topic which deserves further investigation.
- 9) The two definitions of ductility at the member level, moment and rotational, give similar results without the presence of gravity load. The observation is due, primarily, to the following: the tendency for the structure to deform laterally in a symmetric fashion increases, which makes the definition of yield rotation more meaningful for the rotational ductility factor; in columns, the reduction in yield capacity is not as significant for the moment definition. In the more realistic case including gravity, the rotational ductility is generally greater than the moment ductility in girders and vice versa in columns. The arbitrary constant for the yield rotation and the lack of a means to handle the change in yield moment due to interaction may, again, explain these discrepancies and indicate that the

moment definition provides a better index for measuring inelastic deformation at the element level.

- 10) The lateral and interstory displacements for a 4- and 10-story point hinge model compared with those of an "equivalent" shear beam model, whose nonlinear spring properties are obtained from the point hinge model, generally agree within 10%. This implies the following: the hysteretic behavior of a story is approximately bilinear; the story ductility factor, defined herein, is representative of the gross nonlinear deformation of a story; the shear beam model predicts the overall response of the more expensive point hinge model if the proper force-deformation relationships are specified.

Although application of an elastic modal analysis for a multi-degree-of-freedom system may result in local ductilities exceeding the design level, no other procedure is available which is as inexpensive, has a more readily adaptable format for building codes, or offers the potential for serving as a preliminary design tool in a more complex set of procedures. However, the inelastic response spectrum approach requires further investigation to make it a reliable design tool.

5.2 Recommendations

Additional areas of research recommended for the development of adequate inelastic spectrum-based design procedures are outlined as follows.

- 1) Perform safety analyses to determine distributions of ductility associated with uncertainties in ground motion characteristics, member strength properties, the amount of critical damping, period changes due to stiffness deterioration or inelastic action, and the portion of live load present.
- 2) Modify program parameters to test the sensitivity of the inelastic analysis to the time step, alternate forms of damping (e.g., mass proportional, stiffness proportion), the second slope of the dual component model, the P - Δ effect, and foundation rocking.
- 3) Determine the most appropriate distributions of stiffness and mass throughout the structure.
- 4) Measure response in terms of other definitions of ductility.
- 5) Design and model various building types such as reinforced concrete and braced steel frame.
- 6) Extend the work with single-degree-of-freedom systems, which forms the basis of the simplified rules for constructing the inelastic spectra, to more complex systems. Veletsos and Vann (3) have performed such analyses comparing the deformation

spectra of associated elastic and elastoplastic 2- and 3-degree-of-freedom shear beam models.

The complications involved in the continued investigation of non-linear behavior demand extensive computer time and effort. These costs are compensated for by the apparent potential for improved seismic design procedures.

REFERENCES

1. Veletsos, A.S., Newmark, N.M., and Chelapati, C.V., "Deformation Spectra for Elastic and Elastoplastic Systems Subjected to Ground Shock and Earthquake Motions," Proceedings of the Third World Conference on Earthquake Engineering, Wellington, New Zealand, 1965.
2. Veletsos, A.S., "Maximum Deformations of Certain Nonlinear Systems," Proceedings of the Fourth World Conference on Earthquake Engineering, Santiago, Chile, 1969.
3. Veletsos, A.S., and Vann, W.P., "Response of Ground-Excited Elastoplastic Systems," Journal of the Structural Division, ASCE, Vol. 97, No. ST4, April, 1971.
4. Anderson, J.C., and Bertero, V.V., "Seismic Behavior of Multistory Frames Designed by Different Philosophies," Earthquake Engineering Research Center Report No. EERC 69-11, University of California, Berkeley, California, October, 1969.
5. Mahin, S.A., and Bertero, V.V., "An Evaluation of Some Methods for Predicting Seismic Behavior of Reinforced Concrete Buildings," Earthquake Engineering Research Center Report No. EERC 75-5, University of California, Berkeley, California, February, 1975.
6. Haviland, R.W., "A Study of the Uncertainties in the Fundamental Translational Periods and Damping Values for Real Buildings," M.I.T. Department of Civil Engineering Research Report R76-12, Order No. 531, February, 1976.
7. Isbell, J.E., and Biggs, J.M., "Inelastic Design of Building Frames to Resist Earthquakes," M.I.T. Department of Civil Engineering Research Report R74-36, No. 393, May, 1974.
8. Bertero, V.V., and Kamil, H., "Nonlinear Seismic Design of Multi-story Frames," Canadian Journal of Civil Engineering, Vol. 2, No. 4, 1975.
9. Biggs, J.M., Introduction to Structural Dynamics, McGraw-Hill, 1964.
10. Luyties, W.H., Anagnostopoulos, S.A., and Biggs, J.M., "Studies on the Inelastic Dynamic Analysis and Design of Multi-Story Frames," M.I.T. Department of Civil Engineering Research Report R76-29, Order No. 548, July, 1976.

REFERENCES

(continued)

11. Newmark, N.M., and Hall, W.J., "Procedures and Criteria for Earthquake Resistant Design," Building Practices for Disaster Mitigation, Building Science Series 46, National Bureau of Standards, February, 1973.
12. Penzien, J., "Elasto-Plastic Response of Idealized Multi-Story Structures Subjected to a Strong Motion Earthquake," Proceedings of the Second World Conference on Earthquake Engineering, Tokyo, Japan, 1960.
13. Hisada, T., Nakagawa, K., and Izumi, M., "Earthquake Response of Idealized Twenty Story Buildings Having Various Elasto-plastic Properties," Proceedings of the Third World Conference on Earthquake Engineering, Wellington, New Zealand, 1965.
14. Clough, R.W., "Inelastic Earthquake Response of Tall Buildings," Proceedings of the Third World Conference on Earthquake Engineering, Wellington, New Zealand, 1965.
15. Clough, R.W., and Benuska, K.L., "Nonlinear Earthquake Behavior of Tall Buildings," Journal of the Engineering Mechanics Division, ASCE, Vol. 93, No. EM3, June, 1967.
16. Guru, B.P., and Heidebrecht, A.C., "Factors Influencing the Inelastic Response of Multistory Frames Subjected to Strong Motion Earthquakes," Proceedings of the Fourth World Conference on Earthquake Engineering, Santiago, Chile, 1969.
17. Goel, S.C., and Berg, G.V., "Inelastic Earthquake Response of Tall Steel Frames," Journal of the Structural Division, ASCE, Vol. 94, No. ST8, August, 1968.
18. Anderson, J.C., and Gupta, R.P., "Earthquake Resistance Design of Unbraced Frames," Journal of the Structural Division, ASCE, Vol. 98, No. ST11, November, 1972.
19. Applied Technology Council, An Evaluation of a Response Spectrum Approach to Seismic Design of Buildings, A Study Report for Center for Building Technology, Institute of Applied Technology, National Bureau of Standards, September, 1974.
20. Anagnostopoulos, S.A., "Non-Linear Dynamic Response and Ductility Requirements of Building Structures Subjected to Earthquakes," M.I.T. Department of Civil Engineering Research Report R72-54, Structures Publication No. 349, September, 1972.

REFERENCES

(continued)

21. Gasparini, D.A., and Vanmarcke, E.H., "Simulated Earthquake Motions Compatible with Prescribed Response Spectra," M.I.T. Department of Civil Engineering Research Report R76-4, Order No. 527, January, 1976.
22. Manual of Steel Construction, 7th ed., American Institute of Steel Construction, New York, N.Y.
23. Clough, R.W., and Benusha, K.L., FHA Study of Seismic Design Criteria for High-Rise Buildings, A Report Prepared for the Technical Studies Program of the Federal Housing Administration, by T.Y. Lin and Associates, Consulting Engineers, 1966.
24. Veletsos, A.S., and Newmark, N.M., "Effect of Inelastic Behavior on the Response of Simple Systems to Earthquake Motions," Proceedings of the Second World Conference on Earthquake Engineering, Tokyo, Japan, 1960.
25. Newmark, N.M., "Current Trends in the Seismic Analysis and Design of High Rise Structures," Earthquake Engineering, Prentice-Hall, Inc., Englewood Cliffs, N.J., 1971.
26. Aziz, T.S.A., "Inelastic Dynamic Analysis of Building Frames," thesis presented to the Massachusetts Institute of Technology, Cambridge, Mass., in 1974, in partial fulfillment of the requirements for the degree of Doctor of Science.
27. Pique del Pozo, J., "On the Use of Simple Models in Nonlinear Dynamic Analysis," thesis presented to the Massachusetts Institute of Technology, Cambridge, Mass., in 1976, in partial fulfillment of the requirements for the degree of Doctor of Philosophy.
28. Anagnostopoulos, S.A., and Biggs, J.M., "An Evaluation of Response Spectra Design Procedures Through Inelastic Analysis," to be presented at the 6th World Conference on Earthquake Engineering, New Dehli, India, January, 1977.
29. Roesset, J., Unpublished User's Guide for the Computer Program APPLE PIE, M.I.T., Cambridge, Massachusetts.
30. Luyties, W.H., Unpublished User's Guide for the Computer Program FRIEDA, M.I.T., Cambridge, Massachusetts.
31. "ICES STRUDL II - Engineering User's Manual - Frame Analysis," Vol. 1, Publication No. R68-91, Department of Civil Engineering, M.I.T., Cambridge, Mass., November 1968.

APPENDIX A

PROPERTIES OF EQUIVALENT SHEAR BEAM MODELS

TABLE A.1 - EQUIVALENT SHEAR BEAM PROPERTIES FOR 4-STORY FRAME

LEVEL	1 st SLOPE (kips/in)	2 nd SLOPE (kips/in)	YIELD SHEAR (kips)
1	500.0	25.0	120.0
2	463.8	33.0	96.0
3	395.6	26.0	72.0
4	325.0	18.6	39.0

TABLE A.2 - EQUIVALENT SHEAR BEAM PROPERTIES FOR 10-STORY FRAME

LEVEL	1 st SLOPE (kips/in)	2 nd SLOPE (kips/in)	YIELD SHEAR (kips)
1	400.0	27.7	111.0
2	480.0	34.5	96.0
3	450.0	25.0	90.0
4	387.0	20.0	84.0
5	325.0	22.2	76.0
6	287.0	29.8	70.2
7	233.0	30.0	63.0
8	193.0	11.6	56.0
9	153.0	10.5	49.0
10	153.0	16.0	30.0

APPENDIX B

STRENGTH PROPERTIES FOR INELASTIC DESIGNS

TABLE B.1
PROPERTIES OF 4-STORY FRAME FOR SECTION 4.1

STORY	COLUMN M_p 's (k-in)		GIRDER M_p 's (k-in)	
	EXTERIOR	INTERIOR	EXTERIOR	INTERIOR
4	503	974	845	845
3	1063	1879	1290	1240
2	1553	2612	2000	1800
1	2285	3675	2540	2240

TABLE B.2
PROPERTIES OF 10-STORY FRAME FOR SECTION 4.1

STORY	COLUMN M_p 's (k-in)		GIRDER M_p 's (k-in)	
	EXTERIOR	INTERIOR	EXTERIOR	INTERIOR
10	483	834	1025	1025
9	817	1528	1260	1260
8	1118	2051	1180	1265
7	1424	2467	1415	1475
6	1690	2864	1590	1660
5	1986	3233	1750	1815
4	2286	3607	1930	1910
3	2601	3980	2110	2030
2	2916	4351	2300	2140
1	3523	5171	2500	2215

TABLE B.3
PROPERTIES OF 18-STORY FRAME FOR SECTION 4.1

STORY	COLUMN M_p 's (k-in)		GIRDER M_p 's (k-in)	
	EXTERIOR	INTERIOR	EXTERIOR	INTERIOR
18	619	879	1208	1208
17	826	1504	1375	1375
16	1141	2021	1375	1375
15	1469	2597	1584	1584
14	1830	3122	1584	1584
13	2168	3616	1584	1678
12	2494	4154	1748	1978
11	2880	4643	1838	2062
10	3243	5147	1932	2114
9	3616	5707	2127	2385
8	4035	6238	2213	2433
7	4443	6783	2318	2470
6	4871	7390	2557	2717
5	5326	7961	2667	2748
4	5775	8535	2779	2757
3	6258	9177	3048	2942
2	6764	9817	3161	2925
1	7663	11136	3385	2997

TABLE B.4
PROPERTIES OF 4-STORY FRAME FOR SECTION 4.2

STORY	COLUMN M_p 's (k-in)		GIRDER M_p 's (k-in)	
	EXTERIOR	INTERIOR	EXTERIOR	INTERIOR
4	845	1625	909	983
3	1818	3147	2430	2339
2	2656	4318	3805	3433
1	3934	6094	4832	4261

TABLE B.5
PROPERTIES OF 10-STORY FRAME FOR SECTION 4.2

STORY	COLUMN M_p 's (k-in)		GIRDER M_p 's (k-in)	
	EXTERIOR	INTERIOR	EXTERIOR	INTERIOR
10	646	1336	1024	1024
9	1340	2448	1582	1770
8	1819	3240	2346	2523
7	2296	3802	2818	2951
6	2693	4336	3147	3309
5	3166	4827	3461	3612
4	3650	5340	3838	3808
3	4162	5845	4220	4064
2	4663	6328	4598	4279
1	5738	7677	4970	4416

TABLE B.6
PROPERTIES OF 18-STORY FRAME FOR SECTION 4.2

STORY	COLUMN M_p 's (k-in)		GIRDER M_p 's (k-in)	
	EXTERIOR	INTERIOR	EXTERIOR	INTERIOR
18	701	1381	1208	1208
17	1321	2360	1533	1593
16	1789	3074	2053	2049
15	2236	3829	2575	2850
14	2763	4519	2847	3132
13	3252	5153	3115	3345
12	3683	5837	3486	3952
11	4225	6434	3644	4106
10	4736	7043	3819	4201
9	5253	7757	4225	4754
8	5855	8405	4412	4861
7	6434	9058	4618	4931
6	7026	9789	5076	5410
5	7685	10464	5286	5464
4	8347	11159	5527	5491
3	9059	11945	6091	5882
2	9804	12692	6319	5848
1	11317	14726	6732	5966

TABLE B.7
PROPERTIES OF 4-STORY FRAME FOR SECTION 4.4

STORY	COLUMN M_p 's (k-in)		GIRDER M_p 's (k-in)	
	EXTERIOR	INTERIOR	EXTERIOR	INTERIOR
4	450	896	495	530
3	880	1665	1290	1240
2	1225	2220	2000	1800
1	1840	3152	2540	2240

TABLE B.8
PROPERTIES OF 10-STORY FRAME FOR SECTION 4.4

STORY	COLUMN M_p 's (k-in)		GIRDER M_p 's (k-in)	
	EXTERIOR	INTERIOR	EXTERIOR	INTERIOR
10	320	674	335	435
9	574	1119	820	905
8	716	1390	1180	1265
7	889	1563	1415	1478
6	1026	1731	1590	1660
5	1198	1866	1750	1815
4	1371	2012	1930	1910
3	1561	2158	2110	2030
2	1751	2305	2300	2140
1	2239	2973	2500	2215

TABLE B.9
PROPERTIES OF 4-STORY FRAME FOR SECTION 4.5

STORY	COLUMN M_p 's (k-in)		GIRDER M_p 's (k-in)	
	EXTERIOR	INTERIOR	EXTERIOR	INTERIOR
4	709	1126	845	845
3	1488	2160	1548	1488
2	2164	2989	2400	2160
1	3204	4213	3048	2688

TABLE B.10
PROPERTIES OF 10-STORY FRAME FOR SECTION 4.5

STORY	COLUMN M_p 's (k-in)		GIRDER M_p 's (k-in)	
	EXTERIOR	INTERIOR	EXTERIOR	INTERIOR
10	553	950	1025	1025
9	1095	1720	1260	1260
8	1476	2292	1416	1518
7	1869	2739	1698	1770
6	2201	3165	1908	1992
5	2584	3558	2100	2178
4	2972	3956	2316	2292
3	3382	4355	2532	2436
2	3790	4750	2760	2568
1	4642	5680	3000	2658